

# **Synthesis and Reactivity of Ferrocenyl Substituted Bis(amino)gallanes**

INAUGURAL – DISSERTATION

zur  
Erlangung der Doktorwürde  
der  
Naturwissenschaftlich-Mathematischen Gesamtfakultät  
der  
Ruprecht-Karls-Universität Heidelberg

vorlegt von  
Ovidiu Cristian Feier-Iova (M. Sc.)  
aus Ineu, Rumänien

2008



# INAUGURAL – DISSERTATION

zur

Erlangung der Doktorwürde

der

Naturwissenschaftlich-Mathematischen Gesamtfakultät

der

Ruprecht-Karls-Universität Heidelberg

vorlegt von

Ovidiu Cristian Feier-Iova (M. Sc.)

aus Ineu, Rumänien

2008

**Tag der mündlichen Prüfung: 18.07.2008**



# **Synthesis and Reactivity of Ferrocenyl Substituted Bis(amino)gallanes**

Gutachter:

Prof. Dr. Gerald Linti

Prof. Dr. Dr. Hans-Jörg Himmel



**Eidesstattliche Erklärung gemäß § 8 Abs. 3 b) und c) der Promotionsordnung:**

Ich erkläre hiermit, dass ich die vorliegende Dissertation selbst verfasst und mich dabei keiner anderen als der von mir ausdrücklich bezeichneten Quellen und Hilfen bedient habe. Ich erkläre weiterhin, dass ich an keiner anderen Stelle ein Prüfungsverfahren beantragt bzw. die Dissertation in dieser oder anderer Form bereits anderweitig als Prüfungsarbeit verwendet oder einer anderen Fakultät als Dissertation vorgelegt habe.

Heidelberg, den 05 Juni 2008

---

Ovidiu Feier-Iova





*This research work was carried out at the Institute of Inorganic Chemistry of Ruprecht-Karls-University Heidelberg from January, 2005 to June, 2008 under the supervision of Prof. Dr. Gerald Linti.*

***To my wonderful wife and to my parents, who have raised me to be the person I am today.***



## **Acknowledgments**

In my opinion, the great satisfaction for a PhD candidate is to write this part of the thesis. You know that when this task is fulfilled, then only a small step separates you from your “victory”. But the way till there, seems to be an endless one and without receiving invaluable guidance and encouragement, in many ways, nothing would have been possible.

In the following, I would like to express my deepest gratitude to Prof. Dr. Gerald Linti for his support, unselfish guidance, and interesting discussions every time when it was necessary, without previous appointment. I also wish to thank for all the advices, ideas and for giving me the opportunity to materialize this PhD Thesis under his supervision. I am gratefully indebted to Prof. Dr. Hans-Jörg Himmel for having accepted to referee this dissertation.

My special thanks go also to Dr. Jürgen Gross and to his coworkers for the mass spectrometry data. to Mrs. Danuta Gutruf for the electrochemical data, Mrs. Beate Termin for measuring many NMR spectra and to the technologists of Microanalytical Laboratory, Gas Station and Chemical Store.

Further thanks should go to all my colleagues and members of the institute who have contribute to this work. Philipp Butzug, thank you for measuring the crystallographic data sets and for all his assistance. Thomas Zessin and Kirill Monakhov, thank you for the quantum chemical calculations and that together with Tobias Adamczyk succeed to create a friendly atmosphere in the research group. Mrs. Karin Stelzer and Mrs. Marlies Schönebeck-Schilli, thank you for helping me to solve all administrative tasks.

I would also like to send my thanks to the research group of Prof. Dr. Peter Comba, namely: to Christoph Busche, Björn Seibold, for helping me with preparing and measuring the EPR spectrum and to Marta Zajaczkowski, Stefan Helmle, for their assistance in preparing samples for CVs measurements.

My wholehearted thanks goes to my wife Simona Feier-Iova for all her support and for making me shiny when “thunderclouds were into the sky”. I am also much indebted to my parents Sofia and Ioan Feier and to my brother Adrian Feier for their encouragement, although there is a long way between us.

Finally, the opportunity afforded by the Ruprecht-Karls University Heidelberg and by the Deutschen Forschungsgemeinschaft in their financial aid is gratefully acknowledged.



## Abbreviations and Symbols

ave.	average	m	multiplet (in NMR spectroscopy)
Bct	(phenyl)tricarbonyl-chromium	Mal	malonic acid or malonate
br	broad	m <sub>c</sub>	multiplet centered
Bu	butyl	Me	methyl
calcd.	calculated	Mes*	2,4,6-tri( <i>tert</i> -butyl)phenyl
Cp	$\eta^5$ -cyclopentadienyl	ml	milliliter
CV	cyclovoltammetry	mmol	millimole
d	doublet (in NMR spectroscopy)	M.p.	melting point
dd	doublet of doublets (in NMR)	mV	millivolt
dec.	decomposition	NMR	Nuclear Magnetic Resonance
Diox	1, 4-dioxane	Ph	phenol or phenolate
Do	donor	ppm	parts per million
DMSO	dimethylsulfoxide	py	pyridine
dt	doublet of triplets (in NMR)	Pytsi	(dimethyl(pyridin-2-yl)silyl)-bis-(trimethylsilyl)methanide
EA	elementary analysis/analyses	pz	1-pyrazol
EI	Electron Impact	r.t.	room temperature
Eq.	equation	s	singlet (in NMR spectroscopy)
EPR	Electron Paramagnetic Resonance	subst.	substituted
ESI	Electron Spray Ionization	t	triplet
eV	electron volt	<sup>t</sup> Bu	<i>tert</i> -butyl
Et	ethyl	thf	tetrahydrofuran
Fc	Ferrocene	TMEDA	<i>N,N,N',N'</i> -tetramethylethylenediamine
Fig.	Figure	tmp	2,2,6,6-tetramethyl-piperidino
g	gram	unsubst.	unsubstituted
G	gauss	$\delta$	chemical shift
h	hour(s)	$^\circ$	degree (temperature and angle)
K	Kelvin degree		



## Contents

Zusammenfassung.....	1
Abstract.....	2
1. Introduction.....	3
1.1. Monomeric Bis(amino)gallium Halides.....	3
1.2. Ferrocene, Ferrocenyl Derivatives of the Group 13 Elements and Their Possible Applications .....	5
1.3. Aim of this Thesis .....	8
References.....	10
2. Synthesis and Characterization of Amino Gallium Halides. Starting Materials for Gallylferrocene Derivatives .....	15
2.1. Introduction .....	15
2.2. Synthesis Routes .....	16
2.3. Spectroscopic Characterization.....	17
2.3.1. <sup>1</sup> H- and <sup>13</sup> C-NMR Spectroscopy .....	17
2.3.2. Mass Spectrometry .....	19
2.4. Crystal Structure Analysis .....	19
2.4.1. Crystal Structure Analysis of <b>1</b> .....	19
2.4.2. Crystal Structure Analysis of <b>6</b> .....	20
2.4.3. Crystal Structure Analysis of <b>7</b> .....	22
2.5. Summary of Important Bond Lengths.....	24
References.....	25
3. Reaction of Bis(amino)gallium Chlorides with Mono- and Dilithioferrocene.....	27
3.1. Introduction.....	27
3.2. Synthesis Routes .....	29
3.3. Spectroscopic Characterization.....	30
3.3.1. <sup>1</sup> H- and <sup>13</sup> C-NMR Spectroscopy .....	30
3.4. Cyclo Voltammetric Determinations .....	35
3.5. Quantum Chemical Calculations .....	37
3.6. Crystal Structure Analysis .....	39
3.6.1. Crystal Structure Analysis of <b>8</b> .....	39
3.6.2. Crystal Structure Analysis of <b>9</b> .....	40
3.6.3. Crystal Structure Analysis of <b>12</b> .....	41

References.....	44
4. Reactivity Studies on <b>8</b> and <b>9</b> .....	47
4.1. Introduction.....	47
4.2. Reaction of <b>8</b> with Acids .....	47
4.2.1. Synthesis Routes.....	47
4.2.2. Spectroscopic Characterization .....	49
4.2.2.1. <sup>1</sup> H- and <sup>13</sup> C-NMR Spectroscopy .....	49
4.2.2.2. Mass spectrometry.....	57
4.2.3. Cyclovoltammetric Determinations.....	57
4.2.4. Electron Paramagnetic Resonance (EPR) Spectroscopy .....	60
4.2.5. Crystal Structure Analysis .....	61
4.2.5.1. Crystal Structure Analysis of <b>13</b> .....	61
4.2.5.2. Crystal Structure Analysis of <b>14</b> .....	62
4.2.5.3. Crystal Structure Analysis of <b>15</b> .....	63
4.2.5.4. Crystal Structure Analysis of <b>18</b> .....	65
4.2.5.5. Crystal Structure Analysis of <b>19</b> .....	67
4.3. Reaction of <b>9</b> with Acids .....	67
4.3.1. Synthesis Routes.....	67
4.3.2. Spectroscopic Characterization .....	69
4.3.2.1. <sup>1</sup> H- and <sup>13</sup> C-NMR Spectroscopy .....	69
4.3.3. Crystal Structure Analysis.....	73
4.3.3.1. Crystal Structure Analysis of <b>22</b> .....	73
4.4. Comparison of Important Bond Lengths .....	74
References.....	82
5. Conclusion and Outlook .....	83
6. Summary .....	85
7. Experimental .....	93
7.1. General Remarks.....	93
7.1.1. NMR Spectroscopy.....	93
7.1.2. Elementary Analysis .....	93
7.1.3. Mass Spectrometry .....	94
7.1.4. Cyclovoltammetry .....	94
7.1.5. X-ray Analysis.....	94
7.1.6. Quantum Chemical Calculations.....	95



7.1.7. EPR Spectroscopy .....	95
7.1.8. Melting Point.....	96
7.1.9. Chemical used .....	96
7.2. Preparation of Amino Gallium Halides.....	96
7.2.1. Synthesis of <b>6</b> and <b>7</b> .....	96
7.3. Preparation of Ferrocenyl Substituted Bis(amino)gallanes.....	97
7.3.1. Synthesis of <b>8</b> and <b>12</b> .....	97
7.3.2. Synthesis of <b>8a</b> .....	98
7.3.3. Synthesis of <b>9</b> .....	98
7.3.4. Synthesis of <b>10</b> .....	99
7.3.5. Synthesis of <b>11</b> .....	99
7.4. Preparation of Different Derivatives of Mono- and Bisgallyl Substituted Ferrocenes.....	100
7.4.1. Synthesis of <b>13</b> .....	100
7.4.2. Synthesis of <b>14</b> .....	101
7.4.3. Synthesis of <b>15</b> .....	102
7.4.4. Synthesis of <b>16</b> and <b>17</b> .....	102
7.4.5. Synthesis of <b>18</b> .....	103
7.4.6. Synthesis of <b>19</b> .....	103
7.4.7. Synthesis of <b>20</b> .....	104
7.4.8. Synthesis of <b>21</b> and <b>22</b> .....	105
References.....	107
8. Crystal Data.....	109
9. Publications.....	115



## Zusammenfassung

Die vorliegende Arbeit behandelt die Untersuchung verschiedener mono- and disubstituierter Gallylferrocene bzgl. ihrer Synthese und Struktur sowie der sich daraus ergebenden chemischen und physikalischen Eigenschaften.

Das Bis(diaminogallyl)ferrocen  $[\{\text{Fe}(\eta^5\text{-C}_5\text{H}_4)_2\}\{\text{Ga}(\text{tmp})_2\}_2]$  **8** und das monosubstituierte Gallylferrocen  $[\{(\eta^5\text{-C}_5\text{H}_5)\text{Fe}(\eta^5\text{-C}_5\text{H}_4)\}\{\text{Ga}(\text{tmp})_2\}]$  **9** erwiesen auf Grund ihrer einfachen Synthese sich als die am besten geeigneten Startmaterialien zur Synthese von anderen gallyl-substituierten Ferrocenen und Galliaferrocenophanen.

Zudem wurden zwei weitere gallyl-substituierte Ferrocene  $[\{\text{Fe}(\eta^5\text{-C}_5\text{H}_4)_2\}\{\text{Ga}\{\text{N}(\text{SiMe}_3)_2\}_2\}]$  **10** und  $[\{(\eta^5\text{-C}_5\text{H}_5)\text{Fe}(\eta^5\text{-C}_5\text{H}_4)\}\{\text{Ga}\{\text{N}(\text{SiMe}_3)_2\}_2\}]$  **11** erhalten.

Bei der Reaktion von **8** und **9** mit unterschiedlichen Säuretypen wurden verschiedene Reaktionsweisen beobachtet. Die Behandlung von **8** und **9** mit einprotonigen Säuren wie Essigsäure, Ethanol oder Phenol ergab die gallyl-substituierten Ferrocene **14 – 17** und **20 – 22**.

Die so erhaltenen neuen gallyl-substituierte Ferrocene wurden durch Protonierung und Abspaltung der tmp-Gruppen an den Gallium-Atomen gebildet. Dies sind  $[\text{tmpH}_2]^+_2[\{\text{Fe}(\eta^5\text{-C}_5\text{H}_4)_2\}\{\text{Ga}(\text{O}_2\text{CMe})_3\}_2]^{2-}$  **14** und  $[\text{tmpH}_2]^+[\{(\eta^5\text{-C}_5\text{H}_5)\text{Fe}(\eta^5\text{-C}_5\text{H}_4)\}\{\text{Ga}(\text{O}_2\text{CMe})_3\}]^-$  **20**,  $[\text{tmpH}_2]^+_2[\{\text{Fe}(\eta^5\text{-C}_5\text{H}_4)_2\}\{\text{Ga}(\text{O-C}_6\text{H}_5)_3\}_2]^{2-}$  **16**,  $[\text{Li}(\text{thf})_2]^+_2[\{\text{Fe}(\eta^5\text{-C}_5\text{H}_4)_2\}\{\text{Ga}(\text{O-C}_6\text{H}_5)_3\}_2]^{2-}$  **17**,  $[\text{tmpH}_2]^+[\{(\eta^5\text{-C}_5\text{H}_5)\text{Fe}(\eta^5\text{-C}_5\text{H}_4)\}\{\text{Ga}(\text{O-C}_6\text{H}_5)_3\}]^-$  **21**,  $[\text{Li}(\text{thf})_2]^+[\{(\eta^5\text{-C}_5\text{H}_5)\text{Fe}(\eta^5\text{-C}_5\text{H}_4)\}\{\text{Ga}(\text{O-C}_6\text{H}_5)_3\}]^-$  **22** und  $[\{\text{Fe}(\eta^5\text{-C}_5\text{H}_4)_2\}\{\text{GaOEt}\}_2\text{O}]_4$  **15**.

Die Reaktion von **8** oder **9** mit organischen Disäuren wie Malonsäure und Catechol führte unter Spaltung sowohl der GaN- als auch der GaC-Bindungen zu  $[\text{tmpH}_2]^+_3[\{\text{CH}_2(\text{COO})_2\}_3\text{Ga}]^{3-}$  **18** und  $[\text{tmpH}_2]^+_2[(\sigma\text{-C}_6\text{H}_4\text{-O}_2)_2\text{Ga}(\text{OC}_6\text{H}_4\text{OH})]^{2-}$  **19**.

Lässt man **8** mit Kohlenstoffdioxid reagieren, bildet sich unter Insertion in die GaN-Bindungen das Carbaminat  $[\{\text{Fe}(\eta^5\text{-C}_5\text{H}_4)_2\}\{\text{Ga}(\text{O}_2\text{Ctmp})(\mu^2\text{-O}_2\text{Ctmp})\}_2]$  **13**.

## Abstract

In this work, several mono- and disubstituted gallyl ferrocenes were synthesized and their chemical and physical properties have been investigated. In the same time, new information's regarding the stability and atoms arrangement in solid state structures of a series of mono- and disubstituted ferrocenyl gallane are reported.

From all of them, the disubstituted gallyl ferrocene [ $\{\text{Fe}(\eta^5\text{-C}_5\text{H}_4)_2\}\{\text{Ga}(\text{tmp})_2\}_2$ ] **8** and the monosubstituted gallyl ferrocene [ $\{(\eta^5\text{-C}_5\text{H}_5)\text{Fe}(\eta^5\text{-C}_5\text{H}_4)\}\{\text{Ga}(\text{tmp})_2\}$ ] **9** proves to be the most suited starting material for the synthesis of other gallyl substituted ferrocenes and gallaferrocenophanes. That is because of their moderate to high yield syntheses. **8** and **9** have been characterized by means of  $^1\text{H}$ -,  $^{13}\text{C}$ -NMR spectroscopy, elementary analysis, mass spectrometry, cyclovoltammetry and single crystal X-ray analysis. Also, several quantum chemical calculations using the crystal coordinates of **8** and **9** gave an insight into their electronically structures and stabilities.

Other two gallyl substituted ferrocenes [ $\{\text{Fe}(\eta^5\text{-C}_5\text{H}_4)_2\}\{\text{Ga}\{\text{N}(\text{SiMe}_3)_2\}_2\}_2$ ] **10** and [ $\{(\eta^5\text{-C}_5\text{H}_5)\text{Fe}(\eta^5\text{-C}_5\text{H}_4)\}\{\text{Ga}\{\text{N}(\text{SiMe}_3)_2\}_2\}$ ] **11** have been synthesized.

By the reaction of **8** and **9** with different acids, a different behavior could be observed. When **8** and **9** have been treated with monoacids as acetic acid, ethanol or phenol different gallylsubstituted ferrocenes **14** – **17** und **20** – **22** were obtained. These new gallylsubstituted ferrocenes are formed by cleavage of the Ga-N bonds. With acetic acid [ $\text{tmpH}_2$ ] $^+_2\{\{\text{Fe}(\eta^5\text{-C}_5\text{H}_4)_2\}\{\text{Ga}(\text{O}_2\text{CMe})_3\}_2\}^{2-}$  **14** and [ $\text{tmpH}_2$ ] $^+[\{(\eta^5\text{-C}_5\text{H}_5)\text{Fe}(\eta^5\text{-C}_5\text{H}_4)\}\{\text{Ga}(\text{O}_2\text{CMe})_3\}]^-$  **20**, with phenol [ $\text{tmpH}_2$ ] $^+_2\{\{\text{Fe}(\eta^5\text{-C}_5\text{H}_4)_2\}\{\text{Ga}(\text{O-C}_6\text{H}_5)_3\}_2\}^{2-}$  **16**, [ $\text{Li}(\text{thf})_2$ ] $^+_2\{\{\text{Fe}(\eta^5\text{-C}_5\text{H}_4)_2\}\{\text{Ga}(\text{O-C}_6\text{H}_5)_3\}_2\}^{2-}$  **17**, [ $\text{tmpH}_2$ ] $^+[\{(\eta^5\text{-C}_5\text{H}_5)\text{Fe}(\eta^5\text{-C}_5\text{H}_4)\}\{\text{Ga}(\text{O-C}_6\text{H}_5)_3\}]^-$  **21** and [ $\text{Li}(\text{thf})_2$ ] $^+[\{(\eta^5\text{-C}_5\text{H}_5)\text{Fe}(\eta^5\text{-C}_5\text{H}_4)\}\{\text{Ga}(\text{O-C}_6\text{H}_5)_3\}]^-$  **22** and with ethanol [ $\{\text{Fe}(\eta^5\text{-C}_5\text{H}_4)_2\}\{\text{GaOEt}\}_2\text{O}]_4$  **15** were formed.

When **8** or **9** was reacted with the organic diacids malonic acid and catechol, not only the Ga-N bonds, but as well the Ga-C bonds were cleaved and [ $\text{tmpH}_2$ ] $^+_3\{\{\text{CH}_2(\text{COO})_2\}_3\text{Ga}\}^{3-}$  **18** and [ $\text{tmpH}_2$ ] $^+_2\{(\sigma\text{-C}_6\text{H}_4\text{-O}_2)_2\text{Ga}(\text{OC}_6\text{H}_4\text{OH})\}^{2-}$  **19** were obtained. The reaction of **8** with carbon dioxide leads to the formation of the carbamate [ $\{\text{Fe}(\eta^5\text{-C}_5\text{H}_4)_2\}\{\text{Ga}(\text{O}_2\text{Ctmp})(\mu^2\text{-O}_2\text{Ctmp})\}_2$ ] **13**.

## 1. Introduction

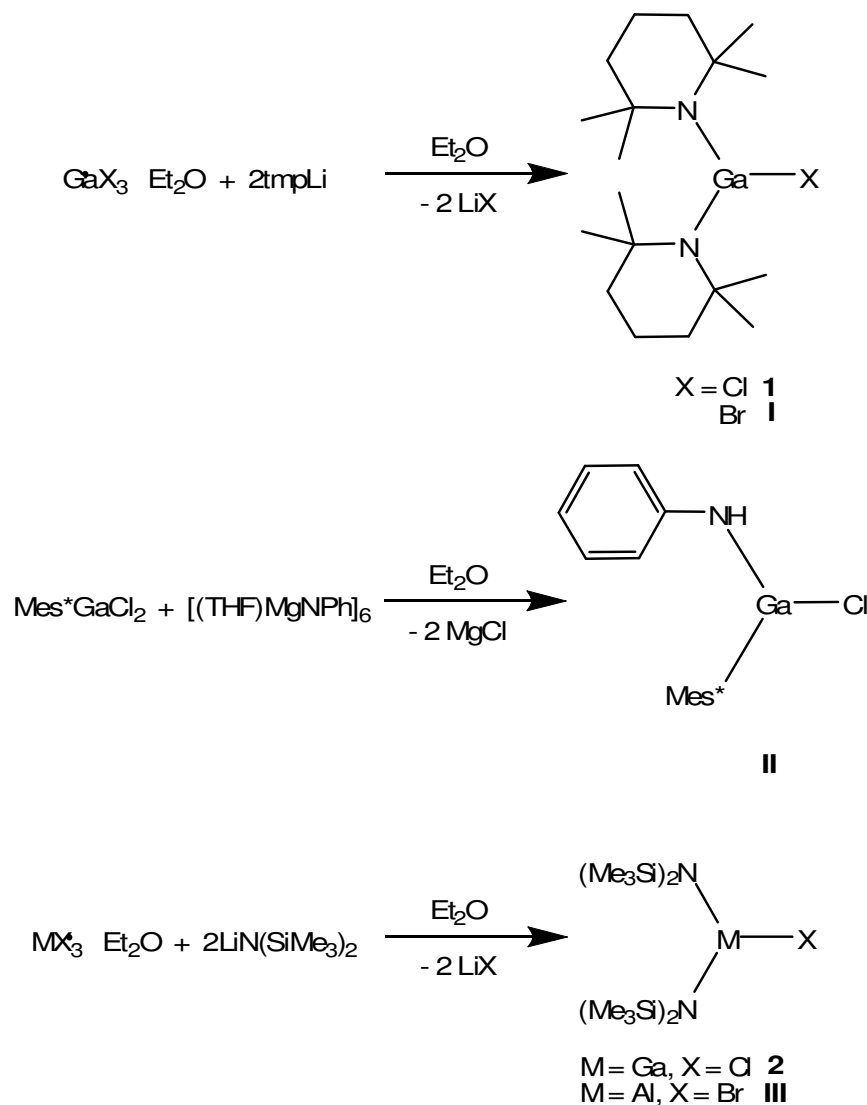
### 1.1. Monomeric Bis(amino)gallium Halides

The chemistry of organyl and amino compounds of the Group 13 elements is well developed because of their potential application in the nitride semiconductors production (MN, M = Al, Ga or In)<sup>[1]-[3]</sup> and then, because of their interesting bonding models in comparison with the lighter elements.<sup>[4]-[6]</sup> These bonding models give rise to unusual structures and properties of the compound with the elements from the Group 13. That is reflected in debate concerning the very definition of chemical bonding.<sup>[7]-[9]</sup> Almost all the amino complexes of the metals from this Group have in common their high tendency to oligomerise through the formation of strong metal-nitrogen bridges.<sup>[10]</sup> This is possible through the interaction between the lone pairs of the nitrogen atoms, with the formally empty p-orbital on the metal center to form dative  $\pi$ -bonds, which are usually reflected by planar core geometry.<sup>[9]</sup>

A special case, where the lone pairs of the nitrogen atom are not involved in a  $\sigma$ - or  $\pi$ -bonding and in the same time, the metal centers are coordinative unsaturated, is that of monomeric bis(amino)gallium halides. These two features, made bis(amino)gallium halides, some of the most versatile starting materials for the synthesis of different organyl gallium derivatives.

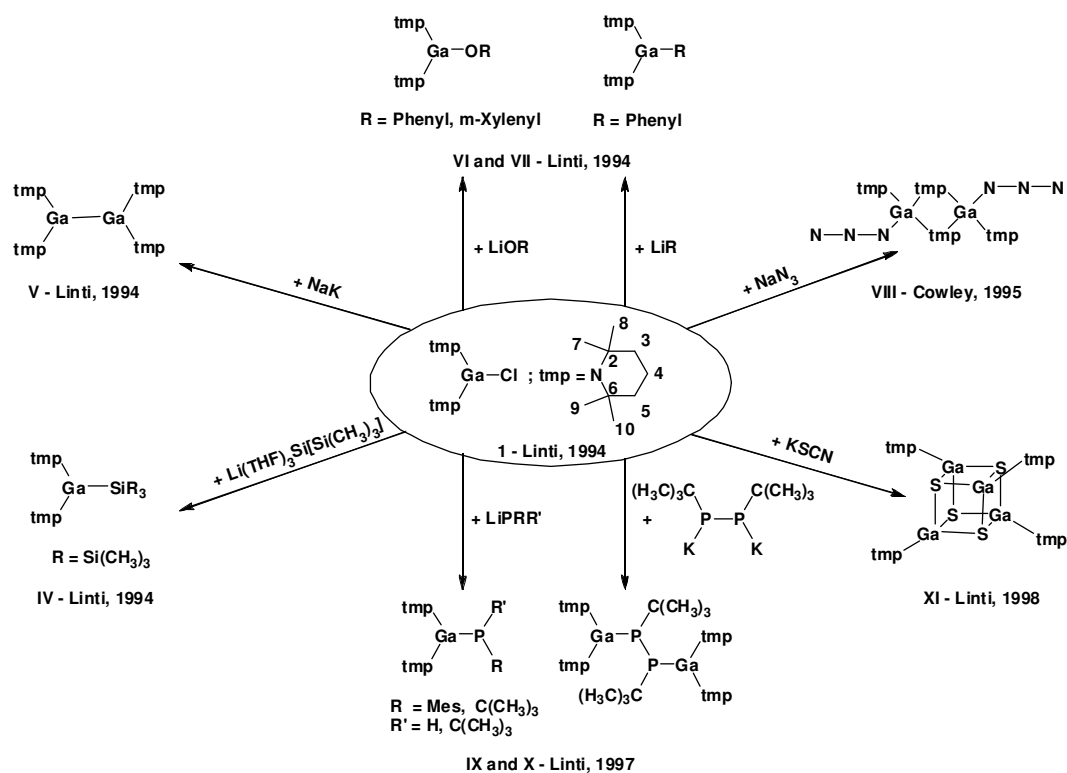
In 1994 G. Linti *et al.*<sup>[11]</sup> and in parallel P. P. Power *et al.*<sup>[12]</sup> published the synthesis of the first reported bis(amino)gallium halides ( $\text{tmp}_2\text{GaX}$ , X = Cl (**1**) or Br (**I**)<sup>[11]</sup>,  $\{(\text{Me}_3\text{Si})_2\text{N}\}_2\text{GaCl}$  (**2**) and  $\text{Mes}^*\text{GaCl}\{\text{N}(\text{H})\text{Ph}$  (**II**)<sup>[12]</sup>) which were a landmark at that time (see Scheme 1).

Scheme 1: Synthesis routes for the first reported bis(amino)gallium halides.



These bis(amino)gallium and corresponding aluminum halides<sup>[13]</sup> found rapidly further applications as precursors in the synthesis of other gallium or aluminum organyls derivatives and from all of them, in the following, it will be mentioned those in which  $\text{tmp}_2\text{GaCl}$  (**1**) was used as starting material (see Scheme 2).

In this thesis, it was appealed again to the versatility of **1** by using it, for the first time, as adduct in the synthesis of new mono- and disubstituted ferrocenyl gallanes.

**Scheme 2:** Using of **1** as starting material on the synthesis of different bis(amino)gallium derivatives.

## 1.2. Ferrocene, Ferrocenyl Derivatives of the Group 13 Elements and Their Possible Applications

There are many years past from the fortunate accident that led to the discovery, made by T. J. Kealy and P. L. Pauson,<sup>[14]</sup> of the first recognized sandwich compound, which is known as ferrocene. Although, its “venerable age”, ferrocene is still one of the most use precursors for the synthesis of many cyclopentadienyl derivatives of various metals and metalloids, some of them having industrial applications ranging from antiknock additives to polymerization catalysts<sup>[15]</sup> or even as building block in supramolecular chemistry.<sup>[16]-[18]</sup>

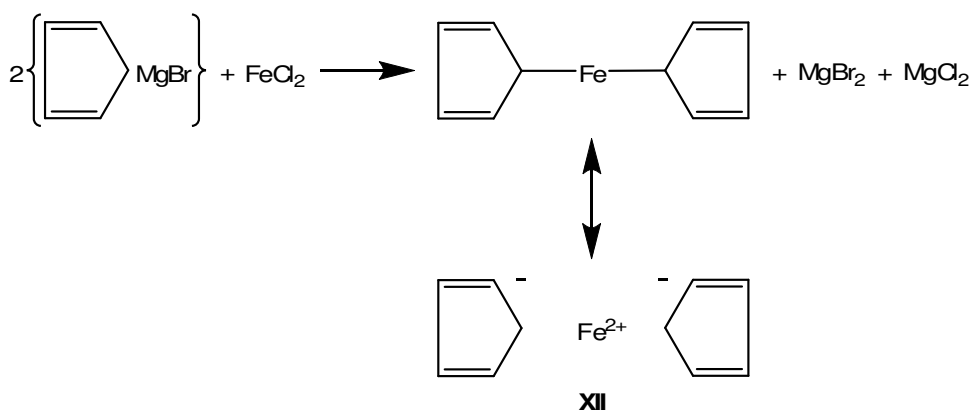
One year before the discovery of ferrocene, R. D. Brown<sup>[19]</sup> predicted a hypothetical hydrocarbon as a non-benzenoid molecule which was called fulvalene. Having this prediction in mind and also the report of H. Gilman and M. Lichtenwalter<sup>[20]</sup> for the

## 1. Introduction

---

successful synthesis of biphenyl, Pauson found a new challenge on attempted fulvalene synthesis. Thus, by refluxing the Grignard reagent cyclopentadienylmagnesium bromide with anhydrous iron (II) chloride (obtained after the initial reduction of  $\text{FeCl}_3$  to  $\text{FeCl}_2$  by the Grignard reagent) in anhydrous ether, a remarkable stable orange solid was afforded, with the analytical data showing iron in its backbone. The first formulated reaction for ferrocene formation is presented in Scheme 3.<sup>[21]</sup>

**Scheme 3:** Proposed reaction route for the synthesis of ferrocene.<sup>[21]</sup>



In the same year, but one month before T. J. Kealy and P. L. Pauson's note, S. A. Miller, J. A. Tebboth, and J. F. Tremaine submitted their article to the *Journal of Chemical Society*, which was first published in the following year.<sup>[22]</sup> By using another synthesis route, reduced iron was reacted with cyclopentadiene vapors in a nitrogen atmosphere and the same product, now familiarly known as ferrocene, was exhibited.

Nevertheless, the first proposal for a sandwich structure of ferrocene came from G. Wilkinson *et al.* after several physical and chemical investigations.<sup>[23]</sup> In the same time with Wilkinson studies, E. O. Fischer succeeded in isolation and analysis *via* X-ray diffraction of suitable single crystals of ferrocene and reported its antiprismatic structure.<sup>[24]</sup> That was one of the most tortuous way for the characterization of a new compound, finalized with a Nobel prize for chemistry in 1973 for the "last two pioneer researchers in organometallic chemistry".<sup>[25]</sup> Since then, ferrocene found its applications in almost all large mineral oil companies as additive in fuel oils, which has the consequence that the fuel combustion is accelerated and the soot formation is



enormously lowered during the burning process.<sup>[26]</sup> Ferrocene is also used in plastic production as flame- and smoke-retardant.<sup>[27]</sup>

Apart from ferrocene applications in industrial processes, in the last 50 years, several thousands ferrocenyl derivatives were synthesized having the ferrocenyl group as substituent and/or backbone in a wide variety of mono- and disubstituted ferrocenyl ligand systems. The most common routes for the synthesis of different ferrocenyl derivatives are: electrophilic aromatic substitution reactions (ex.: Friedel-Craft acylation, intramolecular acylation,<sup>[28]</sup> intermolecular acylation<sup>[29],[30]</sup> etc.), metallation reactions<sup>[31]-[33]</sup> and oxidation reactions.<sup>[34]</sup> From all of them, we will be focus on the ferrocenyl derivatives of the Group 13 elements, on their technical and theoretical applications, especially on the mono- and disubstituted gallyl ferrocenes and respectively on gallaferrocenophanes synthesis.

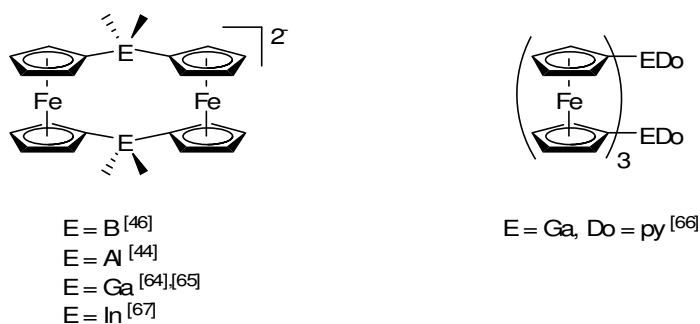
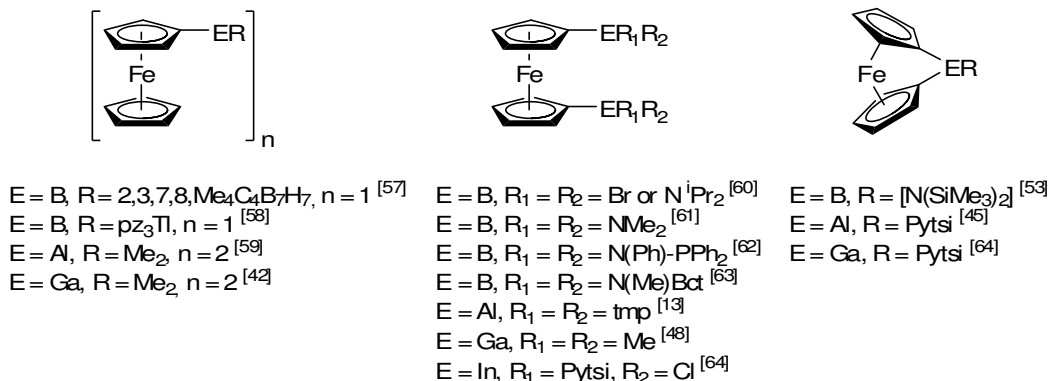
In the past decade, several groups were engaged in the synthesis of new ferrocenyl substituted alanes,<sup>[13],[35]-[41]</sup> gallanes,<sup>[42]</sup> indanes<sup>[43]</sup> and even in the synthesis of some ferrocenophanes with the Group 13 elements.<sup>[44]-[50]</sup> Such systems fulfill the features as precursors to polymeric materials with ferrocenyl repeat fragments and as starting material in the synthesis of new ferrocene-based ligands, that can be used in further catalytic transformations, when are bounded directly to an adequate transition metal.<sup>[51]-[55]</sup> Another possible application is on the metalorganic chemical vapor deposition of GaN : Fe and (Ga,Fe)N<sup>[56]</sup> layers with a previously establish stoichiometry.

The most representative examples of some mono- or disubstituted ferrocenyl derivatives of the Group 13 elements and ferrocenophanes of the same Group are shown in Scheme 4.

From all of these ferrocenyl derivatives of the Group 13 elements, only a few of them have gallium atoms in their backbone and that is because the chemistry of gallylsubstituted ferrocenes was limited to methyl derivatives as:  $[\{(\eta^5\text{-C}_5\text{H}_5)\text{Fe}(\eta^5\text{-C}_5\text{H}_4)\}\{\text{GaMe}_2\}]_2$ ,<sup>[42]</sup>  $[\{(\eta^5\text{-C}_5\text{H}_5)\text{Fe}(\eta^5\text{-C}_5\text{H}_3)\}\{\text{Ga}(\text{Me}_2)\text{-CH}_2\text{NMe}_2\}]$ ,<sup>[43]</sup> [1,1']-digallyl ferrocenes  $[\{\text{Fe}(\eta^5\text{-C}_5\text{H}_4)_2\}\{\text{GaMe}_2\}]_n$  and donor adducts.<sup>[68]</sup>

In the past recent years, several new [1,1']-gallylferrocenophanes were reported in the literature and their redox chemistry has been studied.<sup>[47],[66],[68]-[70]</sup>

Scheme 4: Ferrocenyl derivatives of the Group 13 elements.



This revival of the gallyl ferrocenes and gallyl ferrocenophanes chemistry came as a result of the recently growing interest in using the previous mention compounds as precursor to semiconductors materials.<sup>[70]-[73]</sup> Actually, this is the main reason for the currently great popularity of the organo-gallium compounds, including here, also, the gallyl ferrocenyl derivatives. Apart from that, there are several indices of some potential for using these compounds as precursors for preparing polymers through ring-opening reactions, with interesting electrical, magnetic and optical properties, as a result of electron delocalization.<sup>[74]</sup>

### 1.3. Aim of this Thesis

There are several important aims of this thesis which will be summarized as follow.

The first aim was to synthesize and characterize new mono- and disubstituted gallyl ferrocenes. These substituted gallyl ferrocenes were use as precursors to synthesize new

ferrocenylgallanes and respectively to prepare oligomeric or polymeric gallaferrocenophanes.

Then, the chemical, electrochemical, physical and structural (solid state) properties of the obtained products were analyzed by means of  $^1\text{H}$ - and  $^{13}\text{C}$ -NMR spectroscopy, mass spectrometry, elemental analysis, cyclovoltammetry and where it was possible, through single crystal X-ray analysis. To gain an insight into electronic influence of bis(amino)gallyl substituents on the ferrocenyl rest, a series of quantum chemical calculations have been performed on the model compound  $[\text{Fc}\{\text{Ga}(\text{NR}_2)\}_n]$  ( $\text{Fc} = \{(\eta^5\text{-C}_5\text{H}_5)\text{Fe}(\eta^5\text{-C}_5\text{H}_4)\}$  or  $\{\text{Fe}(\eta^5\text{-C}_5\text{H}_4)_2\}$ ,  $\text{R} = \text{tmp}$ ,  $n = 0, 1$  or  $2$ ). Finally, trying to oxidize the iron atoms from the ferrocenylgallanes and to analyze the magnetically behaviour of this new species.

## References

- [1] D.A. Neumayer, and J.G. Ekerdt, *Chem. Mater.*, **1996**, 8, 9-25.
- [2] D.M. Hoffman, *Polyhedron*, **1994**, 13, 1169-1179.
- [3] S. Strite, H. Morkoç, *J. Vac. Sci. Technol. B*, **1992**, 10, 1237-1266.
- [4] M. F. Lappert, P.P. Power, A. R. Sanger, and R. C. Srivastava, *Metal and Metalloid Amides*, Ellis Horwood-Wiley: Chichester, U.K., **1979**.
- [5] M. J. Taylor, and P. J. Brothers, In *The Chemistry of Aluminum, Gallium, Indium and Thallium*, Downs, A. J.; Ed.; Blackie-Chapman Hall: New York, **1993**, Chapter 3.
- [6] G. H. Robinson, In *Coordination Chemistry of Aluminum*, Robinson, G. H., Ed.; VCH: New York, **1993**; Chapter 5.
- [7] L. Pauling, *The Nature of the Chemical Bond*, 3rd ed., Cornell University Press, **1960**, p. 6.
- [8] P. P. Power, *J. Chem. Soc., Dalton Trans.*, **1998**, 2939-2951.
- [9] P. P. Power, *Chem. Rev.*, **1999**, 99, 3463-3503 (and the literature therein).
- [10] C. J. Carmalt, *Coord. Chem. Rev.*, **2001**, 223, 217-264.
- [11] G.Linti, R. Frey, and K. Polborn, *Chem. Ber.*, **1994**, 127, 1387-1393.
- [12] P. J. Brothers, R. J. Wehmschulte, M. M. Olmstead, K. Ruhlandt-Senge, S. R. Parkin, and P. P. Power, *Organometallics*, **1994**, 13, 2792-2799.
- [13] K. Knabel, I. Krossing, H. Nöth, H. Schwenk-Kircher, M. Schmidt-Amelunxen, and T. Seifert, *Eur. J. Inorg. Chem.*, **1998**, 1095-1114.
- [14] T. J. Kealy, and P. L. Pauson, *Nature*, **1951**, 168, 1039-1040.
- [15] H. Gilman, *Adv. Organomet. Chem.* **1968**, 7, 1-52.
- [16] S. Barlow, and D. O'Hare, *Chem. Rev.*, **1997**, 97, 637-669.
- [17] U. T. Müller-Westerhoff, *Angew. Chem.*, **1986**, 98, 700-716; *Angew. Chem. Int. Ed.*, **1986**, 25, 702-717.
- [18] S. Leininger, B. Olenyuk, and P. J. Stang, *Chem. Rev.*, **2000**, 100, 853-907.
- [19] R. D. Brown, *Nature*, **1950**, 165, 566-567.
- [20] H. Gilman, and M. Lichtenwalter, *J. Am. Chem. Soc.*, **1939**, 61, 957-959.
- [21] G. B. Kauffman, *J. Chem. Ed.*, **1983**, 60, 185-186.
- [22] S. A. Miller, J. A. Tebboth, and J. F. Tremaine, *J. Chem. Soc.*, **1952**, 632-635.

- [23] G. Wilkinson, M. Rosenblum, M. C. Whiting, and R. B. Woodward, *J. Am. Chem. Soc.*, **1952**, *74*, 3458-3459.
- [24] E. O. Fischer, and W. Z. Pfab., *Z. Naturforsch.*, **1952**, *7B*, 377-379.
- [25] D. Seyferth, and A. Davison, *Science*, **1973**, *182*, 699-701.
- [26] K. E. Ritrievi, J. P. Longwell, and A. F. Sarofim, *Combustion and Flame* **1987**, *70(1)*, 17-31.
- [27] H. Jungbluth, and G. Lohmann, *Nachrichten aus der Chemie*, **1999**, *47(5)*, 532, 534-536.
- [28] M. Rosenblum and F. W. Abbate, *J. Am. Chem. Soc.*, **1966**, *88*, 4178-4184.
- [29] T. J. Curphe, J. O. Santer, M. Rosenblum, and J. H. Richards, *J. Am. Chem. Soc.*, **1960**, *82*, 5249-5250.
- [30] A. F. Jr. Cunningham, *Organometallics*, **1994**, *13*, 2480-2485.
- [31] D. Guillaneux, and H. B. Kagan, *J. Org. Chem.*, **1995**, *60*, 2502-2505.
- [32] M. D. Rausch, and D. J. Ciappenelli, *J. Organomet. Chem.*, **1967**, *10*, 127-136.
- [33] I. R. Butler, W. R. Cullen, J. Ni, and S. J. Rettig, *Organometallics*, **1985**, *4*, 2196-2201.
- [34] C. Elschenbroich, In *Organometallchemie*, B. G. Teubner; Ed. B. G. Teubner Verlag, GWV Fachverlage GmbH: Wiesbaden, **2003**, Chapter 15.
- [35] T. Baumgartner, F. Jäkle, R. Rulkens, G. Zech, A. J. Lough, and I. Manners, *J. Am. Chem. Soc.*, **2002**, *124*, 10062-10070.
- [36] F. Voigt, A. Fischer, C. Pietzsch, and K. Jacob, *Z. Anorg. Allg. Chem.*, **2001**, *627*, 2337-2343.
- [37] F. Voigt, K. Jacob, N. Seidel, A. Fisher, C. Pietzsch, and P. Zanello, *J. Prakt. Chem.*, **2000**, *342*, 666-674.
- [38] G. H. Robinson, S. G. Bott, and J. L. Atwood, *J. Coord. Chem.*, **1987**, *16*, 219-224.
- [39] R. D. Rogers, W. J. Cook, and J. L. Atwood, *Inorg. Chem.*, **1979**, *18*, 279-282.
- [40] J. L. Atwood, A. L. Shoemaker, *J. Chem. Soc., Chem. Commun.*, **1976**, 536-537.
- [41] J. L. Atwood, B. L. Bailey, B. L. Kindberg, and W. J. Cook, *Aust. J. Chem.*, **1973**, *26*, 2297-2298.
- [42] B. Lee, W. T. Pennington, J. A. Laske and G. H. Robinson, *Organometallics* **1990**, *9*, 2864-2865.
- [43] E. Hecht, *Z. Anorg. Allg. Chem.*, **2000**, *626(3)*, 759-765.

- [44] J. A. Schachner, C. L. Lund, J. W. Quail, and J. Müller, *Acta Cryst.*, **2005**, *E61*, m682-m684.
- [45] J. A. Schachner, C. L. Lund, J. W. Quail, and J. Müller, *Organometallics*, **2005**, *24*, 785-787.
- [46] M. Scheibitz, R. F. Winter, M. Bolte, H. W. Lerner, and M. Wagner, *Angew. Chem., Int. Ed.*, **2003**, *42*, 924-927.
- [47] A. Althoff, P. Jutzi, N. Lenze, B. Neumann, A. Stammler, and H. G. Stammler, *Organometallics*, **2003**, *22*, 2766-2774.
- [48] A. Althoff, P. Jutzi, N. Lenze, B. Neumann, A. Stammler, and H. G. Stammler, *Organometallics*, **2002**, *21*, 3018-3022.
- [49] A. Berenbaum, H. Braunschweig, R. Dirk, U. Englert, J. C. Green, F. Jäkle, A. J. Lough, and I. Manners, *J. Am. Chem. Soc.*, **2000**, *122*, 5765-5774.
- [50] H. Braunschweig, C. Burschka, G. K. B. Clentsmith, T. Kupfer, and K. Radacki, *Inorg. Chem.*, **2005**, *44*, 4906-4908.
- [51] A. S. Abd-El-Aziz, and E. K. Todd, *Coord. Chem. Rev.*, **2003**, *246*, 3-52.
- [52] I. Manners, *Chem. Commun.*, **1999**, 857-865.
- [53] H. Braunschweig, R. Dirk, M. Muller, P. Nguyen, R. Resendes, D. P. Gates, and I. Manners, *Angew. Chem., Int. Ed. Engl.*, **1997**, *36*, 2338-2340.
- [54] I. Manners, *Adv. Organomet. Chem.*, **1995**, *37*, 131-168.
- [55] A. Togni, and T. Hayashi, Eds. *Ferrocenes Homogeneous Catalysis, Organic Synthesis, Materials Science*, Wiley-VCH: Weinheim, Germany, **1994**.
- [56] A. Bonanni, M. Kiecana, C. Simbrunner, T. Li, M. Sawicki, M. Wegscheider, M. Quast, H. Przybylińska, A. Navarro-Quezada, R. Jakiela, A. Wolos, W. Jantsch, and T. Dietl, *Phys. Rev. B*, **2007**, *75*, 125210-1-125210-18.
- [57] R. N. Grimes, W. M. Maxwell, R. B. Maynard, and E. Sinn, *Inorg. Chem.*, **1980**, *19*, 2981-2985.
- [58] F. Jäkle, K. Polborn, and M. Wagner, *Chem. Ber.*, **1996**, *129*, 603-606.
- [59] B. Wrackmeyer, E. V. Klimkina, T. Ackermann, and W. Milius, *Inorg. Chem. Commun.*, **2007**, *10*, 743-747.
- [60] B. Wrackmeyer, U. Dörfler, W. Milius, and M. Herberhold, *Polyhedron*, **1995**, *14*, 1425-1431.
- [61] M. Herberhold, U. Dörfler, W. Milius, and B. Wrackmeyer, *J. Organomet. Chem.*, **1995**, *492*, 59-63.

- [62] F. Jäkle, M. Mattner, T. Priermeier, and M. Wagner, *J. Organomet. Chem.*, **1995**, 502, 123-130.
- [63] F. Jäkle, T. Priermeier, and M. Wagner, *Chem. Ber.*, **1995**, 128, 1163-1169.
- [64] J. A. Schachner, C. L. Lund, J. W. Quail, and J. Müller, *Organometallics*, **2005**, 24, 4483-4488.
- [65] W. Uhl, I. Hahn, A. Jantschak, and T. Spies, *J. Organomet. Chem.*, **2001**, 637-639, 300-303.
- [66] P. Jutzi, N. Lenze, B. Neumann, and H.-G. Stammler, *Angew. Chem. Int. Ed.*, **2001**, 40, 1423-1427.
- [67] J. A. Schachner, G. A. Orlowski, J. W. Quail, H.-B. Kraatz, and J. Müller, *Inorg. Chem.*, **2006**, 45, 454-459.
- [68] A. Althoff, D. Eisner, P. Jutzi, N. Lenze, B. Neumann, W. W. Schoeller and H.-G. Stammler, *Chem. Eur. J.* **2006**, 12, 5471-5480.
- [69] P. Jutzi and L. O. Schebaum, *J. Organomet. Chem.*, **2002**, 654, 176-179.
- [70] M. A. Banks, O. T. Jr. Beachley, H. J. Gysling, and H. R. Luss, *Organometallics*, **1990**, 9, 1979-1982.
- [71] D. L. Reger, S. J. Knox, and L. Leboida, *Inorg. Chem.*, **1989**, 28, 3092-3093.
- [72] R. L. Wells, A. P. Purdy, A. T. McPhail, and C. G. Pitt, *J. Organomet. Chem.*, **1988**, 354, 287-292.
- [73] A. H. Cowley, R. A. Jones, K. B. Kidd, C. M. Nunn, and D. L. Westmoreland, *J. Organomet. Chem.*, **1988**, 341, C1-C5.
- [74] I. Manners, *Angew. Chem. Int. Ed. Engl.*, **1996**, 35, 1602-1621.





## 2. Synthesis and Characterization of Amino Gallium Halides. Starting Materials for Gallylferrocene Derivatives

### 2.1. Introduction

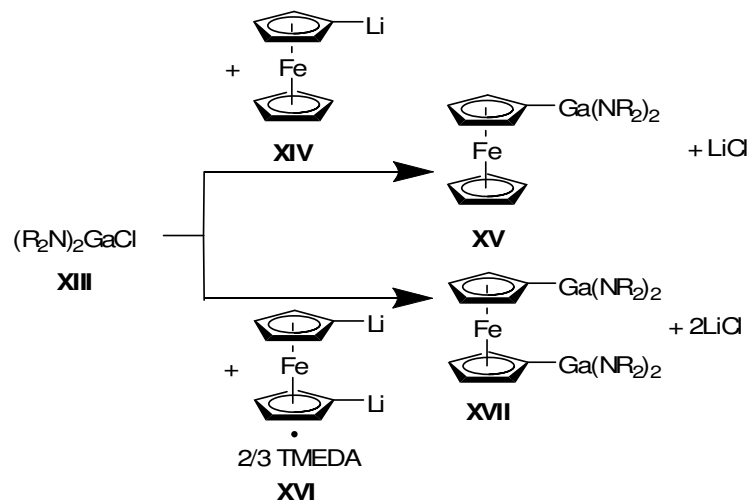
For the synthesis of mono- and digallyl substituted ferrocenes and of gallaferrocenophanes, two building blocks are required: the first one is a gallane derivative, where a reactive bond Ga-X (X = F, Cl, Br or I) is present. That has the possibility to be broken *via* nucleophilic substitution reaction with the building of a new Ga-C bond at the ferrocenyl rest. This second building block is a monolithiated or dilithiated ferrocene.

The approach solution in this thesis was to synthesize monomeric aminogallanes and to use them in substitution reactions with monolithiated or dilithiated ferrocene (see Scheme 5).

In the following, the synthesis routes for some monomeric aminogallanes are presented, which will be used in the synthesis of mono- and digallyl substituted ferrocenes. From all of them the bis(2,2,6,6-tetramethylpiperidino)gallium chloride **1**<sup>[1]</sup> proves to be the best starting material, because of its high yield synthesis. **1** has been a valuable starting material for various bis(amino)gallanes  $\text{tmp}_2\text{GaR}$  (R = H, Me, Si(SiMe<sub>3</sub>)<sub>3</sub>, Ph, OPh, P<sup>t</sup>Bu<sub>2</sub> etc.).<sup>[2]-[6]</sup>

## 2. Synthesis and Characterization of Amino Gallium Halides. Starting Materials for Gallylferrocene Derivatives

**Scheme 5:** Possible synthesis routes to achieve mono- and digallyl substituted ferrocenes, respectively gallaferrocenophanes.



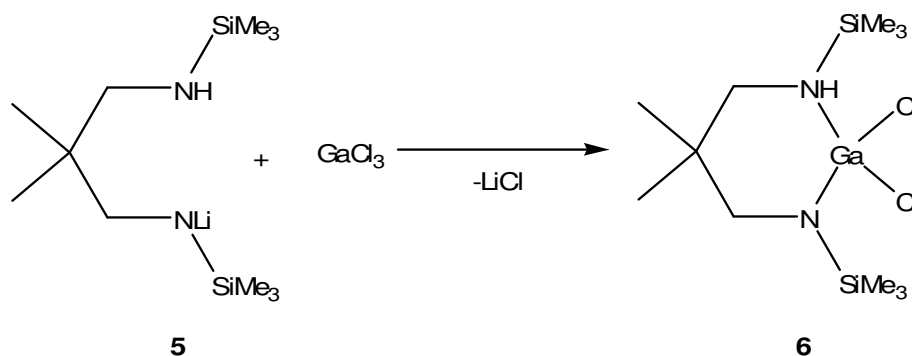
### 2.2. Synthesis Routes

1,3-Bis(trimethylsilylamino)-2,2-dimethylpropane<sup>[7]</sup> **4** was synthesized by the reaction of 1,3-diamino-2,2-dimethylpropane **3** with  $Me_3SiCl$  (Eq. 1). **4** can be easily lithiated, once to obtain 1-trimethylsilyllithioamino-3-trimethylsilylamino-2,2-dimethylpropane **5** and twice to obtain 1,3-bis(trimethylsilyllithioamino)-2,2-dimethylpropane **XVIII**. By the reaction of **XVIII** with galliumtrichloride, the dimeric syn-2,8-dichloro-5,5,11,11-tetramethyl-1,3,7,9-tetrakis(trimethylsilyl)-3,9-diaza-1,7-diazonia-2,8-digallactatricyclo dodecane **XIX** was formed.<sup>[8]</sup> From the reaction of monolithiated **5** with equivalent amounts of  $GaCl_3$  in *thf*/*Diox* (10:1) at  $-78\text{ }^\circ\text{C}$ , the main product 2,2-dichloro-5,5-dimethyl-1,3-bis(trimethylsilyl)-1-aza-3-azonia-2-gallactacyclohexane **6** as a white jelly was obtained (Eq. 2). After several washes with diethyl ether together with filtration of LiCl and cooling at  $-32\text{ }^\circ\text{C}$  for several days, the product **6** crystallized as colorless crystals in good yield. Colorless crystals of the side-product  $[Li(Diox)_2(thf)_2]^+ [GaCl_4]^-$  **7** were grown and further analyzed, too.

Equation 1:



Equation 2:



The monomeric bis(2,2,6,6-tetramethylpiperidino)gallane **1**<sup>[1],[2],[4]</sup> and the monomeric bis[bis(trimethylsilyl)amino]gallane **2**<sup>[9]</sup> were prepared as described in literature. Here, single crystals of **1**<sup>[10]</sup> were obtained, which till now was not possible because of the low melting point of **1**.

## 2.3. Spectroscopic Characterization

### 2.3.1. $^1\text{H}$ - and $^{13}\text{C}$ -NMR Spectroscopy

The  $^1\text{H}$ -NMR spectrum of **6** exhibits four sets of equally intense multiplets corresponding to the four methylene protons (Fig. 1). The multiplets can be separated in two groups: the first one exhibits a doublet and doublet of doublets, having the same value for the coupling constant ( $^2J_{\text{H,H}} = ^4J_{\text{H,H}} = 13.2 \text{ Hz}$ ). The second group consist of a triplet and a doublet of triplets ( $^3J_{\text{H,H}} = ^4J_{\text{H,H}} = 12.4 \text{ Hz}$ ). The triplet structure is a result of an additional coupling with the NH proton. Due to the ring conformation, a large

## 2. Synthesis and Characterization of Amino Gallium Halides. Starting Materials for Gallylferrocene Derivatives

(13.2 Hz) and a small (12.4 Hz) coupling are observed. The further split is due to small  $^4J_{\text{H,H}}$ -couplings (12.4 Hz) between the ring protons. One doublet at  $\delta \text{ } ^1\text{H} = 1.96$  corresponds to the hydrogen atom from the NH group. Four singlets, observed at  $\delta \text{ } ^1\text{H} = 1.05, 0.89, 0.47$  and  $0.09$ , belongs to the methyl groups of the six-membered ring and of the trimethylsilyl substituents.

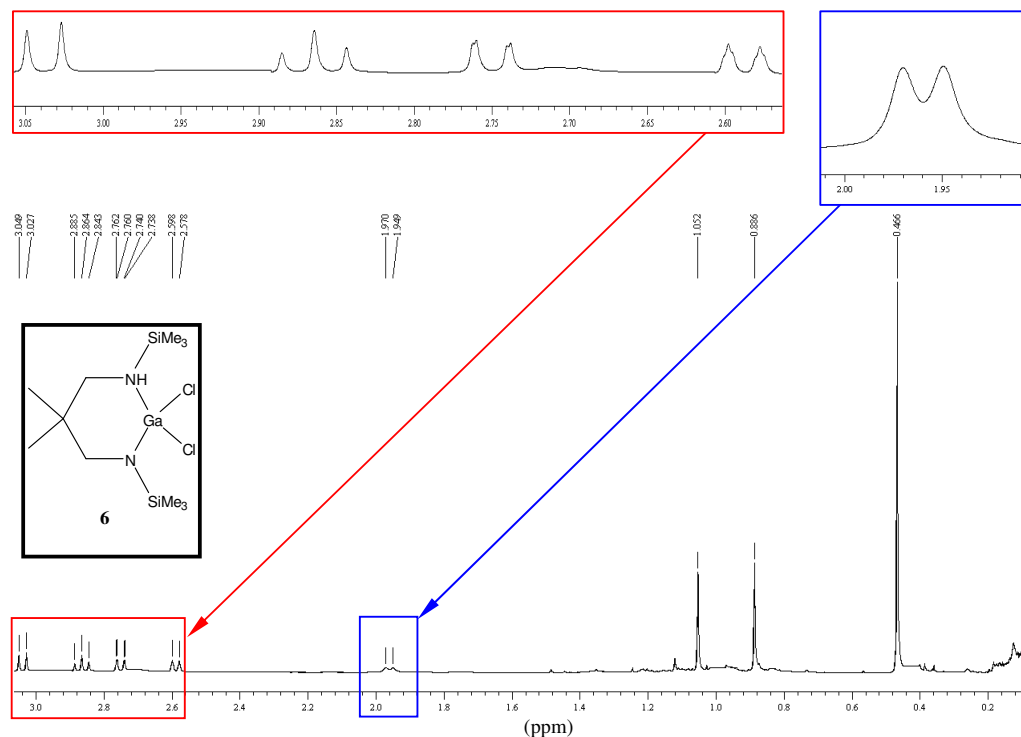


**Figure 1:**  $^1\text{H}$ -NMR spectrum of **6** in  $\text{CDCl}_3$ , at room temperature, with the inset showing an expanded view of the chemical shift range from 3.06 to 2.55 respectively from 2.00 to 1.94 ppm.

In the  $^{13}\text{C}$ -NMR spectrum (Fig. 2), two signals for the methylene carbon atoms ( $\delta \text{ } ^{13}\text{C} = 56.5$  and  $55.2$ ), two for methyl carbon atoms ( $\delta \text{ } ^{13}\text{C} = 26.7$  and  $21.6$ ) and two for trimethylsilyl substituents ( $\delta \text{ } ^{13}\text{C} = 0.8$  respectively  $-1.0$ ) are observed. One singlet at  $\delta \text{ } ^{13}\text{C} = 35.0$  appeared for the quaternary carbon atom. These spectra are in good agreement with the six-membered ring structure of **6**, which will be reported in the next chapter.

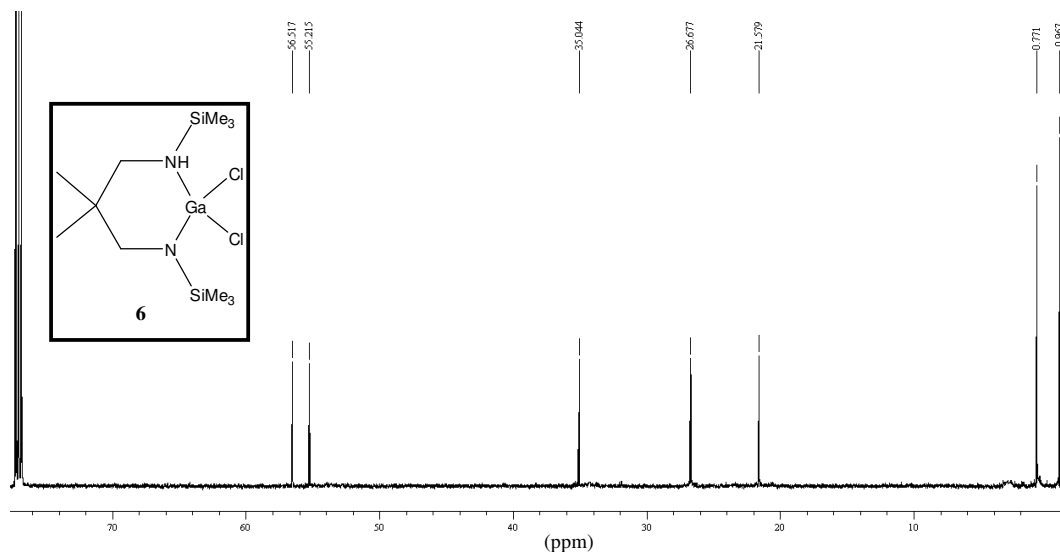


**Figure 2:**  $^{13}\text{C}$ -NMR spectrum of **6** in  $\text{CDCl}_3$ .

Similar spectra were observed and reported for  $\{[(\text{Me}_3\text{Si})\text{N}(\text{H})\text{CH}_2]\text{CMe}_2\{\text{CH}_2\text{N}(\text{SiMe}_3)\}\}\text{GaBr}_2$  **6a**.<sup>[8]</sup> The spectra of the monomeric **1**<sup>[11],[2],[4],[10]</sup> and the monomeric **2**<sup>[9]</sup> are in good agreement with those reported in the literature.

### 2.3.1. Mass Spectrometry

Under the conditions of an EI-MS spectrum, **6** is strongly broken up. The molecular ion of **6**<sup>+</sup> was not observed. The peak at highest mass ( $m/z = 281$ ) correspond to  $[\text{M}-7\text{CH}_3]^+$ . Other peaks are:  $m/z = 268$   $[\text{M} - \text{SiMe}_3 - 3\text{Me}]^+$ ,  $253$   $[\text{M} - \text{SiMe}_3 - 4\text{Me}]^+$ ,  $170$   $[\text{M} - 2\text{SiMe}_3 - \text{Me}_2\text{C}(\text{CH}_2)_2]^+$ . Two methyl units constitute the base peak ( $m/z = 30$ ).

## 2.4. Crystal Structure Analysis

### 2.4.1. Crystal Structure Analysis of **1**

**1**<sup>[11],[2],[4],[10]</sup> crystallizes in prisms of the monoclinic system, space group  $\text{P2}_1/\text{c}$ . A tricoordinated gallium atom is surrounded by two tmp and chlorine substituents (Fig. 3). The Ga-N bond lengths [ $d_{\text{Ga-N}} = 184.2$  pm (ave.)] are in a similar range observed for other compounds  $\text{tmp}_2\text{GaX}$  with electronegative X groups like OR,  $\text{NR}_2$ ,<sup>[4]</sup> but shorter than those for less electron withdrawing groups as:

## 2. Synthesis and Characterization of Amino Gallium Halides. Starting Materials for Gallylferrocene Derivatives

X = Ph [ $d_{\text{Ga-N}} = 188.3(2)$  pm (ave.)],  $\text{tmp}_2\text{Ga}$  [ $d_{\text{Ga-N}} = 190.1(4)$  pm (ave.)],<sup>[3]</sup>  $\text{P}^t\text{Bu}_2$  [ $d_{\text{Ga-N}} = 190.8$  pm (ave.)].<sup>[6]</sup>

A slight pyramidal environment can be observed for the nitrogen atoms, which are built up by two carbon atoms and a gallium atom (sum of bond angles  $354.55^\circ$ ). Other tmp derivatives of gallium reported in the literature show planar and pyramidal coordinated nitrogen atoms, as well, which can be explained by steric factors.

The tmp groups (represented by  $\text{N}_2\text{GaCl}$  mean planes) have angles of  $41^\circ$  and  $70^\circ$  to the  $\text{N}_2\text{GaCl}$  plane. Similar values are characteristic also for other  $\text{tmp}_2\text{GaX}$  derivatives. A wide bond angle ( $130.21(8)^\circ$ ) is observed for the N-Ga-N, which is in agreement with the steric demand of the tmp groups.

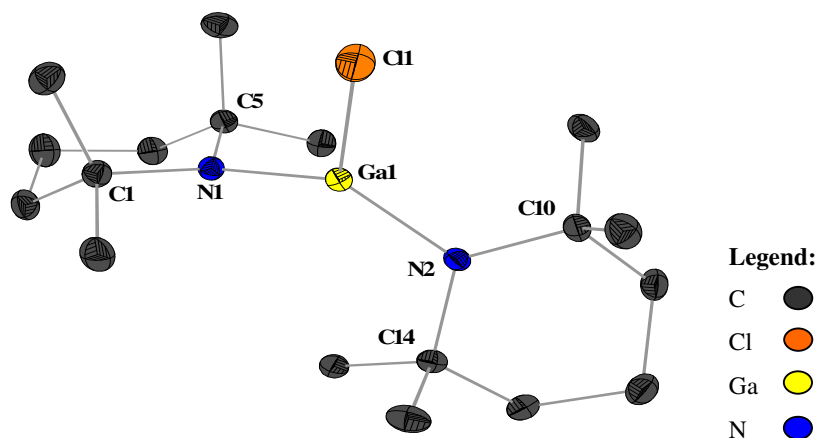


**Figure 3:** View of crystal structure of **1**. Hydrogen atoms have been omitted for more clarity. Selected bond lengths [pm] and angles [ $^\circ$ ]: Ga(1)-Cl(1) 219.9(1), Ga(1)-N(1) 184.5(2), Ga(1)-N(2) 184.0(2); N(1)-Ga(1)-N(2) 130.21(8), N(1)-Ga(1)-Cl(1) 111.78(6), N(2)-Ga(1)-Cl(1) 117.98(6), N(2)-Ga(1)-N(1) 130.21(8), N(2)-Ga(1)-Cl(1) 117.97(6), N(1)-Ga(1)-Cl(2) 111.78(6), C(5)-N(1)-C(1) 118.8(2), C(5)-N(1)-Ga(1) 116.9(1), C(1)-N(1)-Ga(1) 118.6(1), C(10)-N(2)-C(14) 119.6(2), C(10)-N(2)-Ga(1) 117.8(1), C(14)-N(2)-Ga(1) 117.5(1).

### 2.4.2. Crystal Structure Analysis of **6**

From a thf solution, **6** precipitated as colorless crystals at  $-32^\circ\text{C}$ . It crystallizes in the monoclinic system, space group  $\text{P}2_1/\text{n}$ . A twist conformation exhibits the six-membered

ring  $C_3GaN_2$ . The six-membered ring is composed by a gallium atom coordinated in a distorted tetrahedral fashion, an almost planar coordinated nitrogen atom ( $355.5^\circ$  at the triply coordinated nitrogen atom) and a distorted tetrahedral coordinated nitrogen atom (Fig. 4 A). The Ga-N bond lengths are different (184.9 and 199.9 pm) due to the different coordination spheres at the nitrogen atoms. This causes two different Si-N bond lengths [ $d_{Si(1)-N(1)} = 170.7$  pm and  $d_{Si(2)-N(2)} = 182.2$  pm], too. The Ga-N bond lengths vary from approximately 181<sup>[4],[9],[11]</sup> to 209 pm<sup>[8],[12],[13]</sup> in amino compounds of gallium, depending on the coordination number at the gallium and nitrogen atoms.<sup>[14]</sup> For example in  $[(Me_2N)_2Ga(\mu-NMe_2)_2Ga(NMe_2)_2]$ ,<sup>[13]</sup> the bridging Ga-N bonds (200.5(2) and 202.1(3) pm) are longer than the terminal ones (184.9(4) and 186.1(4) pm). The adduct  $[Me_3GaNH_2^tBu]$ <sup>[15]</sup> has relatively long Ga-N distance (212.0(1) pm). Compared to this, the dative Ga-N bond in **6** is quite short. In the homologous bromo derivative  $\{[(Me_3Si)N(H)CH_2]CMe_2\{CH_2N(SiMe_3)\}\}GaBr_2$  **6a**<sup>[8]</sup> this bond is longer (204.0(1) pm). This difference can be explained by the effect of the more electronegative chloro substituents compared to the bromo atoms in **6a** or methyl groups in  $[Me_3GaNH_2^tBu]$ . In the dimeric  $\{[(Me_3Si)NCH_2]_2CMe_2\}GaCl_2$  **XIX**<sup>[8]</sup> two different Ga-N moiety types can be distinguished, the first one is bridging (205.6(2) pm) and longer than the others Ga-N bonds that are involved in the six-membered ring  $C_3GaN_2$  (184.3(2) and 199.3(2) pm). These are in line with those exhibits by **6**. There are also other related amino-amide gallane complexes, which shows similar values for the Ga-N bond lengths with that in **6** as:  $\{[(Me_3Si)NCH_2]_2CMe_2\}_2Ga[LiOEt_2]^+[8]$  (188.1(6) to 198.9(5) pm),  $\{[(Me_3Si)NCH_2]_2CMe_2\}_2Ga_2$ <sup>[16]</sup> (182.9(3) and 183.4(3) pm) and  $\{[(Me_3Si)_2N](H)Ga\{N(H)CH_2CMe_2CH_2NMe_2\}\}_2$ <sup>[17]</sup> (189.3(2) to 201.1(2) pm).

The two C-N bond lengths have similar values of about 150 pm, meaning that the bond length is not effected by the coordination number at the nitrogen atoms. The steric contact is minimized through a *staggered* arrangement of the atoms involved in the crystal structure of **6** (Fig. 4 A and B). Three of the bond angles at the gallium atom deviate from the tetrahedral angle. One is sharp (N(1)-Ga(1)-N(2)) with the bond angle of  $99.4^\circ$  and the other two are wide (N(1)-Ga(1)-Cl(1) and N(1)-Ga(1)-Cl(2)) with an average of the bond angles of about  $116^\circ$ . The Ga-Cl bond lengths [ $d_{Ga-Cl} = 216.4(4)$  pm and  $219.6(4)$  pm] are typical for monomeric gallium chloro compounds reported in literature.

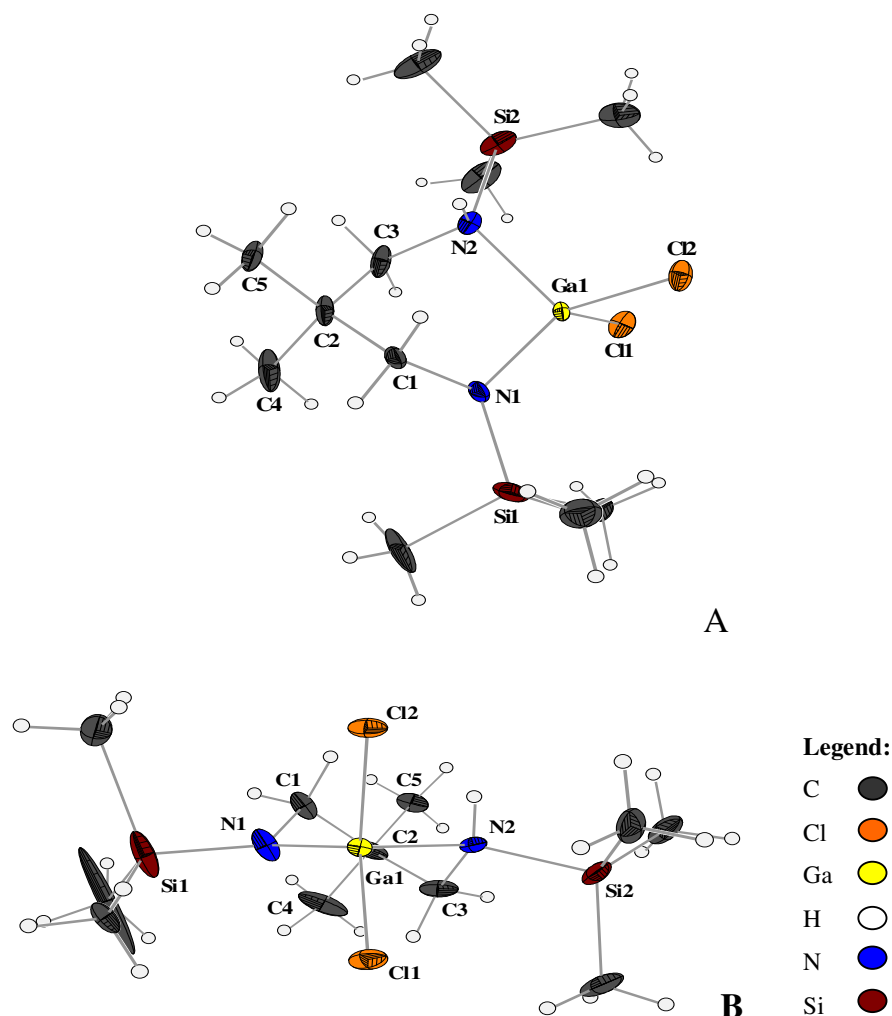


**Figure 4:** View of crystal structure of **3**. (A – molecule top view, B – down the axis Ga(1)-C(2) view). Selected bond lengths [pm] and angles [°]: Ga(1)-N(1) 184.9(3), Ga(1)-N(2) 199.9(7), Ga(1)-Cl(1) 216.4(4), Ga(1)-Cl(2) 219.6(4), N(1)-Si(1) 170.7(4), N(2)-Si(2) 182.2(3); N(1)-Ga(1)-N(2) 99.4(9), Cl(1)-Ga(1)-Cl(2) 107.5(5), Cl(1)-Ga(1)-N(1) 118.6(6), Cl(1)-Ga(1)-N(2) 110.3(7), Cl(2)-Ga(1)-N(1) 113.9(8), Cl(2)-Ga(1)-N(2) 106.3(7), Ga(1)-N(1)-C(1) 109.5(8), Ga(1)-N(2)-C(3) 104.4(9), Ga(1)-N(1)-Si(1) 124.2(10), C(1)-N(2)-Si(2) 121.1(10).

### 2.4.3. Crystal Structure Analysis of **7**

**7** crystallized as side product from the synthesis of **6** in a solution of thf/diox (10:1) at -32 °C (Fig. 5 A and B). It crystallizes in monoclinic system, space group P2<sub>1</sub>/c. One anionic and one cationic part constitute the solid state structure of **7**. The anionic part of the crystal structure is built up by a tetrahedral gallium atom surrounded by four chlorine atoms. A lithium atom surrounded by two thf together with two molecules of



dioxane, also in a tetrahedral environment, affords the counter ion (cationic part) as a polymeric chain (Fig. 5 B). Three Ga-Cl bond lengths are equivalent [ $d_{\text{Ga-Cl}} = 215.2 \text{ pm}$ ] and the axial Ga-Cl bond is a little bit longer [ $d_{\text{Ga-Cl}} = 219.6 \text{ pm}$ ], but all the Ga-Cl bond lengths are in the range of other reported gallium chloride compounds. The Li-O bond lengths are between 187.5 and 197.5 ppm indicates a distorted tetrahedral conformation at the Li atom. The Cl-Ga-Cl bond angles are wider (between  $108.6^\circ$  and  $110.3^\circ$ ) than the tetrahedral angle. The same situation is exhibit also by the O-Li-O angles (average  $109.4^\circ$ ).

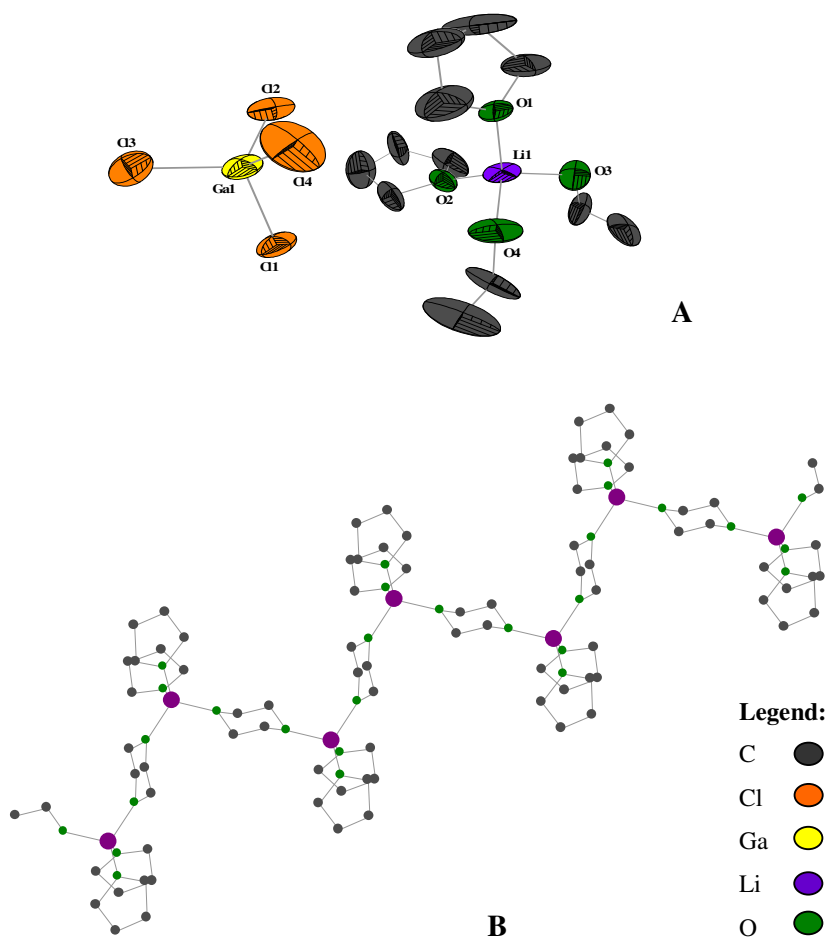


**Figure 5:** View of a molecule of **7** in solid state (**A** – asymmetric unit showing the anionic part and the fragment of the cationic part, **B** – the polymeric chain of the cationic part). Hydrogen atoms have been omitted for clarity. Selected bond lengths [pm] and angles [ $^\circ$ ]: Ga(1)-Cl(1) 215.2(4), Ga(1)-Cl(2) 219.6(6), Ga(1)-Cl(3) 215.2(6), Ga(1)-Cl(4) 215.2(3), Li(1)-O(1) 188.7(4), Li(1)-O(2) 197.5(3), Li(1)-O(3) 193.9(5), Li(1)-O(4) 187.5(5); Cl(1)-Ga(1)-Cl(2) 108.8(6), Cl(1)-Ga(1)-Cl(3) 109.3(7), Cl(1)-Ga(1)-Cl(4) 108.6(7), Cl(2)-Ga(1)-Cl(3) 109.8(7), Cl(2)-Ga(1)-Cl(4) 110.3(6), Cl(3)-Ga(1)-Cl(4) 109.8(6), O(1)-Li(1)-O(2) 115.2(8), O(1)-Li(1)-O(3) 110.7(8), O(1)-Li(1)-O(4) 108.6(8), O(2)-Li(1)-O(3) 107.5(7), O(2)-Li(1)-O(4) 105.8(7), O(3)-Li(1)-O(4) 108.8(7).

## 2.5. Summary of Important Bond Lengths

The Ga-Cl bond lengths in **1** [ $d_{\text{Ga-Cl}} = 219.9(1)$  pm] and respectively in **6** [ $d_{\text{Ga-Cl}} = 216.4(4)$  pm and  $219.6(4)$  pm] are consistent with the terminal Ga-Cl bond lengths in other monomeric compounds.<sup>[18],[8]</sup> Similar Ga-Cl bond lengths are observed in the side product **7** [ $d_{\text{Ga-Cl}} = 215.2$  pm and  $219.6$  pm] which are in agreement with the expected range for a Ga-Cl bond length.

All Ga-Cl and Ga-N bond lengths determined in **1**, **6** and **7** are summarized in Table 1.

**Table 1:** Summary of Ga-Cl and Ga-N bond lengths.

Compound	$d_{\text{Ga-Cl}}$ [pm]	$d_{\text{Ga-N}}$ [pm]
<b>1</b>	219.9(1)	184.5(2) and 184.0(2) 184.2 (ave.)
<b>6</b>	216.4(4) and 219.6(4) 218.0 (ave.)	184.9(3) and 199.9(7) 192.4 (ave.)
<b>7</b>	215.2(4), 215.2(6), 215.2(3) and 219.6(6) 216.3 (ave.)	-

## References

- [1] R. Frey, *Diploma Thesis*, München, **1993**.
- [2] R. Frey, G. Linti, and K. Polborn, *Chem. Ber.*, **1994**, *127*, 101-103.
- [3] G. Linti, R. Frey, and M. Schmidt, *Z. Naturforsch. Teil B*, **1994**, *49b*, 958-962.
- [4] G. Linti, R. Frey, and K. Polborn, *Chem. Ber.*, **1994**, *127*, 1387-1393.
- [5] R. Frey, *PhD Thesis*, München, **1996**.
- [6] G. Linti, R. Frey, W. Köstler, and H. Schwenk, *Chem. Ber.*, **1997**, *130*, 663-668.
- [7] H. Mack, *PhD Thesis*, München, **1995**.
- [8] G. Linti, H. Nöth, K. Polborn, C. Robl, and M. Schmidt, *Chem. Ber.*, **1995**, *128*, 487-492.
- [9] P. J. Brothers, R. J. Wehmschulte, M. M. Olmstead, K. Ruhlandt-Senge, S. R. Parkin, and P. P. Power, *Organometallics*, **1994**, *13*, 2792-2799.
- [10] O. Feier-Iova, and G. Linti, *Z. Anorg. Allg. Chem.*, **2008**, *634*, 559-564.
- [11] D. A. Atwood, V.O. Atwood, A. H. Cowley, R. A. Jones, J. L. Atwood, and S. G. Bott, *Inorg. Chem.*, **1994**, *33*, 3251-3254.
- [12] M. Niemeyer, T. J. Goodwin, S. H. Risbud, and P. P. Power, *Chem. Mater.*, **1996**, *8*, 2745-2750.
- [13] K. M. Waggoner, M. M. Olmstead, and P. P. Power, *Polyhedron*, **1990**, *9*, 257-263.
- [14] C. J. Carmalt, *Coord. Chem. Rev.*, **2001**, *223*, 217-264.
- [15] D. A. Atwood, R. A. Jones, and A. H. Cowley, *J. Organomet. Chem.*, **1992**, *434*, 143-150.
- [16] G. Linti, W. Köstler and A. Rodig, *Z. Anorg. Allg. Chem.*, **2002**, *628*, 1319-1326.
- [17] B. Luo, M. Pink, and W. L. Gladfelter, *Inorg. Chem.*, **2001**, *40*, 307-311.
- [18] O. T. Jr. Beachley, J. R. Gardinier, M. R. Churchill, D. G. Churchill, and K. M. Keil, *Organometallics*, **2002**, *21*, 946-951.



### 3. Reaction of Bis(amino)gallium Chloride with Mono- and Dilithioferrocene

#### 3.1. Introduction

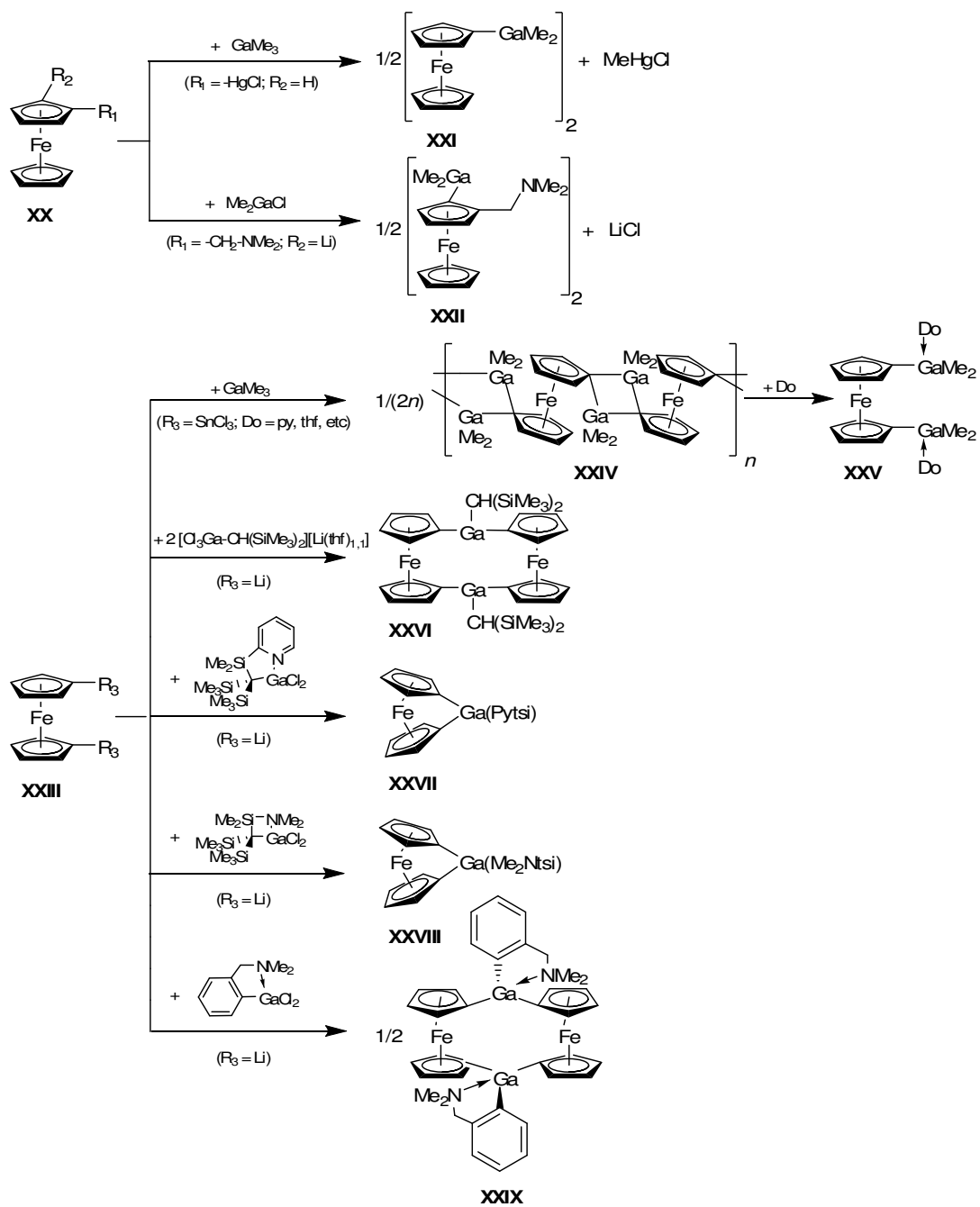
The studies concerning ferrocenylgallanes<sup>[1]-[4]</sup> (structure and bonding) were until the 1990s almost insignificant, notwithstanding the development of the ferrocenyl-based transition metal complexes, which are one of the most investigated species of organotransition-metal chemistry.<sup>[5]</sup> However, seeing the potential utility of organogallium compounds as precursors to semiconductor materials, a new trend started slowly to get outline.

The first example of a ferrocenylgallane dimer reported by G. H. Robinson *et al.* in 1990,<sup>[6]</sup> has been synthesized by reaction of (chloromercurio)ferrocene with trimethylgallium. Since then, several synthesis routes for the mono-, or digallyl substituted ferrocenes and gallaferrocenophanes were reported in the literature (see Scheme 6).

The monogallyl substituted ferrocenes **XXI**<sup>[6]</sup> and **XXII**<sup>[7]</sup> appeared as dimers. From the reaction of disubstituted ferrocene with different alyl- or aryl gallium derivatives, several digallyl substituted ferrocenes (**XXIV** and **XXV**<sup>[8]</sup>) and gallaferrocenophanes (**XXVI**,<sup>[9]</sup> **XXVII**,<sup>[10]</sup> **XXVIII**<sup>[11]</sup> and **XIV**<sup>[12]</sup>) were synthesized.

### 3. Reaction of Bis(amino)gallium Chloride with Mono- and Dilithioferrocene

**Scheme 6:** Mono- or digallyl substituted ferrocenes and gallaferrocenophanes synthesis.

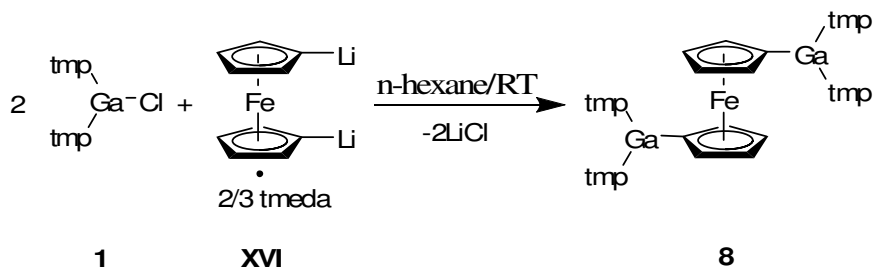


As follows, the reactions of mono- and dilithio ferrocene with **1**<sup>[13]-[16]</sup> and respectively with **2**<sup>[17]</sup> were investigated, giving rise to several new mono-, or digallyl substituted ferrocenes and a gallaferrocenophane, which were further characterized by means of NMR spectroscopy, mass spectrometry, cyclovoltammetry and X-ray structure analyses.

### 3.2. Synthesis Routes

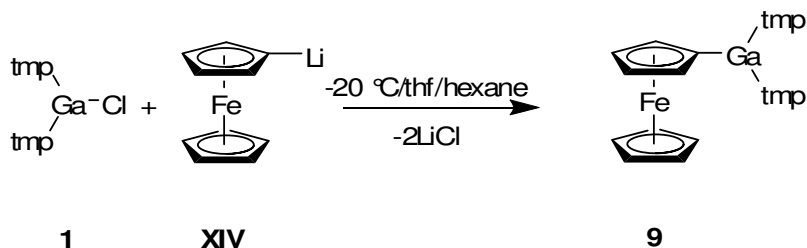
When bis(tmp)gallium chloride **1** is treated with a solution of  $[\text{Li}_2\{\text{Fe}(\eta^5\text{-C}_5\text{H}_4)_2\} \cdot 2/3 \text{ TMEDA}]$  **XVI**<sup>[18]</sup> in hexane (Eq. 3), the digallyl substituted ferrocene  $[\{\text{Fe}(\eta^5\text{-C}_5\text{H}_4)_2\}\{\text{Ga}(\text{tmp})_2\}_2]$  **8** as orange-red crystals is obtained, in good yield. The reaction completed at room temperature in approximately 18 hours, with the formation of a white precipitate of LiCl.

Equation 3:



A similar substitution reaction at one cyclopentadienyl ring (Eq. 4) took place by treating of **1** with a solution of  $[\text{Li}\{(\eta^5\text{-C}_5\text{H}_4)\text{Fe}(\eta^5\text{-C}_5\text{H}_5)\}]$  (*in situ*) **XIV**<sup>[19],[20]</sup> in thf at -20 °C. Here, a mixture of monogallyl substituted ferrocene **9**, digallyl substituted ferrocene **8** and not reacted ferrocene was obtained. The monogallyl substituted ferrocene **9** was isolated as red-orange crystals in good yield.

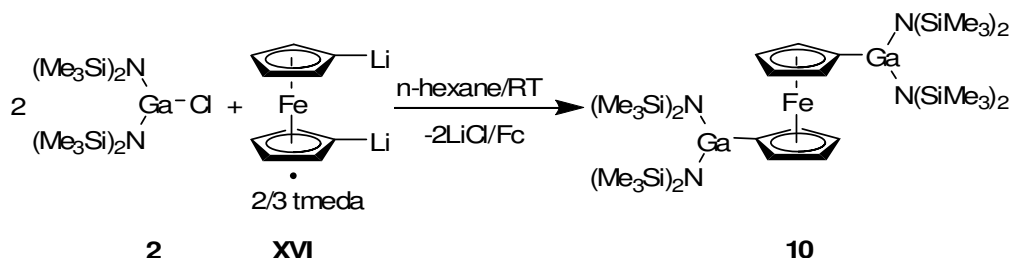
Equation 4:



### 3. Reaction of Bis(amino)gallium Chloride with Mono- and Dilithioferrocene

By treating of **2**<sup>[17]</sup> with a solution of **XVI**<sup>[18]</sup> in hexane (Eq. 5), the bisgallyl-substituted ferrocene **10** was obtained in low yield. **10** appeared as a red-brownish solid.

Equation 5:



The monogallylsubstituted ferrocene **11** was obtained by the reaction of monolithioferrocene **XIV** obtained *in situ* with a stoichiometric quantity of **2**. Here, **11** was isolated in low yield and characterized only by means of <sup>1</sup>H-NMR and <sup>13</sup>C-NMR spectroscopy (Eq. 6).

Equation 6:



### 3.3. Spectroscopic Characterization

#### 3.3.1. <sup>1</sup>H- and <sup>13</sup>C-NMR Spectroscopy

The bisgallyl-substituted ferrocene **8** shows in its <sup>1</sup>H-NMR spectrum two pseudo-triplets of an AA'BB'-system with a 1:2:1 intensity ratio at  $\delta^1\text{H} = 4.62$  and 4.53. These signals correspond to the hydrogen atoms from the substituted cyclopentadienyl rings. The coupling constants <sup>3</sup>J<sub>H,H</sub> and <sup>4</sup>J<sub>H,H</sub> have the same value of 1.6 Hz. A single signal set was recorded for the tmp groups that prove for the free rotation about the Ga-N bonds. One centered multiplet ( $\delta^1\text{H} = 1.77$ ) corresponding to the hydrogen atoms from the  $\gamma$  position was observed and also one singlet ( $\delta^1\text{H} = 1.57$ ) and one pseudo triplet



( $\delta^1\text{H} = 1.51$ ) corresponding to the hydrogen atoms from the terminal methyl groups and to the  $\beta$  hydrogen atoms from the methylene groups of tmp rests (Fig. 6), respectively.

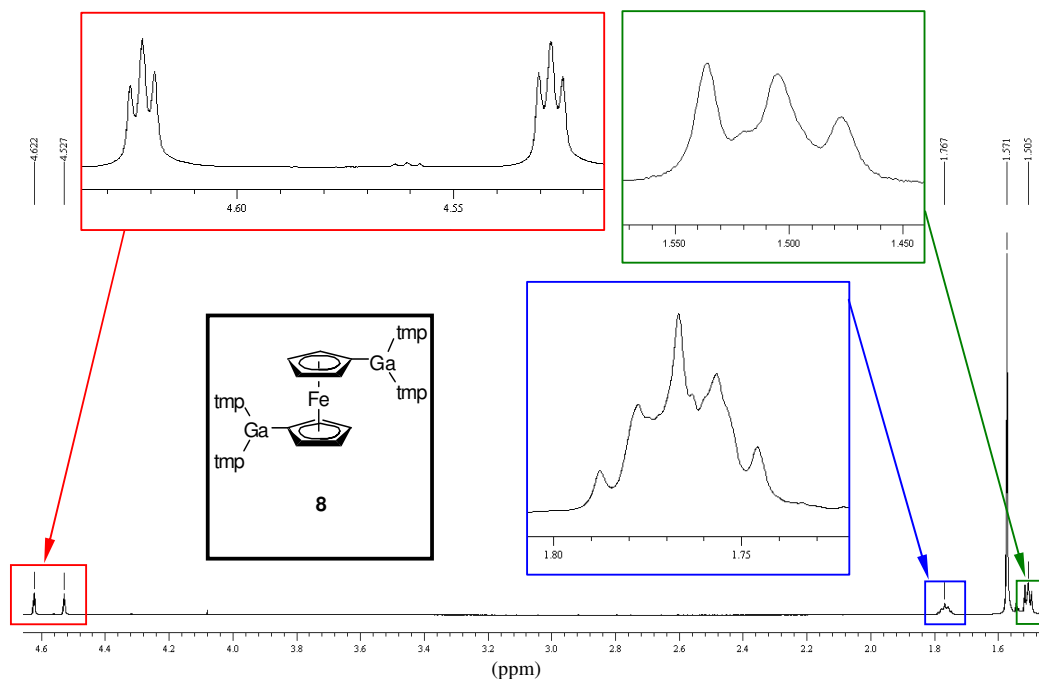


**Figure 6:**  $^1\text{H}$ -NMR spectrum of **8** in  $\text{C}_6\text{D}_6$ , at room temperature, with the inset showing an expanded view of the chemical shift range from 4.65 to 4.50, from 1.57 to 1.45 and from 1.80 to 1.73 ppm.

Three signals are observed for the Cp-rings in the  $^{13}\text{C}$ -NMR spectrum (Fig. 7). The signals for the carbon atoms of the cyclopentadienyl rings are shifted low field ( $\delta^{13}\text{C} = 77.9$  and  $71.9$ ) compared to ferrocene ( $\delta^{13}\text{C} = 68$ ).<sup>[21]</sup> The *ipso*-carbon atoms resonance's appeared at  $\delta^{13}\text{C} = 80.4$ . For the *ipso*-carbon atoms in 1,1'-dimethylgallylferrocene ( $\delta^{13}\text{C} = 76.2$ )<sup>[22]</sup> a less strong low field shift was observed. The chemical shifts for the tmp groups in **8** are in the typical region observed for other  $\text{tmp}_2\text{Ga}$  derivatives.<sup>[15]</sup> Especially, the chemical shift for the carbon atoms bonded to the nitrogen atoms ( $\delta^{13}\text{C} = 54.2$ ) are typical. For the  $\text{tmp}_2\text{GaPh}$ ,<sup>[15]</sup> the chemical shift for the carbon atoms bonded to the nitrogen atoms was reported at the same value as for **8**.

### 3. Reaction of Bis(amino)gallium Chloride with Mono- and Dilithioferrocene

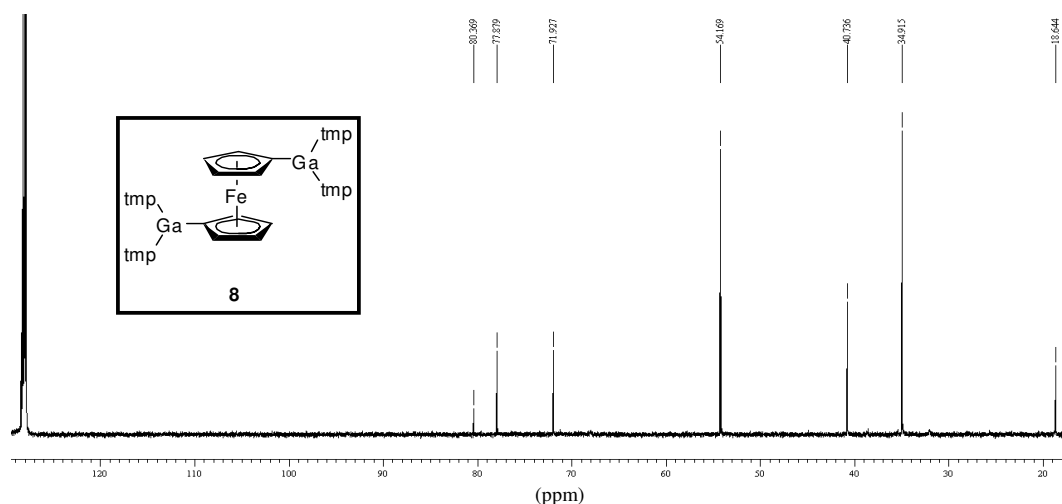


**Figure 7:**  $^{13}\text{C}$ -NMR spectrum of **8** in  $\text{C}_6\text{D}_6$ .

In the  $^1\text{H}$ -NMR spectrum of monogallyl-substituted ferrocene **9** a singlet ( $\delta^1\text{H} = 4.07$ ) for unsubstituted Cp-ring, two pseudo-triplets for the substituted Cp-ring ( $\delta^1\text{H} = 4.55$  and 4.31) are observed. These are shifted to lower frequencies compared to **8**. The coupling constants have the same value as in **8** ( $^3J_{\text{H,H}} = ^4J_{\text{H,H}} = 1.6$  Hz). One single set of signals is recorded for the both tmp terminal groups (Fig. 8). That is in good agreement with the values reported in the literature.<sup>[15]</sup>

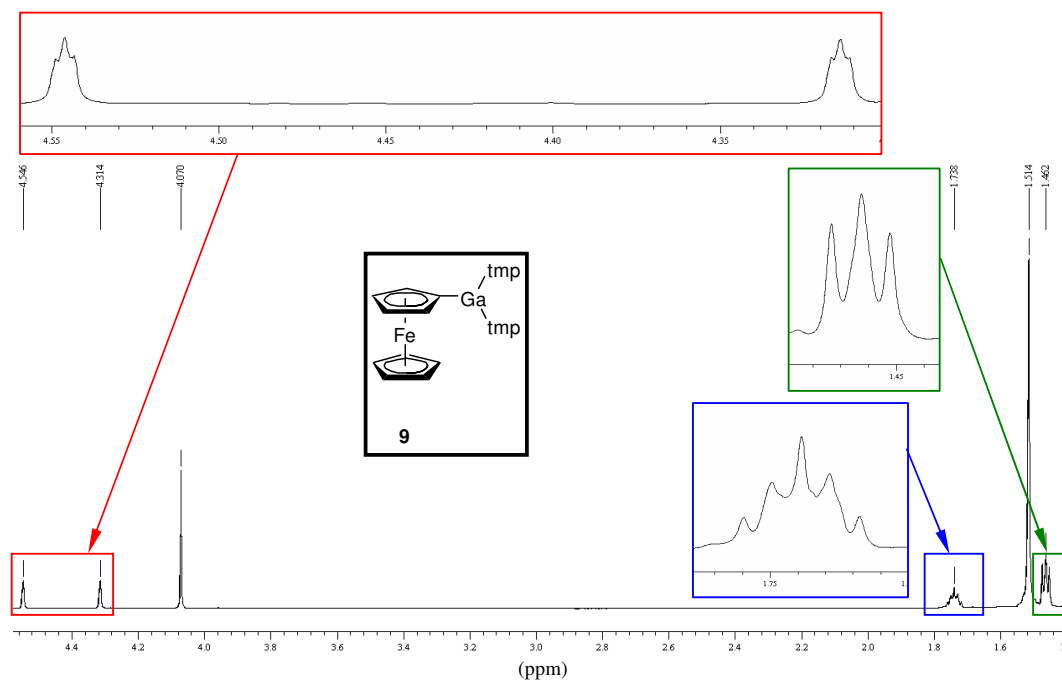


**Figure 8:**  $^1\text{H}$ -NMR spectrum of **9** in  $\text{C}_6\text{D}_6$ , at room temperature, with the inset showing an expanded view of the chemical shift range from 4.56 to 4.30, from 1.77 to 1.70 and respectively from 1.49 to 1.44 ppm.

In the  $^{13}\text{C}$ -NMR spectrum of **9** (Fig. 9) three signals for the substituted Cp-ring and one signal for the unsubstituted Cp-ring are observed. The *ipso*-carbon resonated at  $\delta^{13}\text{C} = 81.0$ , which is a similar value as for the *ipso*-carbon atoms signals in the bisgallyl-substituted ferrocene **8**. As expected, the tmp groups in **9** give rise only to one set of signals as an effect of the free rotation of tmp groups about the Ga-N bond.

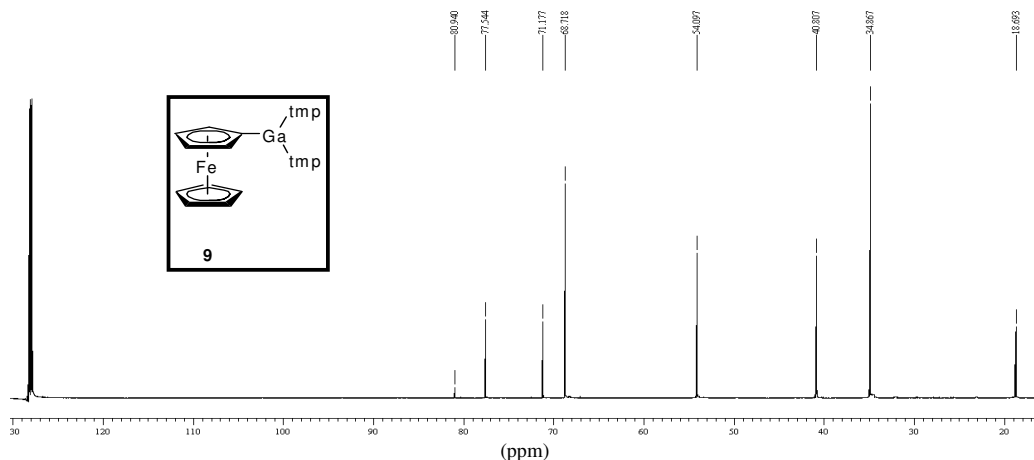


**Figure 9:**  $^{13}\text{C}$ -NMR spectrum of **9** in  $\text{C}_6\text{D}_6$ .

Two pseudo-triplets ( $\delta^1\text{H} = 4.61$  and  $4.41$ ) corresponding to the hydrogen atoms from the cyclopentadienyl rings, are observed in the  $^1\text{H}$ -NMR spectrum of bisgallyl-substituted ferrocene **10**. The coupling constant has the same value as in **8** and **9** ( $^3J_{\text{H,H}} = ^4J_{\text{H,H}} = 1.6$  Hz). A single signal is recorded for the methyl groups ( $\delta^1\text{H} = 0.40$ ) (see Fig. 10).

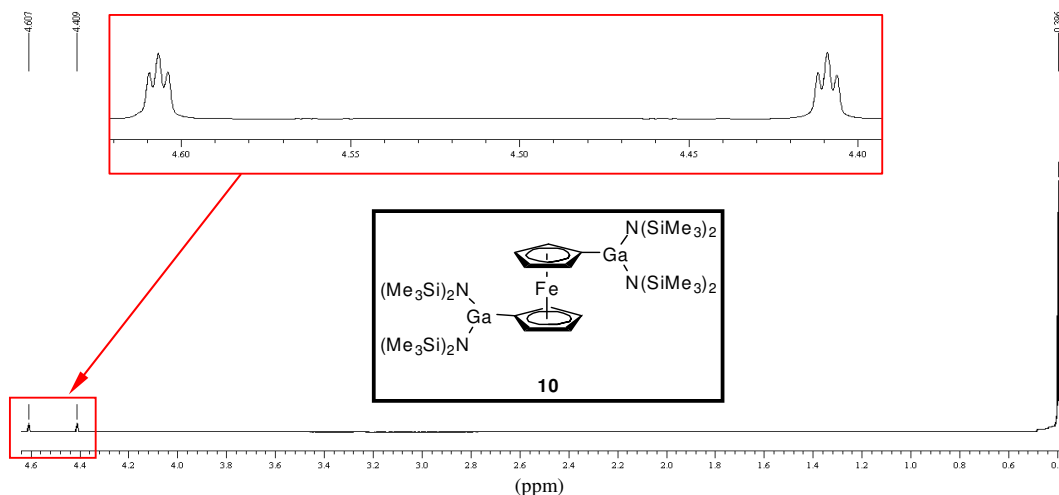


**Figure 10:**  $^1\text{H}$ -NMR spectrum of **10** in  $\text{C}_6\text{D}_6$ , at room temperature, with the inset showing an expanded view of the chemical shift range from 4.62 to 4.40 ppm.

### 3. Reaction of Bis(amino)gallium Chloride with Mono- and Dilithioferrocene

The  $^{13}\text{C}$ -NMR spectrum of **10** (Fig. 11) shows the expected signals for the substituted cyclopentadienyl rings resonating at  $\delta^{13}\text{C} = 77.4$  and  $72.0$ . One signal for the carbon atoms from the methyl rests ( $\delta^{13}\text{C} = 6.1$ ) was observed. The signal corresponding to the *ipso*-carbons could not be observed.

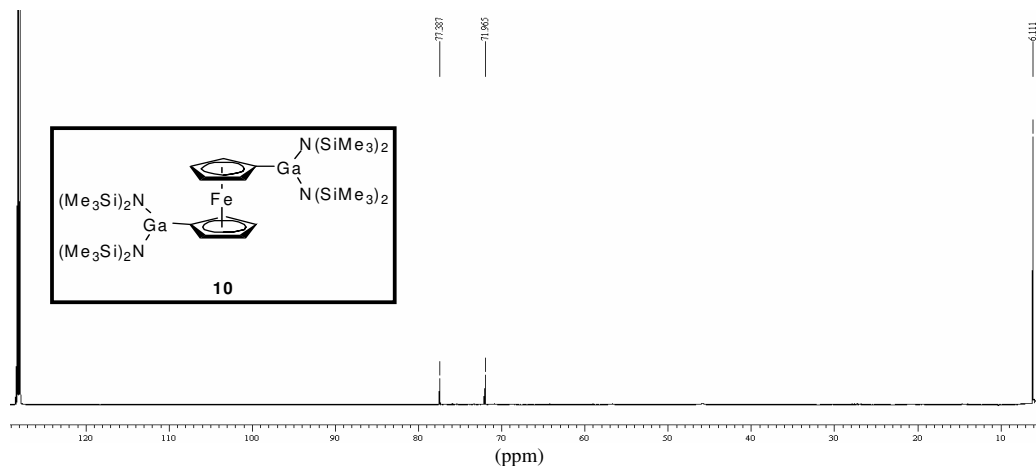


**Figure 11:**  $^{13}\text{C}$ -NMR spectrum of **10** in  $\text{C}_6\text{D}_6$ .

The  $^1\text{H}$ -NMR and  $^{13}\text{C}$ -NMR spectra for the monogallyl-substituted ferrocene **11** were also recorded (Fig. 12 and Fig. 13). In the proton spectrum two sets of signals corresponding to the substituted respectively unsubstituted cyclopentadienyl rings were observed ( $\delta^1\text{H} = 4.31$  and  $4.27$  - pseudo-triplets,  $^3J_{\text{H,H}} = ^4J_{\text{H,H}} = 1.6$  Hz for the substituted Cp-ring and one singlet at  $4.11$  for the unsubstituted Cp-ring). The two pseudo-triplets are less separated. The methyl rests give rise to one singlet ( $\delta^1\text{H} = 0.51$ ).

The  $^{13}\text{C}$ -NMR spectrum exhibits the expected signals for the carbon atoms, with the exception that, again, the signal for the *ipso*-carbon could not be observed ( $\delta^{13}\text{C} = 76.7$  -subst. Cp- $\text{C}^3/\text{C}^4$  or Cp- $\text{C}^2/\text{C}^5$ ,  $71.8$  - subst. Cp- $\text{C}^3/\text{C}^4$  or Cp- $\text{C}^2/\text{C}^5$ ,  $68.9$  - unsubst. Cp,  $6.3$  -  $\text{CH}_3$ ).

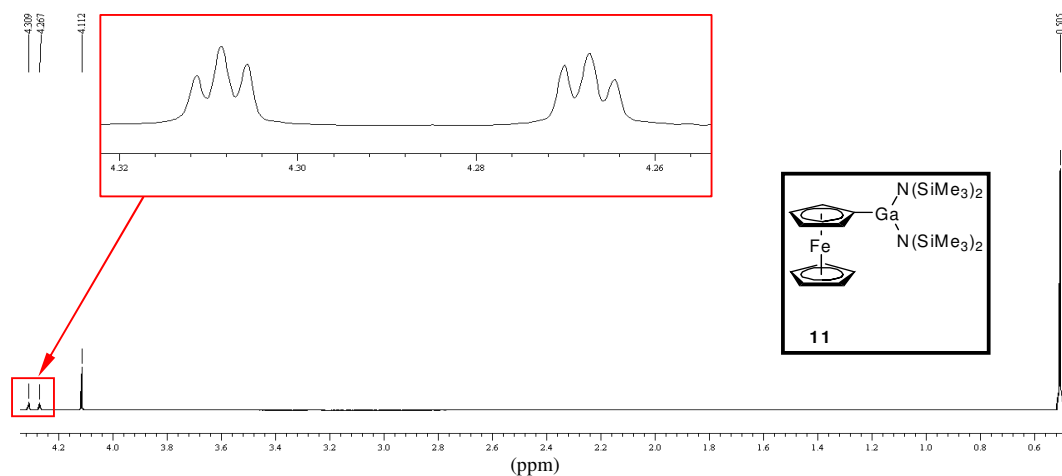


**Figure 12:**  $^1\text{H}$ -NMR spectrum of **11** in  $\text{C}_6\text{D}_6$ , at room temperature, with the inset showing an expanded view of the chemical shift range from 4.32 to 4.26 ppm.

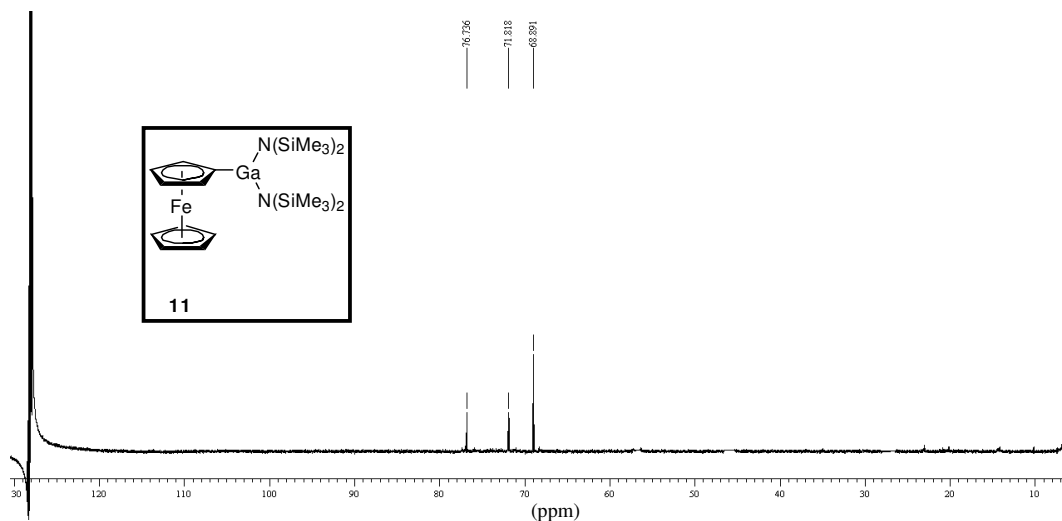


**Figure 13:**  $^{13}\text{C}$ -NMR spectrum of **11** in  $\text{C}_6\text{D}_6$ .

### 3.4. Cyclo Voltammetric Determinations

The electrochemical properties of **8** and **9** were investigated *via* cyclic voltammetry. The cyclic voltammograms were recorded in thf solution with  $\text{NBu}_4\text{PF}_6$  as supporting electrolyte and decamethylcobaltocene/decamethylcobaltocenium as internal reference (see Fig. 14). Reversible oxidation potentials were observed for both compounds at  $E_{1/2} = -199$  mV (**8**) and  $E_{1/2} = 23$  mV (**9**) (*vs.* ferrocene/ferrocenium) with peak separations of 218 mV (**8**) and 241 mV (**9**).

### 3. Reaction of Bis(amino)gallium Chloride with Mono- and Dilithioferrocene

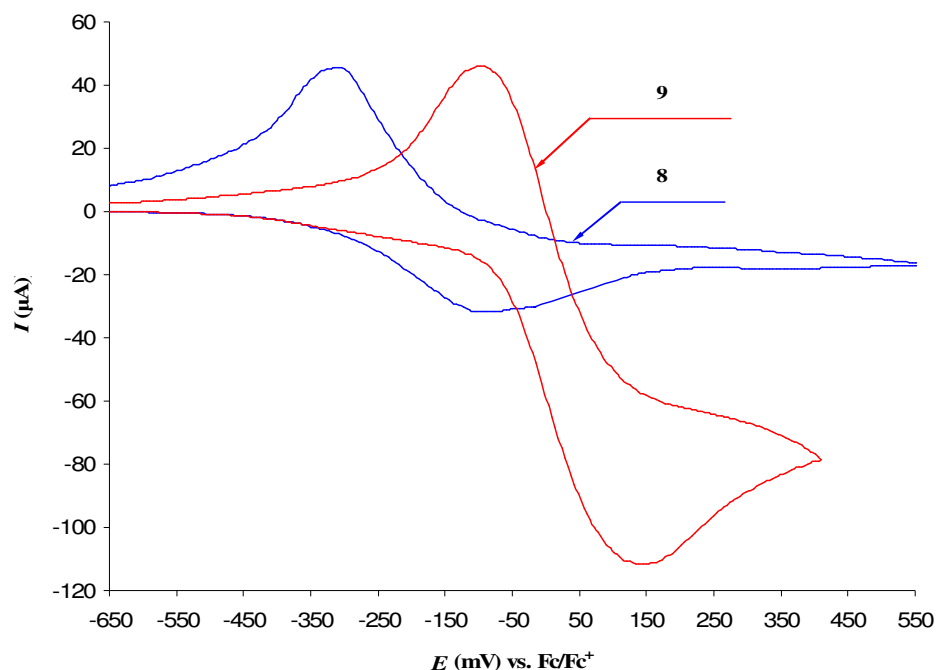


**Figure 14:** Cyclic voltammograms of **8** and **9** versus  $\text{Fc}/\text{Fc}^+$  in thf, internal standard  $\text{CoCp}_2^*/\text{CoCp}_2^{*+}$

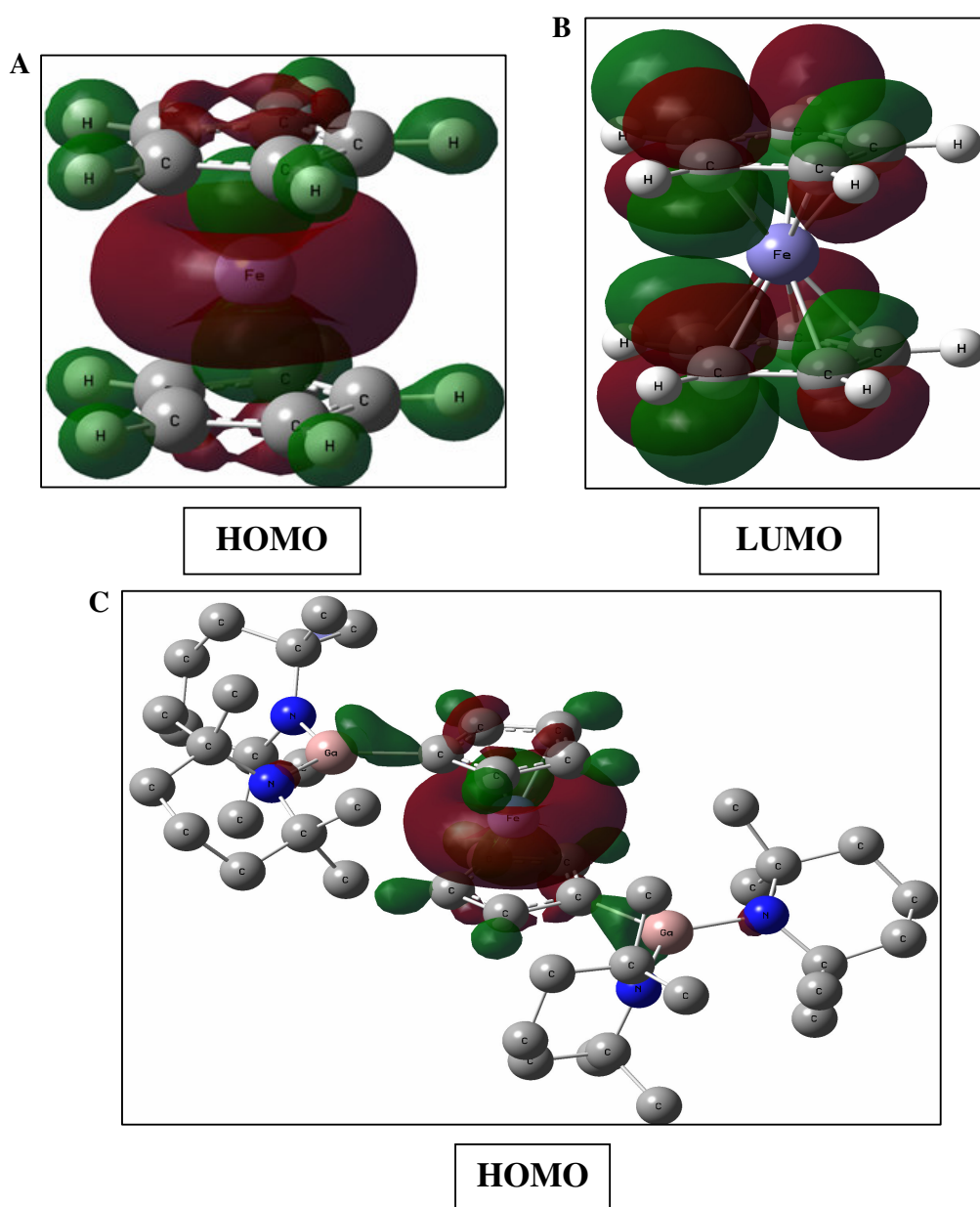
The oxidation waves of **8** are shifted to a high oxidation potential in comparison with other reported gallyl substituted ferrocenes. For example  $[\{\text{Fe}(\eta^5\text{-C}_5\text{H}_4)_2\}\{\text{GaMe}_2\}_2]_n^{[22]}$  shows a lower oxidation potential [ $E_{1/2} = -370$  mV, in pyridine] and  $[\{\text{Fe}(\eta^5\text{-C}_5\text{H}_4)_2\}_2\{\text{GaMe}(\text{Py})\}_2]^{[23]}$  exhibits two oxidation potentials [ $E_{1/2} = -314$  mV and  $E_{1/2} = -114$  mV, in pyridine]. This indicates that the bisgallyl substituted ferrocene **8** is more easily oxidized than ferrocene, but more difficult oxidized than the other gallyl substituted ferrocenes. This can be explained by the electron withdrawing substituents at the gallium atoms. The  $\text{tmp}_2\text{Ga}$  groups are less able to donate electrons into the ring than the substituents with tetra coordinated gallium atoms.

On the other hand, the monogallyl substituted ferrocene **9** exhibits the highest oxidation potential from all gallyl substituted ferrocenes, reported in this thesis. The shift of the oxidation wave to a higher oxidation potential in comparison with the oxidation wave of ferrocene/ferrocenium was observed. Thus, the electron donating ability decreases in the order  $[\{\text{Fe}(\eta^5\text{-C}_5\text{H}_4)_2\}\{\text{GaMe}_2\}_2]_n^{[22]} < [\{\text{Fe}(\eta^5\text{-C}_5\text{H}_4)_2\}_2\{\text{GaMe}(\text{Py})\}_2]^{[23]} < \mathbf{8} < [\text{Fe}(\eta^5\text{-C}_5\text{H}_5)_2] < \mathbf{9}$ . For a more detailed discussion see Chapter 4.2.3.

## 3.5. Quantum Chemical Calculations

Quantum chemical calculations were carried out for **8**, **9** and ferrocene at the B3LYP/6-311G(d) level of theory. For single point quantum chemical calculations the crystal coordinates of **8** and **9** have been used.

These calculations show a larger  $\pi$ -electron delocalization from the ferrocenyl unit to the Ga atom in **9** than that in **8**. This can also be seen, by comparing the HOMO and LUMO of **8** and **9** with that of ferrocene (Fig. 15).



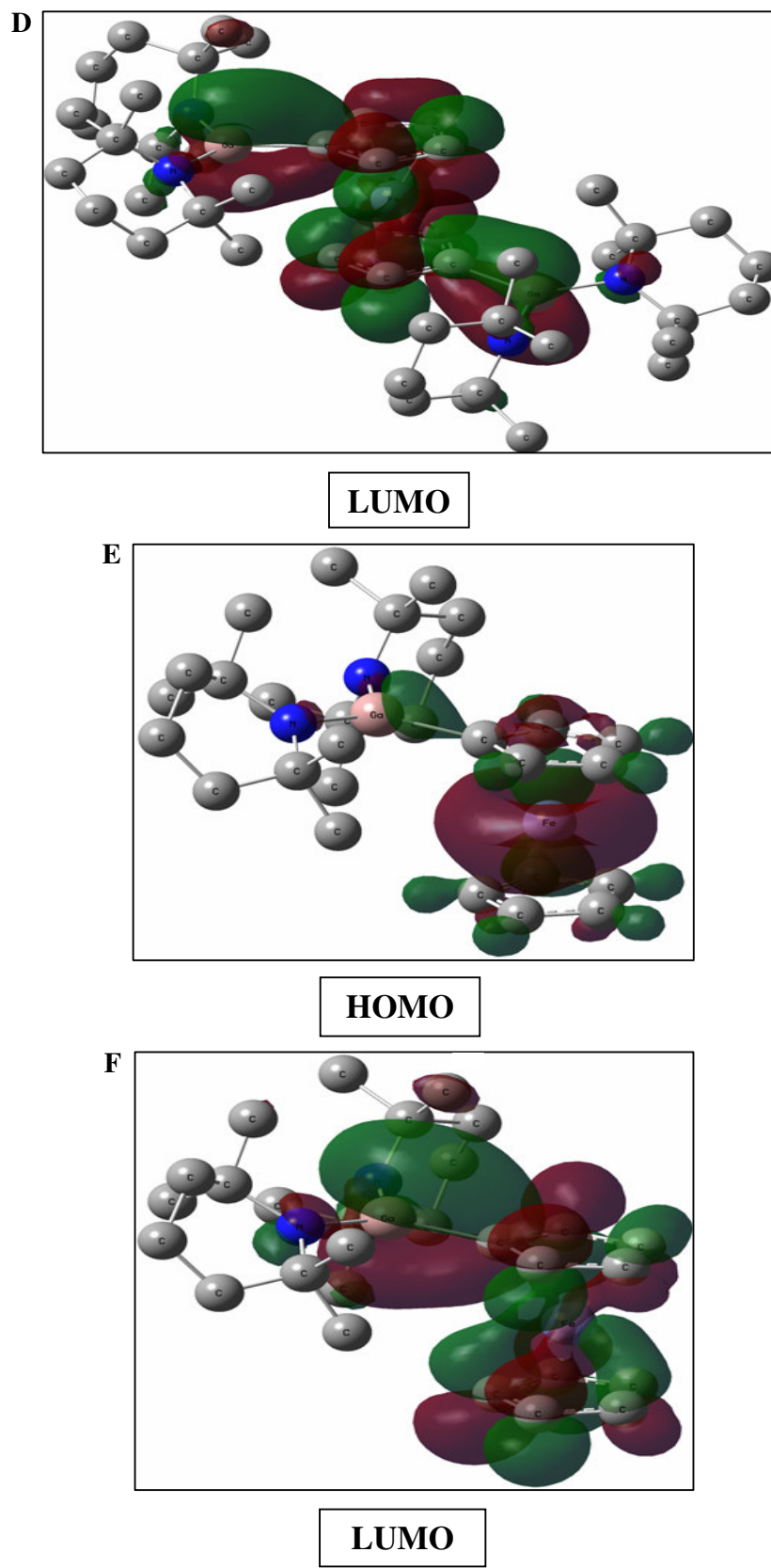


**Figure 15.:** Frontier molecular orbitals of **Fc** (A and B), **8** (C and D) and **9** (E and F).



The HOMO energies are identical for both compound (-4.99 eV) and larger than the HOMO energy for ferrocene (-5.49 eV). In the same time, the LUMO energies are different (-0.95 eV **8**, -0.52 eV **9**) indicating a different electron donating ability. Both values are smaller than that of LUMO in ferrocene (-0.07 eV).

The charge densities are summarized in Table 2:

**Table 2:** Charge density in **Fc**, **8** and **9**.

Compound	Charge density		
	Ga	Fe	N
<b>Fc</b>	-	+0,954	-
<b>8</b>	+0,887 ÷ +0,900	+0,960	-0,482 ÷ -0,505
<b>9</b>	+1,208	+0,952	-0,698 ÷ -0,724

### 3.6. Crystal Structure Analysis

#### 3.6.1. Crystal Structure Analysis of **8**

From a solution of **8** in *n*-hexane suitable orange crystals were grown at 6°C during several days. **8** crystallizes in the triclinic space group  $P\bar{1}$  (Fig. 16). The parallel Cp rings are in an eclipsed conformation and the tmp<sub>2</sub>Ga-substituents are in *anti* position. The Ga-N do not differ largely (187.2(2) - 188.0(2) pm). This is a hint to a minor Ga-N pp- $\pi$ -bonding interaction. The nitrogen atoms of e.g. tmp<sub>2</sub>Ga group show a different environment, respectively two of them are coordinated planar and the others less are slightly pyramidal coordinated (sum of angles 355°).

The NGaN and C<sub>2</sub>N planes intersect with angles of 71° and 40°. That means, only one of the tmp groups is nearly orthogonal to the N<sub>2</sub>GaC planes. This is similar to the situation found in tmp<sub>2</sub>GaOPh.<sup>[15]</sup> Because of a higher steric demand of the tmp groups compared to the ferrocenyl unit, the N-Ga-N angles are slightly larger than 120°. A roughly coplanar arrangement of N<sub>2</sub>Ga planes to the cyclopentadienyl rings is observed. The Ga-C bond lengths [ $d_{\text{Ga-C}} = 197.4$  pm and 197.9 pm] are in the same range as gallium aryl bonds. Also, Ga-C bonds of similar length were reported by Jutzi *et al.* for [Fe( $\eta^5$ -C<sub>5</sub>H<sub>4</sub>)<sub>2</sub>]<sub>2</sub>{GaMe<sub>2</sub>(Do)}<sub>2</sub><sup>[22]</sup> (Do = Phenazine) [ $d_{\text{Ga-C}} = 197.1(4)$  pm].

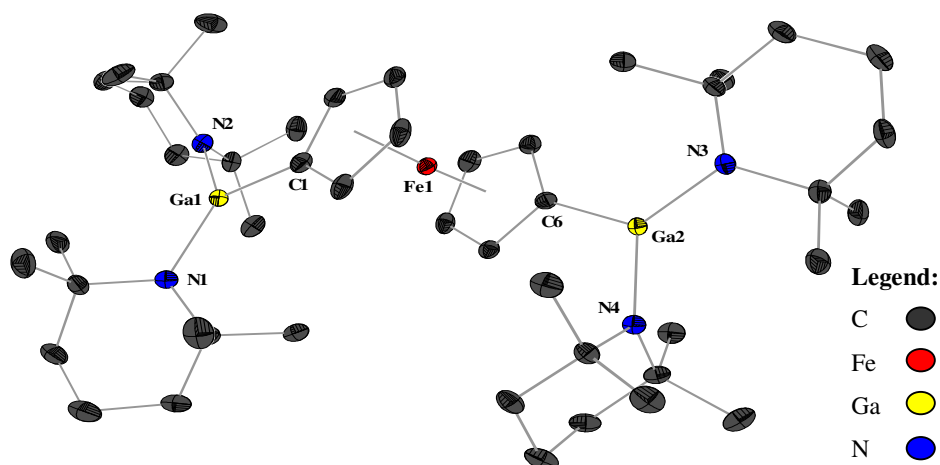


**Figure 16:** View of a molecule of **8**. Hydrogen atoms are omitted for clarity. Selected bond lengths [pm] and angles [°]: Ga(1)-N(2) 187.9(2), Ga(1)-N(1) 188.0(2), Ga(1)-C(1) 197.4(3), Ga(2)-N(4) 187.2(2), Ga(2)-N(3) 187.3(2), Ga(2)-C(6) 197.9(3); N(2)-Ga(1)-N(1) 123.3(11), N(2)-Ga(1)-C(1) 112.0(12), N(1)-Ga(1)-C(1) 124.7(1), N(4)-Ga(2)-N(3) 123.3(1).

### 3.6.2. Crystal Structure Analysis of **9**

**9** crystallizes in the monoclinic space group  $P2_1/n$  (Fig. 17). The Cp rings are in eclipsed conformation. **9** is the first monosubstituted gallyl ferrocene in monomeric conformation.<sup>[6]</sup> The Ga-N bond lengths are 188.0(4) and 190.7(3) ppm, respectively. These values are comparable with the reported values of the Ga-N bond lengths.<sup>[16],[24]-[27]</sup> Both nitrogen atoms of the tmp<sub>2</sub>Ga group exhibit a planar coordination environment (sum of angles: 360° and 358°). The higher steric demand of the tmp groups compared to the ferrocenyl unit have an effect in an N-Ga-N angles slightly larger than 120° (121.7(15)°). The Ga-C (200.9(4) ppm) bond is a little bit longer than the range of gallium aryl bonds and in the same time longer as the other reported gallyl substituted ferrocenes.<sup>[16],[22],[28]</sup>

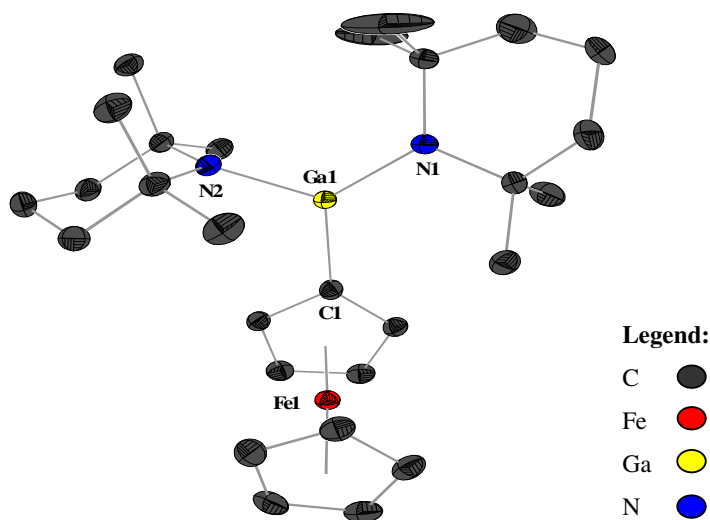
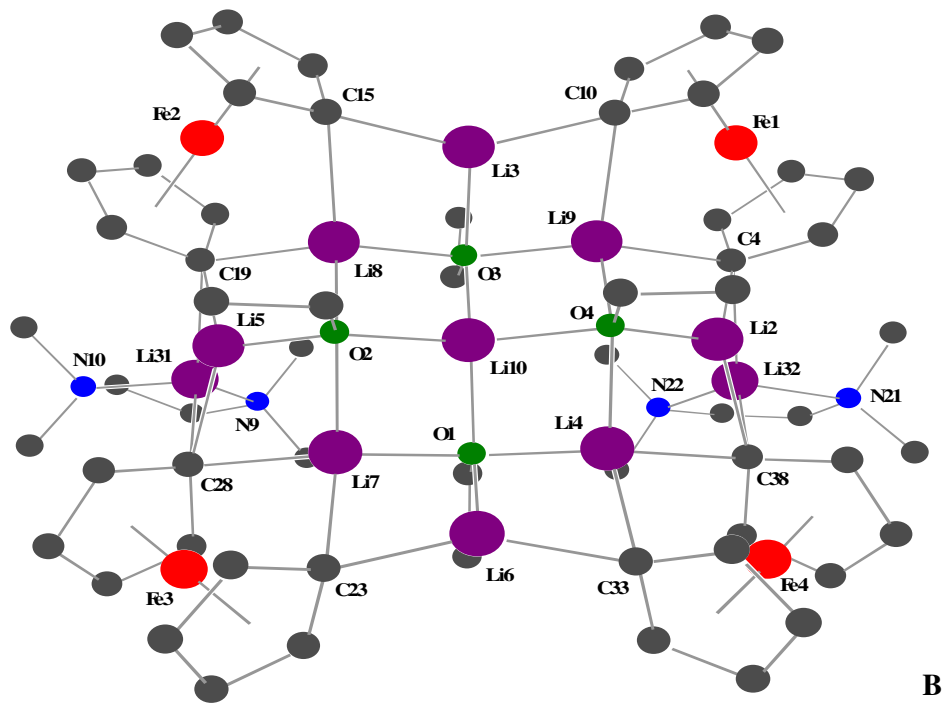
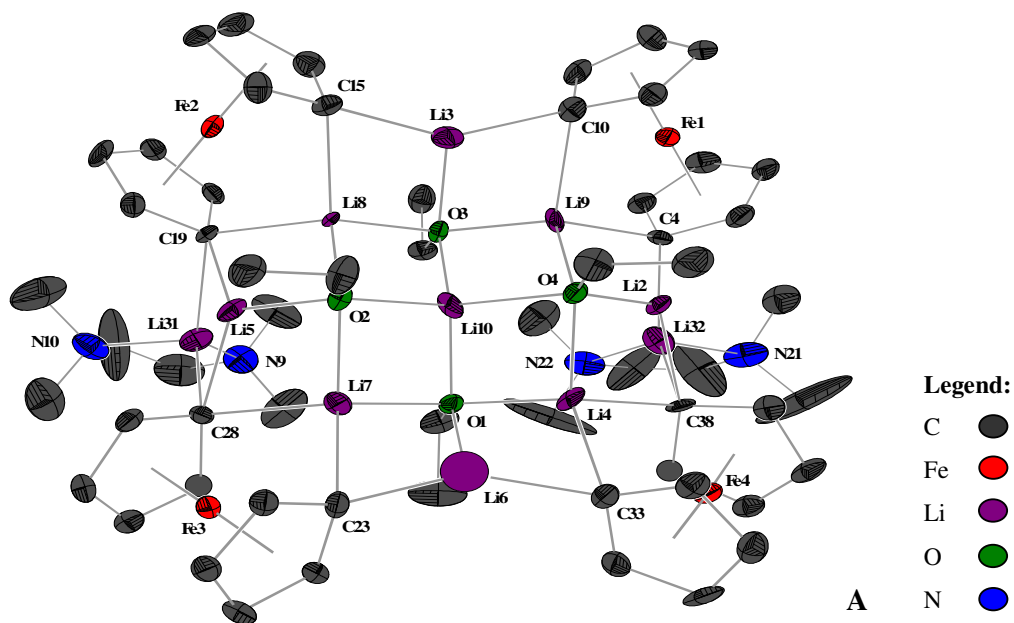


**Figure 17:** Solid state structure of a molecule of **9**. Thermal ellipsoids show 25% probability level. Hydrogen atoms are omitted for clarity. Selected bond lengths [pm] and angles [°]: Ga(1)-N(1) 188.0(4), Ga(1)-N(2) 190.7(3), Ga(1)-C(1) 200.9(4); N(1)-Ga(1)-N(2) 121.7(15), N(1)-Ga(1)-C(1) 124.4(16), N(2)-Ga(1)-C(1) 113.9(15).

### 3.6.3. Crystal Structure Analysis of **12**

The red crystals of **12** were isolated as side-product from an *n*-hexane solution from the synthesis of **8**. **12** crystallizes in the triclinic space group  $P\bar{1}$  (Fig. 18 A, B and C). Further discussions about the bonding nature and other features of the crystal structure of **12** could not be taken in consideration because of its low quality ( $R$  indices for all data is 23.3%). The crystals of **12** diffracted very poorly and the data do not give a complete crystal structure of **12** with accurate bond lengths and bond angles, but shows with certainty the presence of a lithium ferrocenophane cage.

### 3. Reaction of Bis(amino)gallium Chloride with Mono- and Dilithioferrocene



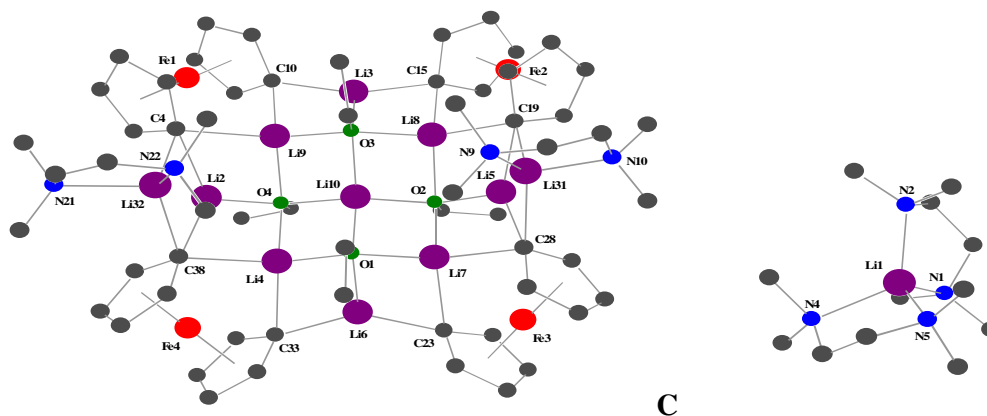


**Figure 18:** Stereoscopic views of the crystal structure of **12** (A), where two diethyl ether molecules, the molecule of  $[\text{Li}(\text{TMEDA})_2]^+$  and respectively all hydrogen atoms have been omitted for clarity. The next two figures exhibits the perspective views of **12**, without the counter ion molecule of  $[\text{Li}(\text{TMEDA})_2]^+$  (B) and with the counter ion molecule of  $[\text{Li}(\text{TMEDA})_2]^+$  (C). Thermal ellipsoids show 25% probability level.

## References

- [1] A. H. Cowley, R. A. Jones, K. B. Kidd, C. M. Nunn, and D. L. J. Westmoreland, *J. Organomet. Chem.*, **1988**, *341*, C1-C5.
- [2] R. L. Wells, A. P. Purdy, A. T. McPhail, and C. G. Pitt, *J. Organomet. Chem.*, **1988**, *354*, 287-292.
- [3] D. L. Reger, S. J. Knox, and L. Leboida, *Inorg. Chem.*, **1989**, *28*, 3092-3093.
- [4] M. A. Banks, O. T. Jr. Beachley, H. J. Gysling, and H. R. Luss, *Organometallics*, **1990**, *9*, 1979-1982.
- [5] G. Marr, B. W. Rockett, *J. Organomet. Chem.*, **1988**, *343*, 79-146.
- [6] B. Lee, W. T. Pennington, J. A. Laske, and G. H. Robinson, *Organometallics*, **1990**, *9*, 2864-2865.
- [7] E. Hecht, *Z. Anorg. Allg. Chem.*, **2000**, *626*, 759-765.
- [8] P. Jutzi, N. Lenze, B. Neumann, and H.-G. Stammer, *Angew. Chem. Int. Ed.*, **2001**, *40(8)*, 1423-1427.
- [9] W. Uhl, I. Hahn, A. Jantschak, and T. Spies, *J. Org. Chem.*, **2001**, *637-639*, 300-303.
- [10] J. A. Schachner, C. L. Lund, J. W. Quail, and J. Müller, *Organometallics*, **2005**, *24*, 4483-4488.
- [11] C. L. Lund, J. A. Schachner, J. W. Quail, and J. Müller, *Organometallics*, **2006**, *25*, 5817-5823.
- [12] J. A. Schachner, G. A. Orłowski, J. W. Quail, H. -B. Kraatz, and J. Müller, *Inorg. Chem.*, **2006**, *45*, 454-459.
- [13] R. Frey, *Diploma Thesis*, München, **1993**.
- [14] R. Frey, G. Linti, and K. Polborn, *Chem. Ber.*, **1994**, *127*, 101-103.
- [15] G. Linti, R. Frey, and K. Polborn, *Chem. Ber.*, **1994**, *127*, 1387-1393.
- [16] O. Feier-Iova, and G. Linti, *Z. Anorg. Allg. Chem.*, **2008**, *634*, 559-564.
- [17] P. J. Brothers, R. J. Wehmschulte, M. M. Olmstead, K. Ruhlandt-Senge, S. R. Parkin, and P. P. Power, *Organometallics*, **1994**, *13*, 2792-2799.
- [18] I. R. Butler, W. R. Cullen, J. Ni, and S. J. Rettig, *Organometallics*, **1985**, *4*, 2196-2201.
- [19] F. Rebiere, O. Samuel, and H. B. Kagan, *Tetrahedron Lett.*, **1990**, *31*, 3121-3124.

- [20] U. T. Mueller-Westerhoff, Z. Yang, and G. Ingram, *J. Organomet. Chem.*, **1993**, *463*, 163-167.
- [21] T. J. Kealy, P. L. Pauson, *Nature*, **1951**, *168*, 1039-1040.
- [22] A. Althoff, P. Jutzi, N. Lenze, B. Neumann, A. Stammler, and H. G. Stammler, *Organometallics*, **2002**, *21*, 3018-3022.
- [23] A. Althoff, P. Jutzi, N. Lenze, B. Neumann, A. Stammler, and H.-G. Stammler, *Organometallics*, **2003**, *22*, 2766-2774.
- [24] D. A. Atwood, R. A. Jones, A. H. Cowley, S. G. Bott, and J. L. Atwood, *J. Organomet. Chem.*, **1992**, *434*, 143-150.
- [25] J. T. Park, Y. Kim, J. Kim, K. Kim, and Y. Kim, *Organometallics*, **1992**, *11*, 3320-3323.
- [26] K. M. Waggoner, M. M. Olmstead, and P. P. Power, *Polyhedron*, **1990**, *9*, 257-263.
- [27] G. Linti, H. Noeth, K. Polborn, C. Robl, and M. Schmidt, *Chem. Ber.*, **1995**, *128*, 487-492.
- [28] O. Feier-Iova, and G. Linti, *WCECS*, 2007, Proceedings, ISBN: 978-988-98671-6-4, 182-187.





## 4. Reactivity Studies on **8** and **9**

### 4.1. Introduction

Usually, the mono- or digallyl substituted ferrocenes and gallaferrocenophanes, reported in the literature, were synthesized from mono- or disubstituted ferrocenes *via* nucleophilic substitution reactions at the cyclopentadienyl rings with the formation of a Ga-C bond.<sup>[1]-[5]</sup> To the best of our knowledge, until now, no studies on the modification of the gallyl substituents in ferrocenyl gallanes have been made. There are some studies made by Jutzi *et al.*<sup>[6]-[9]</sup> regarding the formation of different monomeric adducts in donor solvents (py, thf, phenazine, etc.) with the purpose of using these adducts as starting materials for the synthesis of di- or trinuclear ferrocenophane complexes. Also, some of those adducts were fully characterized by means of NMR spectroscopy, single crystal structure analysis and even cyclovoltammetry.

### 4.2. Reaction of **8** with Acids

#### 4.2.1. Synthesis Routes

If CO<sub>2</sub>, in the form of dry ice, is added to a chilled (at -78 °C) solution of **8**<sup>[10]</sup> in hexane, the color changes immediately from red-orange to yellow. The carbamate **13**<sup>[10]</sup> is formed. Here an insertion of CO<sub>2</sub> into all four gallium-nitrogen bonds takes place. After several weeks of standing at room temperature, yellow crystals of **13** are collected.

The reaction of **8** with different Brønsted acids (e.g. MeCOOH, CH<sub>2</sub>(COOH)<sub>2</sub>, EtOH/H<sub>2</sub>O, C<sub>6</sub>H<sub>5</sub>OH and C<sub>6</sub>H<sub>4</sub>(OH)<sub>2</sub>) is investigated. When a solution of water free acetic acid is added dropwise to a chilled (at -78 °C) solution of **8**, [tmpH<sub>2</sub>]<sup>+</sup><sub>2</sub>[{Fe(η<sup>5</sup>-C<sub>5</sub>H<sub>4</sub>)<sub>2</sub>}{Ga(O<sub>2</sub>CMe)<sub>3</sub>}<sub>2</sub>]<sup>2-</sup> **14**<sup>[11]</sup> in good yield is obtained.

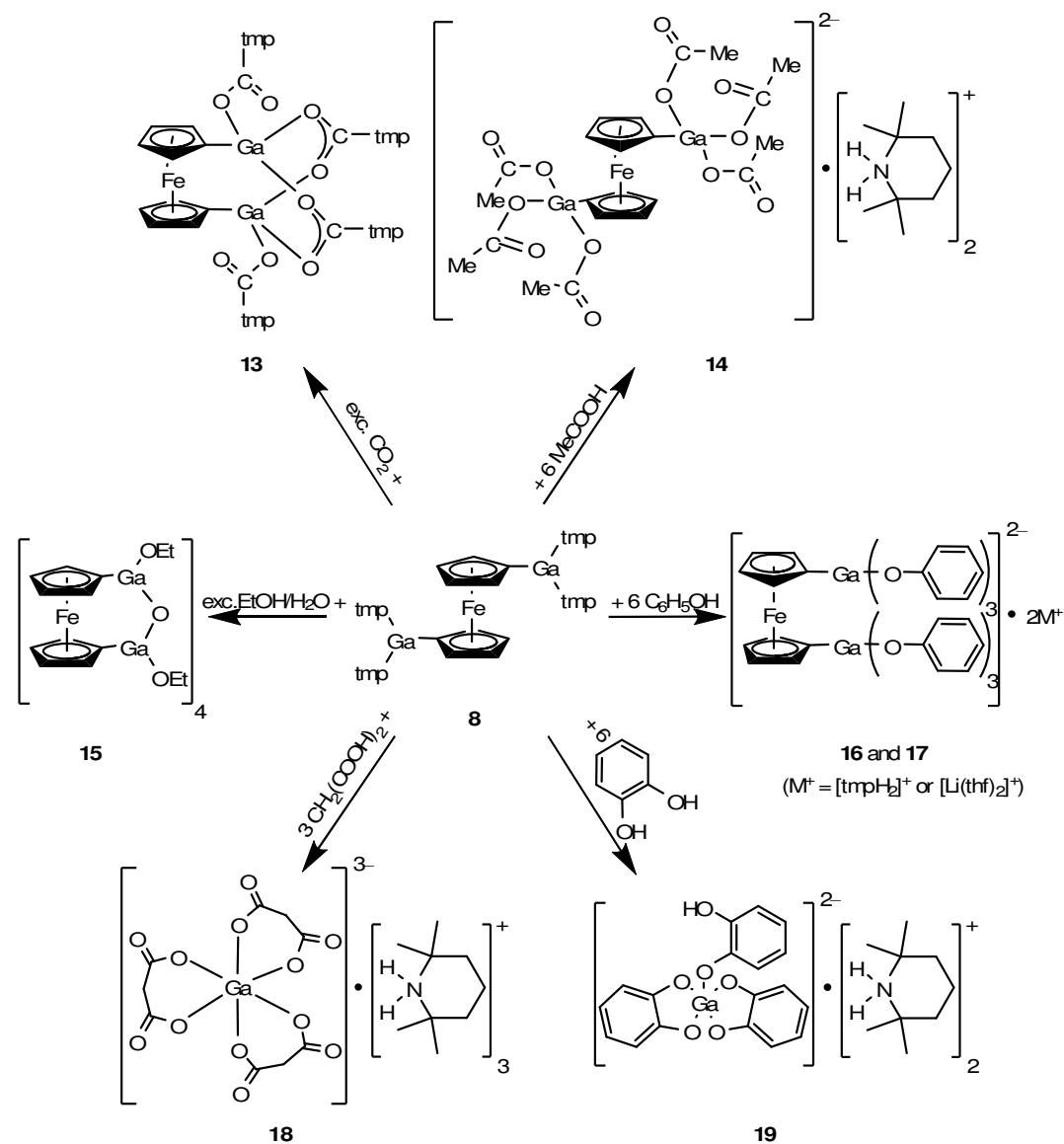
The gallaferrocenophane [{Fe(η<sup>5</sup>-C<sub>5</sub>H<sub>4</sub>)<sub>2</sub>}{GaOEt}<sub>2</sub>O]<sub>4</sub> **15**<sup>[11]</sup> which appeared as an oligomeric structure with four ferrocenyl units in its backbone, is obtained by treating a solution of **8** with an excess of ethanol with water traces. The reaction takes place at room temperature. The product **15** is obtained as yellow crystal by standing several days at -32 °C.

A mixture of digallyl substituted ferrocenes [tmpH<sub>2</sub>]<sup>+</sup><sub>2</sub>[{Fe(η<sup>5</sup>-C<sub>5</sub>H<sub>4</sub>)<sub>2</sub>}{Ga(O-C<sub>6</sub>H<sub>5</sub>)<sub>3</sub>}<sub>2</sub>]<sup>2-</sup> **16** and [Li(thf)<sub>2</sub>]<sup>+</sup><sub>2</sub>[Fe{(η<sup>5</sup>-C<sub>5</sub>H<sub>4</sub>)<sub>2</sub>}{Ga(O-C<sub>6</sub>H<sub>5</sub>)<sub>3</sub>}<sub>2</sub>]<sup>2-</sup> **17** has been obtained from the reaction of **8** with phenol in thf at room temperature. The reaction control is made by using <sup>1</sup>H-NMR technique. The product's ratio of 2:1 is observed (see Fig. 23). Thus, the end of reaction can be also visually observed, through color changing from red-orange to yellow. The products appeared as a yellow-light orange powder.

Compound [tmpH<sub>2</sub>]<sup>+</sup><sub>3</sub>[{CH<sub>2</sub>(COO)<sub>2</sub>}<sub>3</sub>Ga]<sup>3-</sup> **18**, isolated as colorless crystals is prepared by the reaction of **8** with malonic acid. Tetrahydrofuran is used as solvent for this reaction, which took place at room temperature. The product is obtained in good yield.

Finally when a solution of catechol (1,2-dihydroxobenzene) in thf, is added dropwise to a chilled solution of **8**, the gallium catecholate [tmpH<sub>2</sub>]<sup>+</sup><sub>2</sub>[(σ-C<sub>6</sub>H<sub>4</sub>-O<sub>2</sub>)<sub>2</sub>Ga(σ-OC<sub>6</sub>H<sub>4</sub>OH)]<sup>2-</sup> **19**<sup>[11]</sup> as main product is yield (Scheme 7).

Scheme 7: Reactions of 8 with different acids.



## 4.2.2. Spectroscopic Characterization

### 4.2.2.1. $^1\text{H}$ - and $^{13}\text{C}$ -NMR Spectroscopy

The ferrocenyl derivative **13**<sup>[10]</sup> gives rise to two pseudo triplets ( $\delta$   $^1\text{H}$  = 4.39 and 4.36) for the protons of the Cp-rings in the  $^1\text{H}$  NMR spectrum (see Fig. 19). The coupling constant is  $^3J_{\text{H,H}} = ^4J_{\text{H,H}} = 1.5$  Hz. A different bonding mod of the tmpCO<sub>2</sub> units was observed in the  $^1\text{H}$  NMR spectrum. These agree well with the solid state structure of **13**. Two signal sets for tmp-methyl groups were recorded ( $\delta$   $^1\text{H}$  = 1.53 and 1.44). This

#### 4. Reactivity Studies on **8** and **9**

brings to different bonding modes of tmpCO<sub>2</sub> groups or hindered rotation. One pseudo-triplet ( $\delta^1\text{H} = 1.70$ ) and one centered and multiplet ( $\delta^1\text{H} = 1.58$ ) were recorded for the  $\gamma$  and for the  $\beta$  hydrogen atoms of the tmp groups.

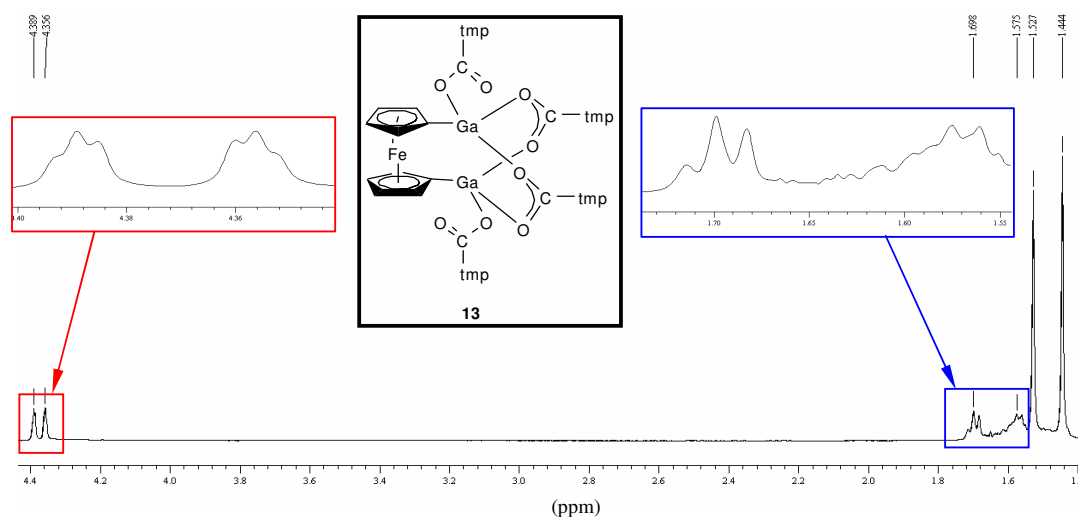


**Figure 19:** <sup>1</sup>H-NMR spectrum of **13** in CDCl<sub>3</sub>, at room temperature, with the inset showing an expanded view of the chemical shift range from 4.40 to 4.31, from 1.88 to 1.54 and from 1.35 to 1.29 ppm.

The <sup>13</sup>C-NMR spectrum of **13** (Fig. 20) shows a double signal for the carbon atoms of the tmp groups ( $\delta^{13}\text{C} = 29.7$  and  $29.6$ ) and two signals for the NCO<sub>2</sub> atoms ( $\delta^{13}\text{C} = 165.8$  and  $161.3$ ). This is indicative for two different bonding modes. This finding is consistent with the crystal structure of **13**. The signal for the *ipso*-carbon atoms exhibit a high field shifting ( $\delta^{13}\text{C} = 64.7$ ) compared to ferrocene and **8**<sup>[10]</sup> which can be explain as a result of the higher coordination number of the attached gallium atoms (C.N. 4-5). In other reported organyl substituted [1, 1]-digallyl ferrocenophanes<sup>[4]</sup> the *ipso*-carbon atoms resonated at about  $\delta^{13}\text{C} = 70$ .

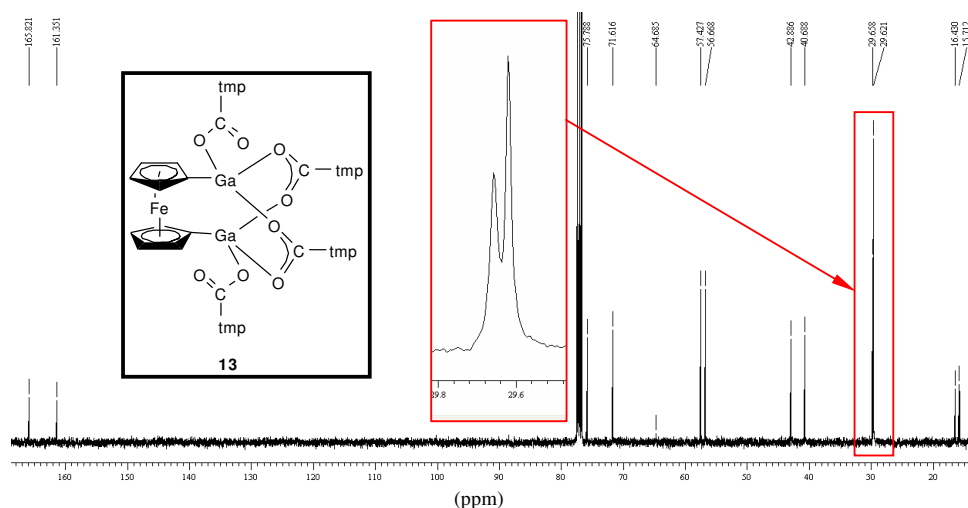


**Figure 20:**  $^{13}\text{C}$ -NMR spectrum of **13** in  $\text{CDCl}_3$ , at room temperature, with the inset showing an expanded view of the chemical shift range from 29.8 to 29.6 ppm.

The  $^1\text{H}$  NMR spectrum of a solution of **14**<sup>[11]</sup> in  $\text{CDCl}_3$  displays broad signals for all the hydrogen atoms from its molecule. A single signal set for both 2,2,6,6-tetramethylpiperidinium ions, one signal for all methyl units of the acetates groups ( $\delta^1\text{H} = 2.02$ ) and two signals for the  $\alpha$ -CH and  $\beta$ -CH units of the Cp rings ( $\delta^1\text{H} = 4.28$  and 4.24) are observed (Fig. 21). The signal corresponding to the  $\gamma$ -CH<sub>2</sub> protons from the tetramethylpiperidinium ions resonate at 1.69 ppm. The signal corresponding to the hydrogen atoms from the amine rests is observed ( $\delta^1\text{H} = 2.10$ ).

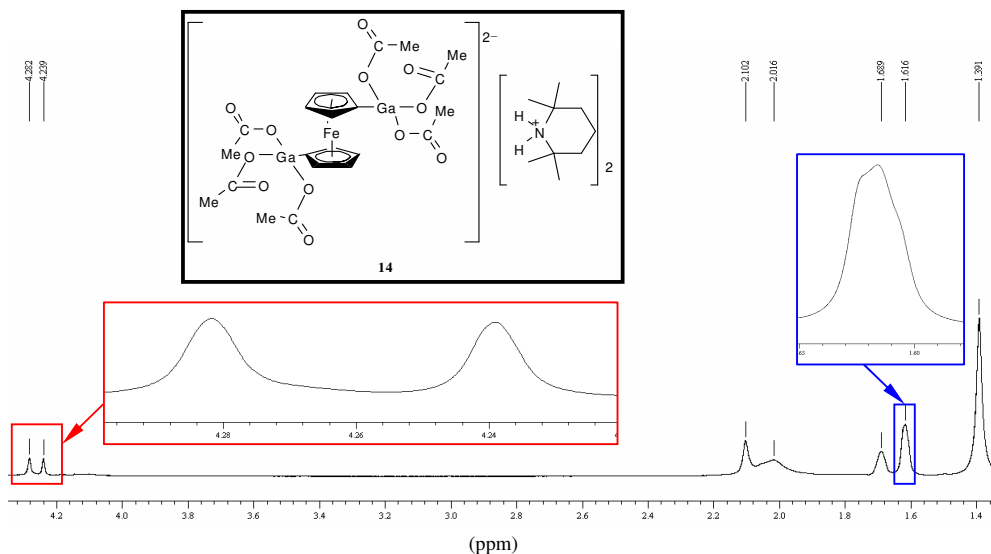


**Figure 21:**  $^1\text{H}$ -NMR spectrum of **14** in  $\text{CDCl}_3$ , at r. t., with the inset showing an expanded view of the chemical shift range from 4.29 to 4.20, from 1.84 to 1.80 and respectively from 1.65 to 1.58 ppm.

The  $^{13}\text{C}$  NMR spectrum of **14** display two signals for the carbon atoms of the Cp rings (see Fig. 22). This indicate a highly symmetrically structure in solution. The signal for the *ipso*-carbon atoms could not be observed. The signals for the carbons atoms of the Cp rings are shifted to lower field, compared to ferrocene, as well as almost all other reported gallylferrocenophanes. Three broad signals are recorded for the acetate groups ( $\delta^{13}\text{C} = 23.6 - \text{CH}_3$ , 177.8 and 177.3 -  $\text{H}_3\text{CCO}_2$ ). This is in contrast with the solid structure of **14**, where only two acetate groups are involved in hydrogen bonding. That is indicative for a migration of the methyl units between the acetate fragments in the molecule of **14**.

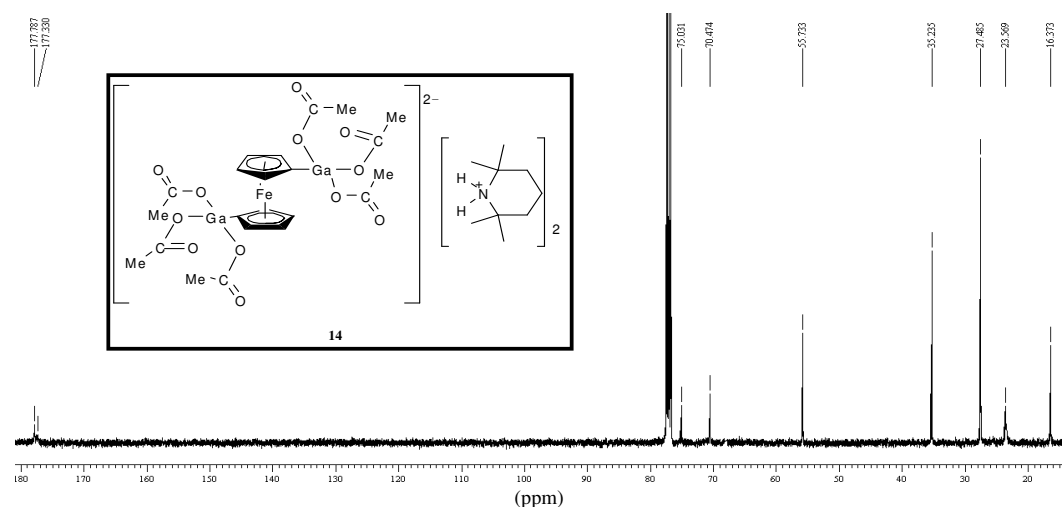


**Figure 22:**  $^{13}\text{C}$ -NMR spectrum of **14** in  $\text{CDCl}_3$ .

From the  $^1\text{H}$ -NMR spectrum of **16** and **17** (Fig. 23), the typical signal set for a  $[\text{tmpH}_2]^+$  ( $\delta^1\text{H} = 1.66 \text{ m}_c$ ,  $1.47 \text{ m}_c$  and  $1.31 \text{ s}$ ) and in addition signals for  $[\text{Li}(\text{thf})]^+$  shifted high field ( $\delta^1\text{H} = 3.74$  and  $1.84$ ) compared to free thf are presented. The anionic part gives a double set of signals for the phenolate group ( $\delta^1\text{H} = 7.11$ ,  $6.91$  and  $6.75$ ). The multipletts are overlapping. The hydrogen atoms from the Cp-ring give rise only to two broad signals ( $\delta^1\text{H} = 3.81$  and  $3.55$ ) (again overlapping). This lent to a coordination of  $\text{Li}(\text{thf})_2$  even in solution. From the integrals of the hydrogen atoms signals of both cationic parts, it is concluded that in solution is a 1:1 mixture of the products (see Fig. 23).

The structure predictions of these two digallyl substituted ferrocenes **16** and **17** and the spectral interpretations were made taking in consideration the crystal structure of  $[\text{Li}(\text{thf})_2]^+[\{(\eta^5\text{-C}_5\text{H}_5)\text{Fe}(\eta^5\text{-C}_5\text{H}_4)\}\{\text{Ga}(\text{C}_6\text{H}_5\text{-O})_3\}]^-$  **22** (see Chapter 4.3.3.1.).

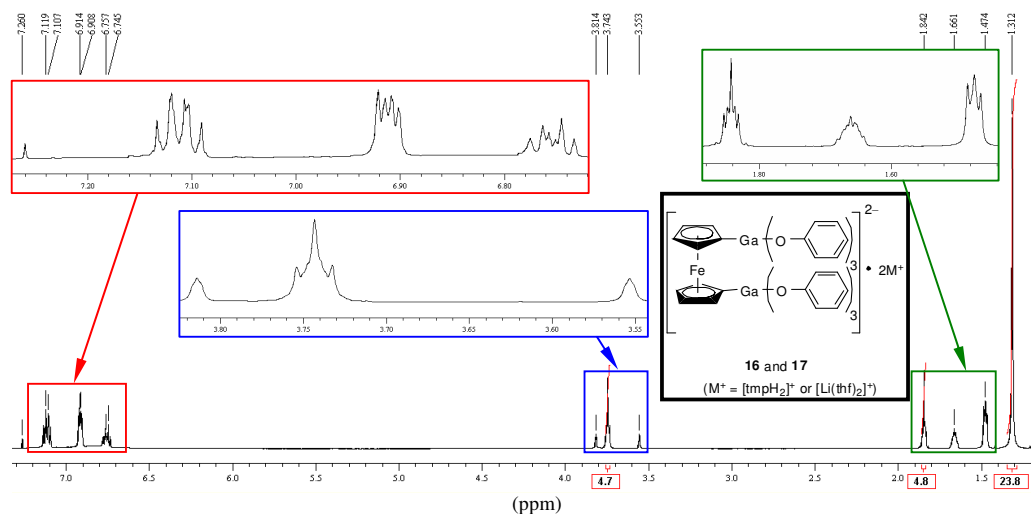
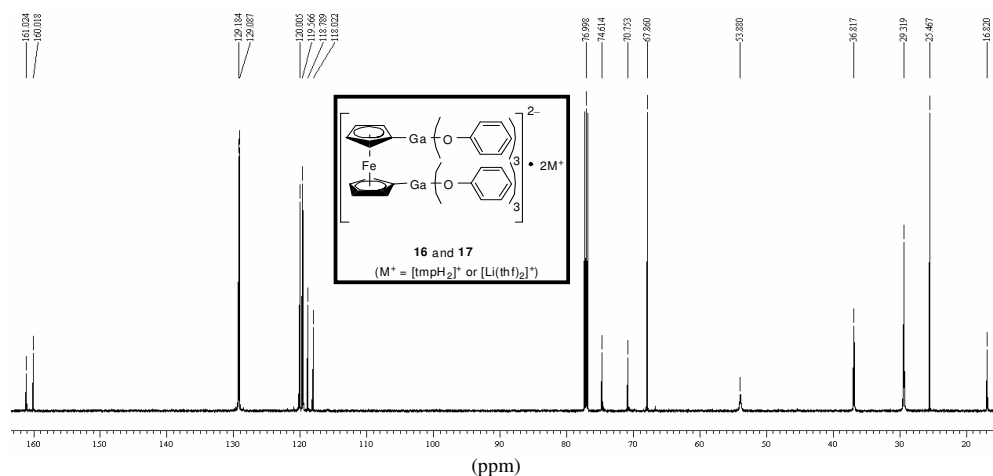


**Figure 23:**  $^1\text{H}$ -NMR spectrum of **16** and **17** in  $\text{CDCl}_3$ , at room temperature, with the inset showing an expanded view of the chemical shift range from 7.28 to 6.72, 3.81 to 3.54 and respectively from 1.88 to 1.44 ppm.

In the  $^{13}\text{C}$ -NMR spectrum (Fig. 24), the two sets of signals were observed corresponding to the phenolate rests of **16** and **17** ( $\delta^{13}\text{C} = 161.0 - 160.0, 129.2 - 129.1, 120.0 - 119.6$  and  $118.8 - 118.0$ ). For the ferrocenyl fragments, only one set of signals is observed for the CH groups ( $\delta^{13}\text{C} = 74.6$  and  $70.7$ ) showing again isochronic nuclei. Last but not least the signals for the carbon atoms of tetramethylpiperidinium cations ( $\delta^{13}\text{C} = 53.9, 36.8, 29.3$  and  $16.8$ ) and the signals for the carbon atoms of the  $[\text{Li}(\text{thf})_2]^+$  ( $\delta^{13}\text{C} = 67.9$  and  $25.5$  ppm) were clearly observed. The signals for the *ispo*-C could not be observed.

#### 4. Reactivity Studies on **8** and **9**



Figure

**24:**  $^{13}\text{C}$ -NMR spectrum of **16** and **17** in  $\text{CDCl}_3$ .

The  $^1\text{H}$ -NMR spectrum of **18** consists of three broad peaks with relative intensities of 6:18:36 (Fig. 25). This is not in agreement with the structure of **18**, because in its  $^1\text{H}$ -NMR spectrum are expected five signals, corresponding to the hydrogen atoms, on different environment bonding mode. Taking in consideration the peaks ratio's mention before, it can be assumed that the hydrogen atoms from the malonate fragments are resonated at 3.34 ppm, the hydrogen atoms of the methyl groups of the  $[\text{tmpH}_2]^+$  cations are resonated at 1.41 ppm and the other hydrogen atoms from the methylene groups of the counter ion are overlapping and resonated at 1.67 ppm. The resonance for the hydrogen atoms from the amine groups could not be observed.

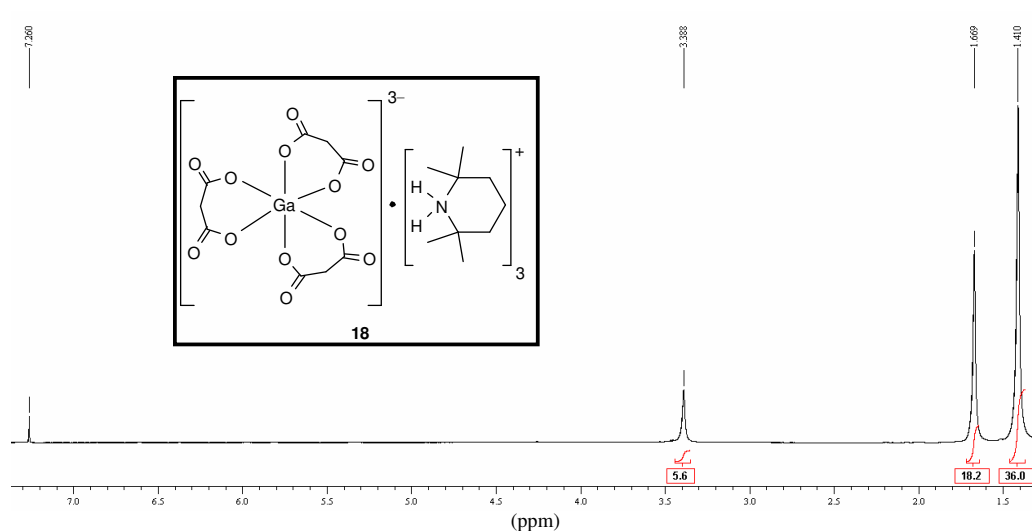


**Figure 25:**  $^1\text{H}$ -NMR spectrum of **18** in  $\text{CDCl}_3$ , at room temperature.



The  $^{13}\text{C}$ -NMR spectrum of **18** at room temperature shows six signals for the carbon atoms' resonances. The two signals at 174.1 and 45.0 ppm belong to the carbon atoms of the malonate fragments and the other four are the signals of the carbon atoms' resonance of the three  $\text{tmpH}_2^+$  counter ions ( $\delta^{13}\text{C} = 56.5, 34.8, 27.4$  and 16.3 ppm). That is in agreement with the solid state structure of **18** (Fig. 26).

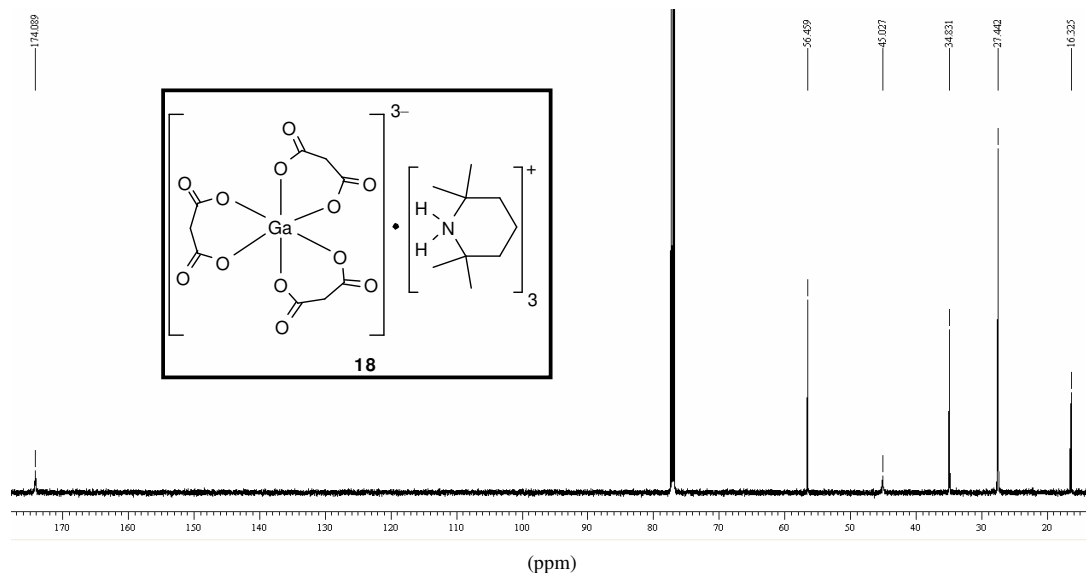


**Figure 26:**  $^{13}\text{C}$ -NMR spectrum of **18** in  $\text{CDCl}_3$ .

A  $^1\text{H}$ - and  $^{13}\text{C}$ -NMR examination of **19**<sup>[11]</sup> was performed. In the  $^1\text{H}$ -NMR spectrum (Fig. 27), **19** exhibits a broad signal for the proton of the  $-\text{OH}$  group ( $\delta^1\text{H} = 8.40$ ), three broad signals corresponding to the protons of the catecholate-rings in a ratio of 2:6:4 ( $\delta^1\text{H} = 6.85, 6.66$  and  $6.55$ , respectively) and also one single set of signals for the 2,2,6,6-tetramethylpiperidinium ions ( $\delta^1\text{H} = 1.69, 1.58$  and  $1.28$ ). As already mentioned before, the catecholate moieties of **19** gives rise only to four signals in the proton NMR spectrum, which is not in line with the solid state structure of **19**. This and the broad signals might be explained as an effect of the proton migration between different oxygen atoms. The signal for the N bonded hydrogen atoms could not be observed.

#### 4. Reactivity Studies on 8 and 9

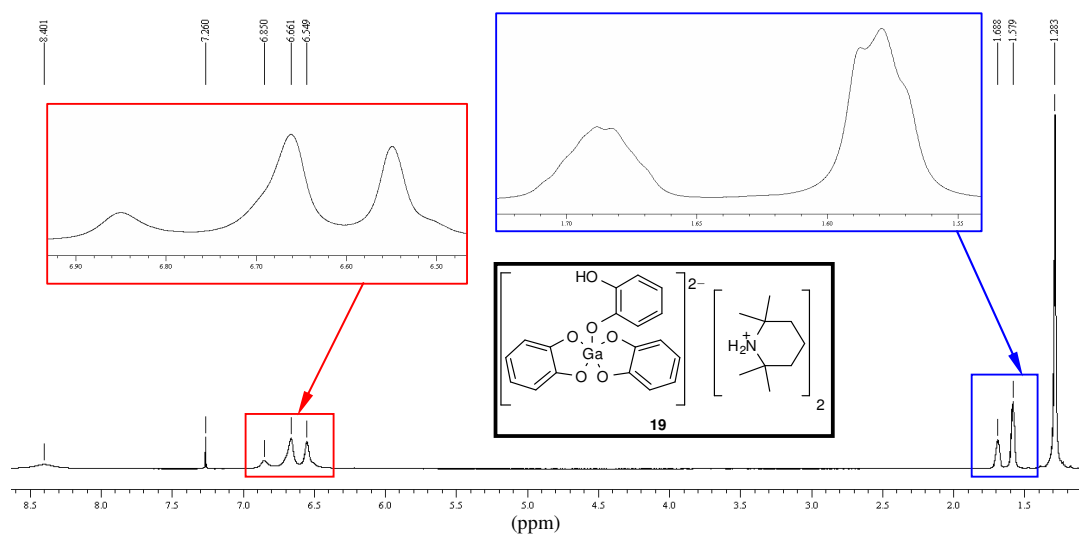


**Figure 27:**  $^1\text{H}$ -NMR spectrum of **19** in  $\text{CDCl}_3$ , at room temperature, with the inset showing an expanded view of the chemical shift range from 6.90 to 6.50 respectively from 1.72 to 1.55 ppm.

In the  $^{13}\text{C}$ -NMR spectrum of **19**, the six observed signals for the aromatic part are very broad. The substituted carbon atoms of the aromatic-rings afforded two broad signals at  $\delta^{13}\text{C} = 150.0$  and  $145.2$ , as well (Fig. 28). For the carbon atoms of the CH groups four signals are observed ( $\delta^{13}\text{C} = 120.3$ ,  $116.9$ ,  $117.7$  and  $114.2$ ). This is indicative for a dynamic structure, too. The tmp rests give rise to one single set of signals for the corresponding carbon atoms, resonated at  $56.0$ ,  $35.8$ ,  $27.9$  and  $16.1$  ppm.

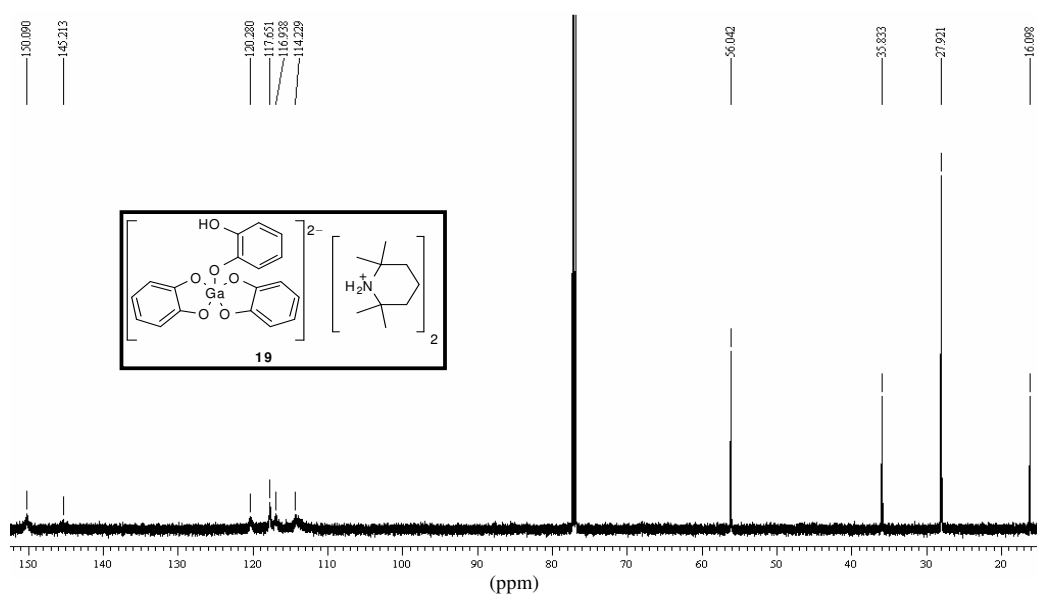


**Figure 28:**  $^{13}\text{C}$ -NMR spectrum of **19** in  $\text{CDCl}_3$ .

#### 4.2.2.2. Mass spectrometry

The peak corresponding to the molecular ion of **13**<sup>+</sup> was observed ( $m/z = 1060$  (0.4)). This indicates a highest stability for **13** in comparison with **8** or **9**. The molecule of **13** loses very easily, under mass spectrometric conditions, one after other CO<sub>2</sub> and tmp units and the following fragments could be found: [M-2CO<sub>2</sub>]<sup>+</sup>, [M-tmpCO<sub>2</sub>]<sup>+</sup>, [M- tmp<sub>2</sub>CO<sub>2</sub>]<sup>+</sup> ( $m/z = 972$ , 875 and 832). In addition [tmpGa-Me]<sup>+</sup> ( $m/z = 194$ ) and seven other fragments are recorded ( $m/z = 186$  [C<sub>10</sub>H<sub>10</sub>Fe]<sup>•+</sup>, 141 [tmpH]<sup>•+</sup>, 126 [tmpH-Me]<sup>+</sup>, 121 [C<sub>5</sub>H<sub>5</sub>Fe]<sup>+</sup>, 69 [Ga]<sup>+</sup>, 58 [Fe]<sup>+</sup>, 44 [CO<sub>2</sub>]<sup>•+</sup>). The base peak of the spectrum is: [tmpH-Me]<sup>+</sup>, [Ga]<sup>+</sup> and [Fe]<sup>+</sup>, as well.

Using the Electron Spray Ionization technique, a mass spectrum of **14** was recorded. The molecular ion peak could not be observed. Only some fragments as [{{Fe( $\eta^5$ -C<sub>5</sub>H<sub>4</sub>)<sub>2</sub>}{GaAc<sub>3</sub>}]<sup>-</sup> and [{{Fe( $\eta^5$ -C<sub>5</sub>H<sub>4</sub>)<sub>2</sub>}{GaAc<sub>2</sub>OH}]<sup>-</sup> ( $m/z = 431$  respectively 389) were obtained.

In the mass spectrum of **15**, the peak of the half molecular ion was recorded ( $m/z = 858$  [M - 2({Fe( $\eta^5$ -C<sub>5</sub>H<sub>4</sub>)<sub>2</sub>){Ga(OEt)<sub>2</sub>}\_2O])<sup>+</sup>). [Ga]<sup>+</sup> was the base peak. Also, some decomposition fragments with different intensities were observed ( $m/z = 186$  (96) [C<sub>10</sub>H<sub>10</sub>Fe]<sup>+</sup>, 121 (60) [C<sub>5</sub>H<sub>5</sub>Fe]<sup>+</sup>, 56 (30) [Fe]<sup>+</sup>).

A gas phase pyrolysis study of **19** was conducted in a mass spectrometer having He as carrier gas. The ESI mass spectrum monitoring of the anions, afforded one fragment having one gallium atom in its backbone ( $m/z = 321$  (100) [{{Ga( $\sigma$ -C<sub>6</sub>H<sub>4</sub>-O<sub>2</sub>)}{C<sub>6</sub>H<sub>4</sub>O(OH)}(OH)<sub>2</sub>]) and the catechol anionic rest [C<sub>6</sub>H<sub>4</sub>O(OH)]<sup>-</sup> ( $m/z = 109$ ).

#### 4.2.3. Cyclovoltammetric Determinations

The cyclo-voltammograms of **13**, **14** and **15**<sup>[11]</sup> were recorded (Fig. 29). Tetrahydrofuran was used as solvent, NBu<sub>4</sub>PF<sub>6</sub> as supporting electrolyte and decamethylcobaltocene/decamethylcobaltocenium as internal reference. The voltammograms show one oxidation and reduction process for each product separated by 169 mV (**13**), 196 mV (**14**) and 130 mV (**15**). The corresponding half wave

potentials are:  $E_{1/2} = -196$  mV (**13**),  $E_{1/2} = -277$  mV (**14**) and  $E_{1/2} = -222$  mV (**15**) (vs. ferrocene/ferrocenium).

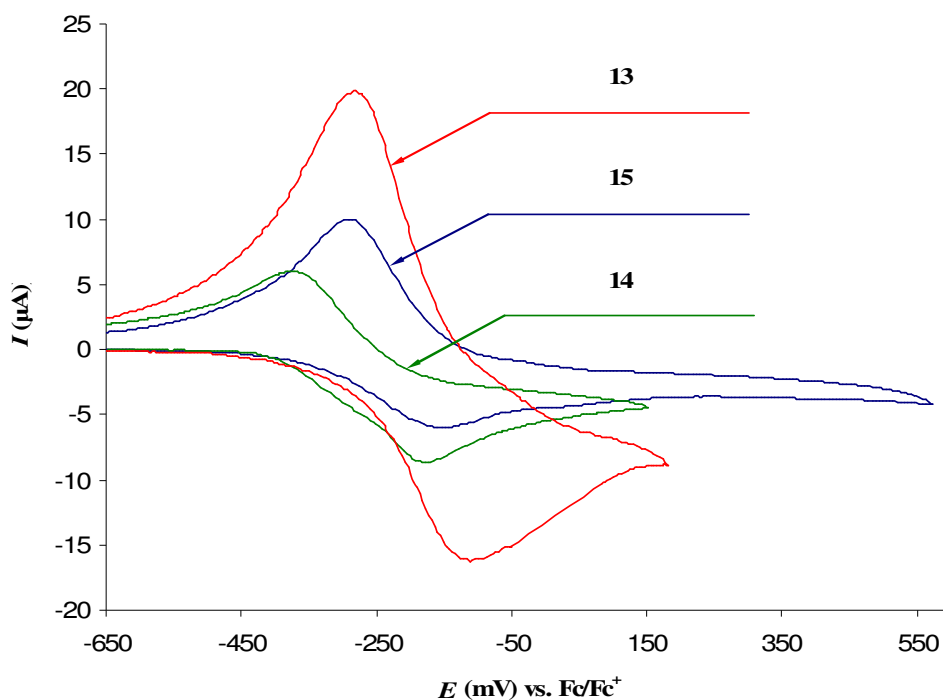


**Figure 29:** Cyclic voltammograms of **13**, **14** and **15** versus  $\text{Fc}/\text{Fc}^+$  in thf, internal standard  $\text{CoCp}_2^*/\text{CoCp}_2^{*+}$ .

As it was already mentioned in **Chapter 3**, again higher oxidation potentials are observed, in comparison with other gallaferrocenophanes.<sup>[3],[4],[6]-[9]</sup> This is an effect of the groups directly bonded to the gallium atoms and the influence of the solvent. Interesting to mention is that, for the tetranuclear species **15** only one oxidation-reduction peak is observed. On the other hand, the trinuclear ferrocenophane  $[\{\text{Fe}(\eta^5\text{-C}_5\text{H}_4)_2\}_3\{\text{Ga}\}_2]$ <sup>[9]</sup> shows three peaks. This behaviour could be an effect of the well separated ferrocenyl units and because of that, probable, no delocalization is possible.

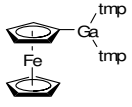
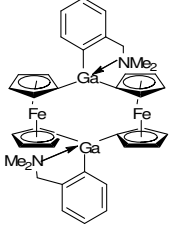
In Table 3 are summarized the first oxidation potentials of different gallyl substituted ferrocenes and gallaferrocenophanes reported in the literature, respectively determined in this thesis, measured in pyridine, tetrahydrofuran, dichloromethane or even DMSO and compared with ferrocene's oxidation potential.

**Table 3:** Summary of the first oxidation potentials recorded for different gallyl substituted ferrocenes, gallaferrocenophanes and respectively ferrocene.

Compound	Structure	Solvent	$E_{1/2}$ [mV]
$[\{\text{Fe}(\eta^5\text{-C}_5\text{H}_4)_2\}\{\text{GaMe}_2\}_2]_n^{[7]}$		Pyridine	-370
$[\{\text{Fe}(\eta^5\text{-C}_5\text{H}_4)_2\}_3\{\text{Ga}\}_2 \cdot 2\text{Py}]^{[6]}$		DMSO	-360
$[\{\text{Fe}(\eta^5\text{-C}_5\text{H}_4)_2\}_3\{\text{GaDMSO}\}_2]^{[9]}$		Pyridine	-356
$[\{\text{Fe}(\eta^5\text{-C}_5\text{H}_4)_2\}_2\{\text{GaMe(Py)}\}_2]^{[8]}$		Pyridine	-314
<b>14</b> <sup>[11]</sup>		Tetrahydrofuran	-277
<b>15</b> <sup>[11]</sup>		Tetrahydrofuran	-222
<b>8</b> <sup>[10]</sup>		Tetrahydrofuran	-199
<b>13</b> <sup>[11]</sup>		Tetrahydrofuran	-196
$[\text{Fe}(\eta^5\text{-C}_5\text{H}_5)_2]$		Tetrahydrofuran	0

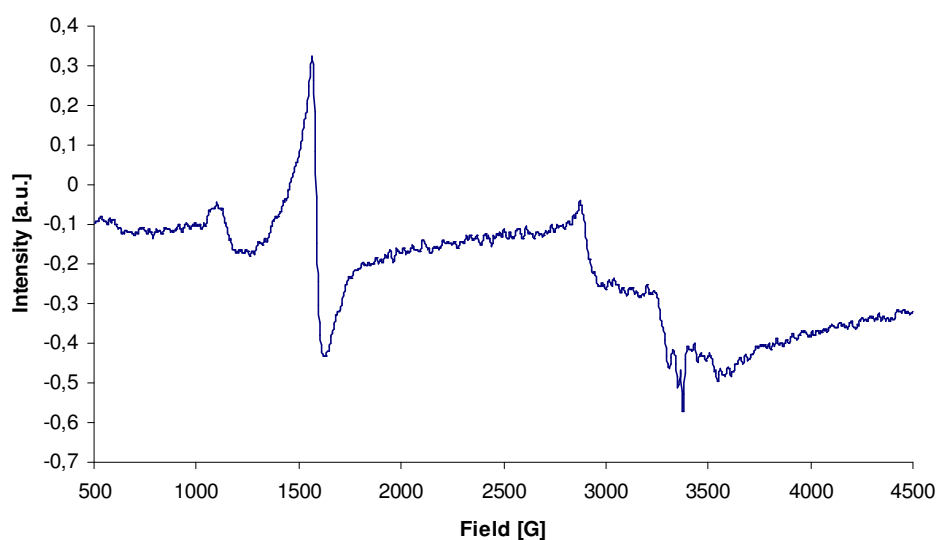
#### 4. Reactivity Studies on 8 and 9

Table 3: (Continuation).

Compound	Structure	Solvent	$E_{1/2}$ [mV]
9		Tetrahydrofuran	23
$[\{\text{Fe}(\eta^5\text{-C}_5\text{H}_4)_2\}_2\{\text{Ga}(\text{Pytsi})_2\}_2]^{[4]}$		Dichloromethane	50

#### 4.2.4. Electron Paramagnetic Resonance (EPR) Spectroscopy

Figure 30 shows the EPR signal observed upon reaction of **8** with bromine. A sample of the blue-green disubstituted gallyl ferricenium **8a** was prepared by solving it in a mixture of thf/toluene (1/1). The split isotropic signal is generated at  $g = 2.00$  (from the experimental data). The spectrum indicated that only a single paramagnetic center is generated by the preparation of disubstituted gallyl ferricenium species, as expected. Similar EPR spectra are also reported in the literature for different substituted ferricenium ions.<sup>[12],[13]</sup>



**Figure 30:** EPR spectrum of disubstituted gallyl ferricenium in thf/toluene (1/1) mixture. Spectrum was recorded at 105 K, with a 9.44 GHz microwave frequency, a 19.92 mW power, and a 5 G modulation amplitude.

#### 4.2.5. Crystal Structure Analysis

##### 4.2.5.1. Crystal Structure Analysis of **13**

**13** (Fig. 31) crystallizes in crystals of the system, space group triclinic  $P\bar{1}$ . By the insertion of four  $\text{CO}_2$  molecules in all four Ga-N bonds of **8** a ferrocenophane with a  $\text{Ga}[\text{OC}(\text{tmp})\text{O}]_2\text{Ga}$  bridge is afforded. Each gallium atom is surrounded distorted tetrahedral. The cyclopentadienyl rings are staggered (angles of  $25.29^\circ$  respectively  $26.44^\circ$  to each other). The gallyl groups are in *syn*-position with a torsion angle  $\text{Ga}(2)\text{-C}(36)\text{-C}(31)\text{-Ga}(1)$  of  $43^\circ$ .

The Ga-C bond lengths [ $d_{\text{Ga-C}} = 192.8$  pm (ave.)] are shorter than those in **8** and even other organyl gallium substituted ferrocenes and -ferrocenophanes.<sup>[8]</sup> Two of the carbamates coordinate bridging and the others are terminal. Therefore, a boat shaped eight-membered  $\text{Ga}(\text{OCO})_2\text{Ga}$ -ring is built. An example of a gallium carbamate with bridging carbamates similar with those exhibits in **13**, is presented by the dimethyl(2,2,6,6-tetramethylpiperidinocarbaminato)gallan-dimer **XXX**.<sup>[10]</sup> Here, a heterocyclic built from the same atoms as in **13**, is in crown like conformation. The relevant distances are in the same range to those of **13**. The Ga-O bond distances are between 189.2 and 194.6 pm and the C-O bonds are at an average bond length of 130 pm. The terminal carbamate groups are coordinated to gallium by a short Ga-O moiety [ $d_{\text{Ga-O}} = 189$  pm]. The other oxygen atoms have distances of 234.1 and 242.4 pm to the gallium atoms. The terminal bonding mode of this ligand is found in bis(2,2,6,6-tetramethylpiperidino)- $\eta^2$ -(2,2,6,6-tetramethylpiperidinocarbaminato)gallane **XXXI**.<sup>[10]</sup> Here the gallium atom is tetra coordinated by two tmp groups [ $d_{\text{Ga-N}} = 187$  pm] and a  $\eta^2$ -carbamato ligand [ $d_{\text{Ga-O}} = 202.7(2)$  pm and  $200.4(2)$  pm]. This is different from **13**, where the terminal carbamate groups are to be regarded as  $\eta^1$ -ligated to tetra coordinated gallium atoms. The resulting  $\text{GaO}_2\text{C}$ -ring has two similar Ga-O and C-O bonds, but the difference is significant, as the longer Ga-O bond is connected to the shorter C-O bond.

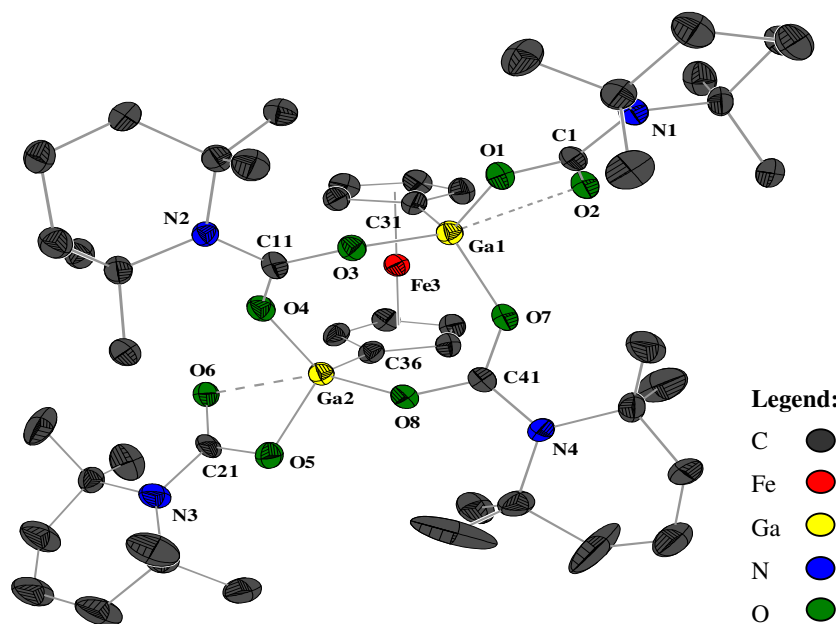


**Figure 31:** Molecular structure of **13** with thermal ellipsoids at the 25 % probability level. Hydrogen atoms and solvent molecules are omitted for clarity. Selected bond lengths [pm] and angles [°]: Ga(1)-O(1) 188.6(5), Ga(1)-O(2) 242.4(5), Ga(1)-O(3) 193.6(6), Ga(1)-O(7) 189.2(5), Ga(1)-C(31) 193.8(9), O(1)-C(1) 131.3(9), O(2)-C(1) 125.2(9), O(3)-C(11) 130.5(9), O(7)-C(41) 129.4(9), N(1)-C(1) 138.8(8), N(2)-C(11) 137.0(9), N(4)-C(41) 136.5(9), Ga(2)-O(4) 189.8(5), Ga(2)-O(5) 190.7(6), Ga(2)-O(8) 194.6(6), Ga(2)-O(6) 234.1(5), Ga(2)-C(36) 191.7(9); O(1)-Ga(1)-O(3) 88.8(2), O(1)-Ga(1)-O(7) 104.5(2), O(3)-Ga(1)-O(7) 102.2(2), O(1)-Ga(1)-C(31) 125.7(3), O(3)-Ga(1)-C(31) 109.2(3), O(7)-Ga(1)-C(31) 119.8(3), C(1)-O(1)-Ga(1), O(4)-Ga(2)-O(5) 104.7(2), O(4)-Ga(2)-C(36) 120.8(3).

#### 4.2.5.2. Crystal Structure Analysis of **14**

The pale yellow crystals of **14** (Fig. 32) are found to be triclinic, space group  $P\bar{1}$ . **14**, is the 2,2,6,6-tetramethylpiperidinium salt of a 1,1'-bis(trisacetatogallyl)ferrocenate(2-). The centro symmetric anionic part of **14** has staggered Cp rings, the substituents are in *anti* position. The gallium atoms are coordinated distorted tetrahedral by a  $\eta^1$ -Cp ring and three  $\eta^1$ -acetate groups. The O-Ga-O bond angles are (99.3° - 103.4°) less widely distorted tetrahedral coordinated. The O-Ga-C bond angles (107.6° - 121.6°) are wider than the tetrahedral angle. Values of Ga-O distances [ $d_{\text{Ga-O}} = 189.4$  pm (ave.)] are typical for Ga-O distances with gallium atoms in a tetrahedral conformation. The carboxylate groups are coordinated different at the gallium atoms *via* oxygen atoms, which is indicated by one short and two large distances to the gallium atoms [ $d_{\text{Ga-O}} = 276.2$  pm (O6), 318.7 pm (O4), 403.6 pm (O2)]. The C-O distances



in the carboxylate groups are different, the gallium bonded oxygen atoms [ $d_{\text{Ga-O}} = 131.0$  pm] are larger bonds than the other ones [ $d_{\text{Ga-O}} = 123.2$  pm]. The cationic counter ions are bonding to the anionic part *via* hydrogen bonds [ $d_{\text{O(2)-H(1)}} = 192.1$  pm,  $d_{\text{O(4)-H(2)}} = 214.6$  pm]. Due to the high electronegativity of the substituents bonded to the gallium atoms, the Ga-C bonds [ $d_{\text{Ga(1)-C(1)}} = 194.3$  pm] are shorter than those in **8** and similar with those in **13**. This is agreement with the Bent's rule.

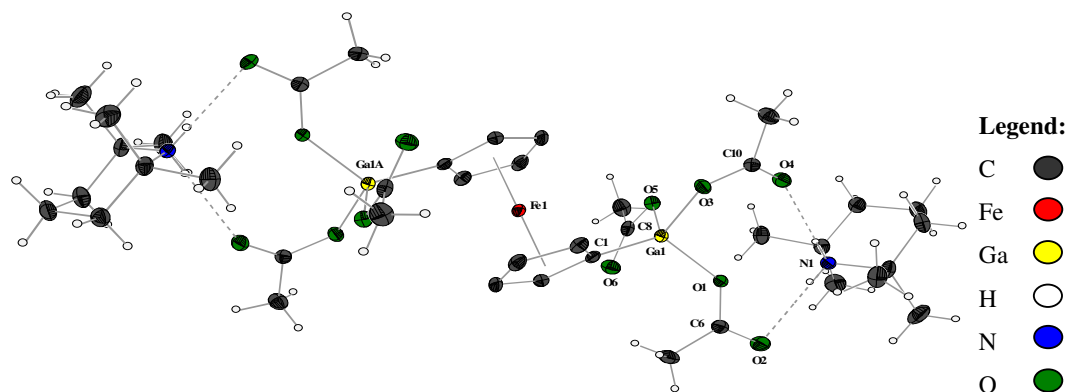
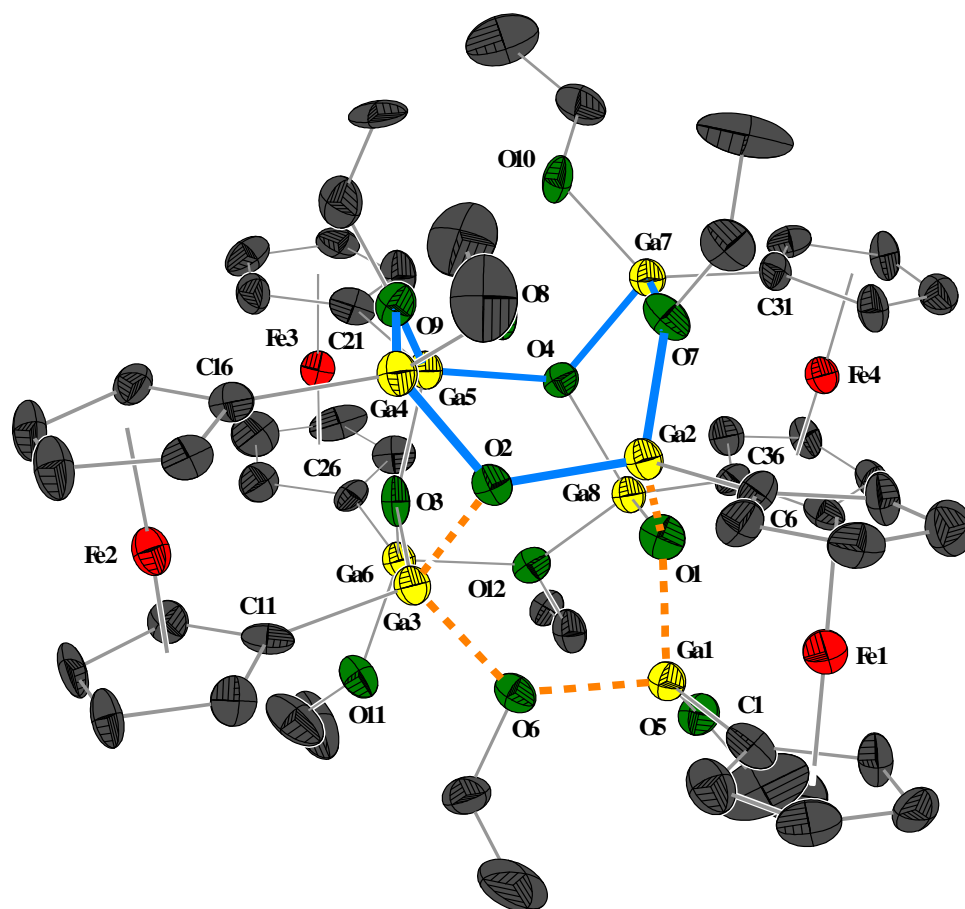


**Figure 32:** Molecular structure of **14** in solid state with the hydrogen bonds between cations and anion. Hydrogen atoms at the Cp-ring are omitted for clarity. Additional bond lengths [pm] and angles [°]: Ga(1)-C(1) 194.4(3), Ga(1)-O(1) 189.5(2), Ga(1)-O(3) 189.2(2), Ga(1)-O(5) 189.4(2), C(6)-O(1) 131.4(3), C(6)-O(2) 124.0(3), C(8)-O(5) 130.9(4), C(8)-O(6) 123.5(4), C(10)-O(3) 131.0(3), C(10)-O(4) 123.3(3); O(1)-Ga(1)-O(3) 101.95(9), O(1)-Ga(1)-O(5) 103.38(9), O(3)-Ga(1)-O(5) 99.3(1), O(1)-Ga(1)-C(1) 119.55(9), O(3)-Ga(1)-C(1) 107.6(1), O(5)-Ga(1)-C(1) 121.6(1), O(1)-C(6)-O(2) 120.0(3).

#### 4.2.5.3. Crystal Structure Analysis of **15**

**15** crystallizes in yellow needles together with two molecules of benzene (Fig. 33 A and B) of the monoclinic system, space group  $P2_1$ . **15** has a gallium-oxygen cage (the central core) built up by eight gallium atoms and eight oxygen atoms. The oxygen atoms are of different nature: four of them are part of the ethoxy groups and the others four are oxide ions. This cage shows two stacked boat-shaped  $\text{Ga}_4\text{O}_4$  rings, which are linked by four Ga-O bonds. This gives rise to four sides faces each of them looking as a distorted hexagon made up by three gallium atoms, two oxygen atoms and one  $\mu^2$ -OEt groups. Four additional OEt groups are in terminal positions directly bonded to the gallium atoms. As a result of the bonding manner, mentioned before, the gallium atoms

have a tetra-coordinated environment made up by three oxygen atoms and one carbon atom, which is part of the ferrocenyl unit. The Ga-O distances in the cage are varying between 179.5 and 194.0 pm. The Cp ring planes of the four ferrocenyl units are intersecting at angles between 5 and 17°, which mean that the ferrocenyl units are in an almost mutually coplanar orientation. The distances between iron atoms are relatively large (730 to 780 pm), that is about 200 pm larger than in  $[\{\text{Fe}(\eta^5\text{-C}_5\text{H}_4)_2\}_3\{\text{Ga}\}_2]$ .<sup>[9]</sup> This might explain the different electrochemical behavior of both compounds.



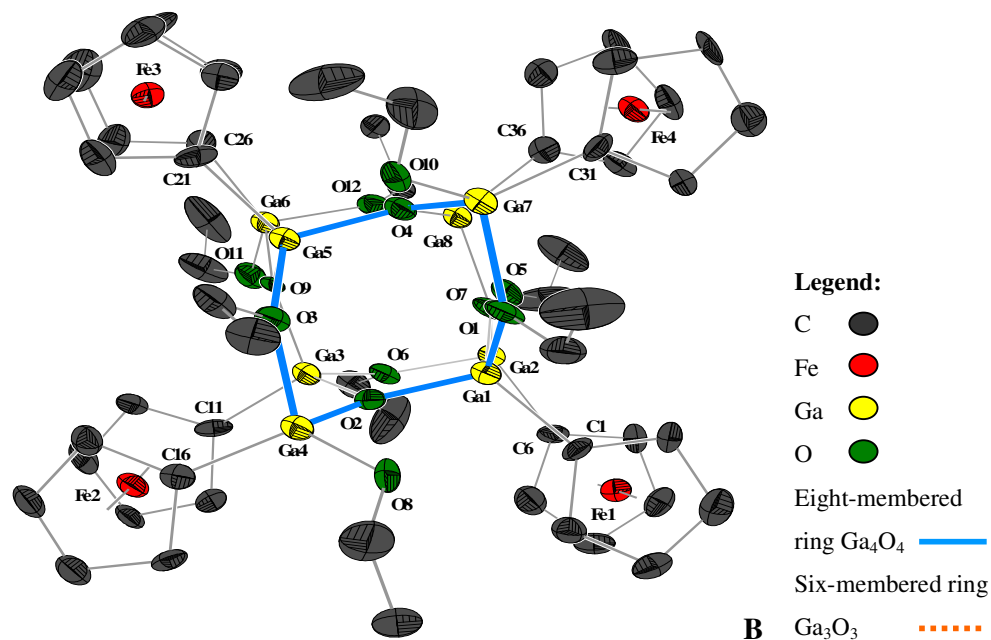


**Figure 33:** ORTEP plot of compound **15** (A-one side view, B-top view). Thermal ellipsoids are drawn at the 25 % probability level. Hydrogen atoms and benzene molecules are omitted for clarity. Selected bond lengths [pm] and angles [°]: Ga-O from 179.5(12) to 194.3(13), Ga-C from 192.3(19) to 199.3(19), O-Ga-O from 93.2(5) to 115.7(5), O-Ga-C from 106.5(6) to 122.6(7), Ga-O-Ga from 111.3(6) to 127.6(6), C-O-Ga from 113.7(11) to 126.3(18), C-C-Ga from 122.1(13) to 132.1(15), Ga-C-Fe from 123.1(10) to 126.9(9).

#### 4.2.5.4. Crystal Structure Analysis of **18**

Colorless crystals of **18**, space group  $P2_1$ , were obtained from a concentrated solution in acetonitrile, after several days standing at 6°C. The structure of **18** was determined by single X-ray crystallography (Fig. 34 A and B) and can be described as a  $\text{Ga}^{3+}$  ion coordinated with three carboxylate units. Thus, the central Ga atom is chelated in a bidentate fashion through two oxygen atoms of the three  $\text{CH}_2(\text{COO})_2^-$  units, therefore the Ga atom is octahedral coordinated. Each of the three six-membered chelate rings has a boat conformation flattened at the Ga end. The anion has a distorted octahedral geometry with significantly different Ga-O bond lengths which vary from 193.0(3) to 197.3(4) pm. The mean angle subtended at the Ga atom by the malonate ligands O-Ga-O is 90.7°.

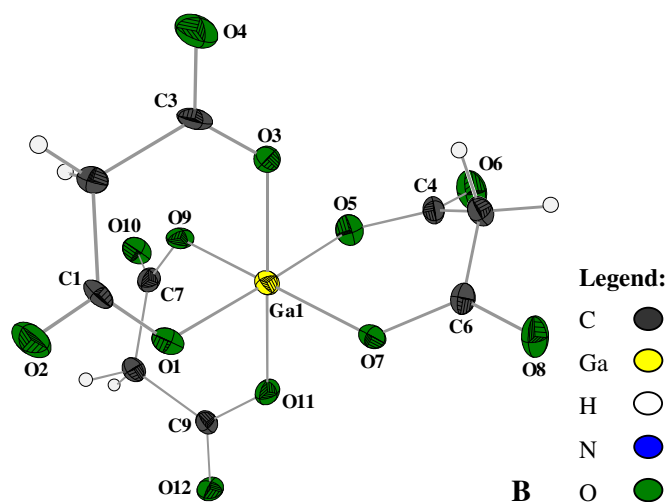
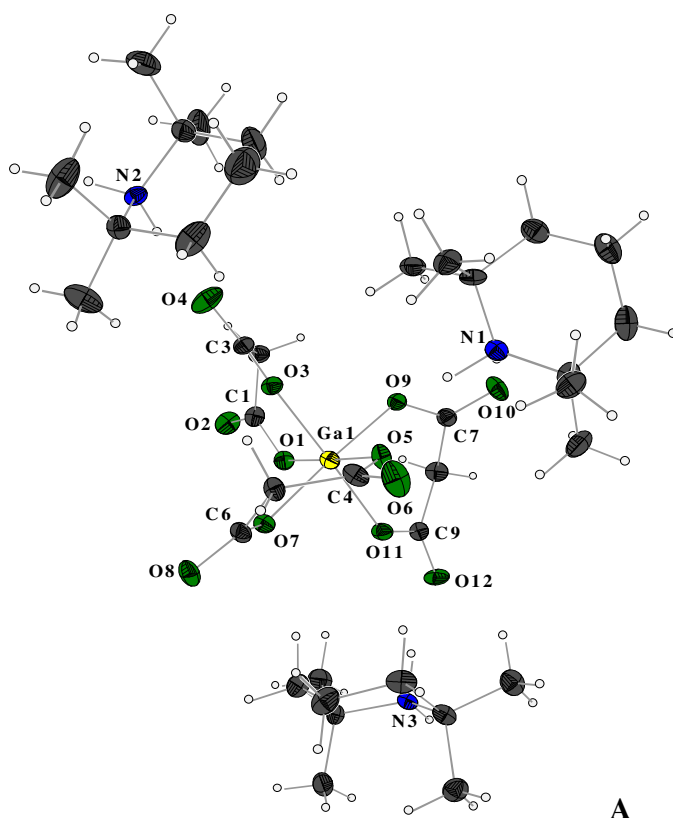


**Figure 34:** Molecular structure of **18** (**A** - the anionic part together with the three cations; **B** - in the scaled view of the anion) showing thermal ellipsoids at the 25% probability level. Selected bond lengths [pm] and angles [°]: Ga(1)-O(1) 197.3(4), Ga(1)-O(3) 197.2(4), Ga(1)-O(5) 197.2(4), Ga(1)-O(7) 193.0(3), Ga(1)-O(9) 194.0(4), Ga(1)-O(11) 195.2(4), O(1)-C(1) 129.0(6), O(2)-C(1) 122.4(6), O(3)-C(3) 126.7(7), O(4)-C(3) 120.6(6), O(5)-C(4) 132.8(6), O(6)-C(4) 121.3(6), O(7)-C(6) 130.7(6), O(8)-C(6) 124.4(5), O(9)-C(7) 130.6(6), O(10)-C(7) 121.4(6), O(11)-C(9) 129.4(6), O(12)-C(9) 121.2(6); O(1)-Ga(1)-O(3) 90.16(16), O(5)-Ga(1)-O(7) 91.95(15), O(9)-Ga(1)-O(11) 89.94(15).

#### 4.2.5.5. Crystal Structure Analysis of 19

After several days at 6°C, colorless crystals of **19** were grown. **19** crystallizes in plates of the orthorhombic system, space group  $P2_12_12_1$  together with a molecule of thf in its unit cell (Fig. 35). **19** exhibits two 2,2,6,6-tetramethylpiperidinium cations which balance the charge of one dianionic gallanate. A rare coordination of the central gallium atom as square pyramidal was observed. Two chelating catecholate ligands build the base of the pyramid and a further  $\eta^1$ -catecholates in the axial position is acting as a tip. The oxygen atom O(6) which belong to the  $\eta^1$ -catecholates is protonated. The Ga-O bonds in the square base have lengths that varying between 189.7 and 194.9 pm. The shortest Ga-O bond length is the axial one [ $d_{\text{Ga-O}(5)} = 183.2$  pm].

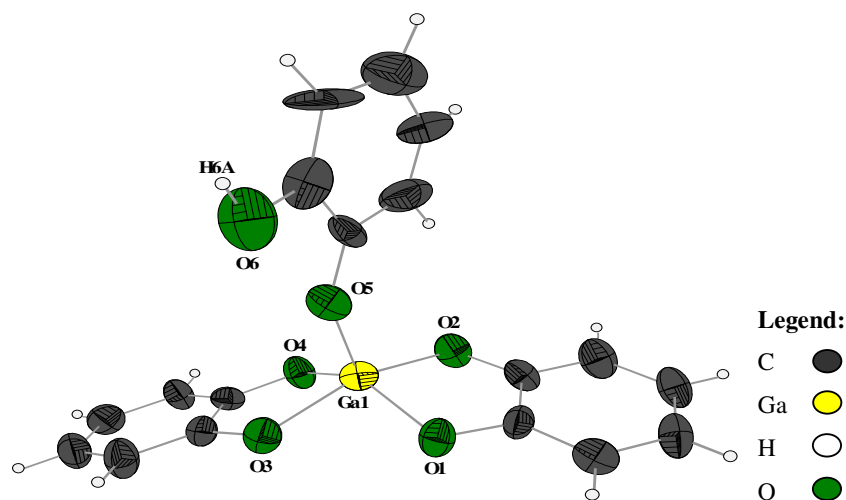


**Figure 35:** Thermal ellipsoid plot of the anion of **19**. The  $\text{tmpH}_2^+$  cations and thf molecule are omitted for clarity. Selected bond lengths [pm] and angles [°]: Ga(1)-O(1) 189.8(7), Ga(1)-O(2) 192.2(6), Ga(1)-O(3) 194.9(6), Ga(1)-O(4) 191.2(6), Ga(1)-O(5) 183.2(8); O(1)-Ga(1)-O(2) 84.4(3), O(1)-Ga(1)-O(3) 89.2(3), O(3)-Ga(1)-O(4) 83.0(3), O(1)-Ga(1)-O(5) 104.2(3), O(4)-Ga(1)-O(5) 113.0(3), O(3)-Ga(1)-O(5) 90.7(3).

### 4.3. Reaction of 9 with Acids

#### 4.3.1. Synthesis Routes

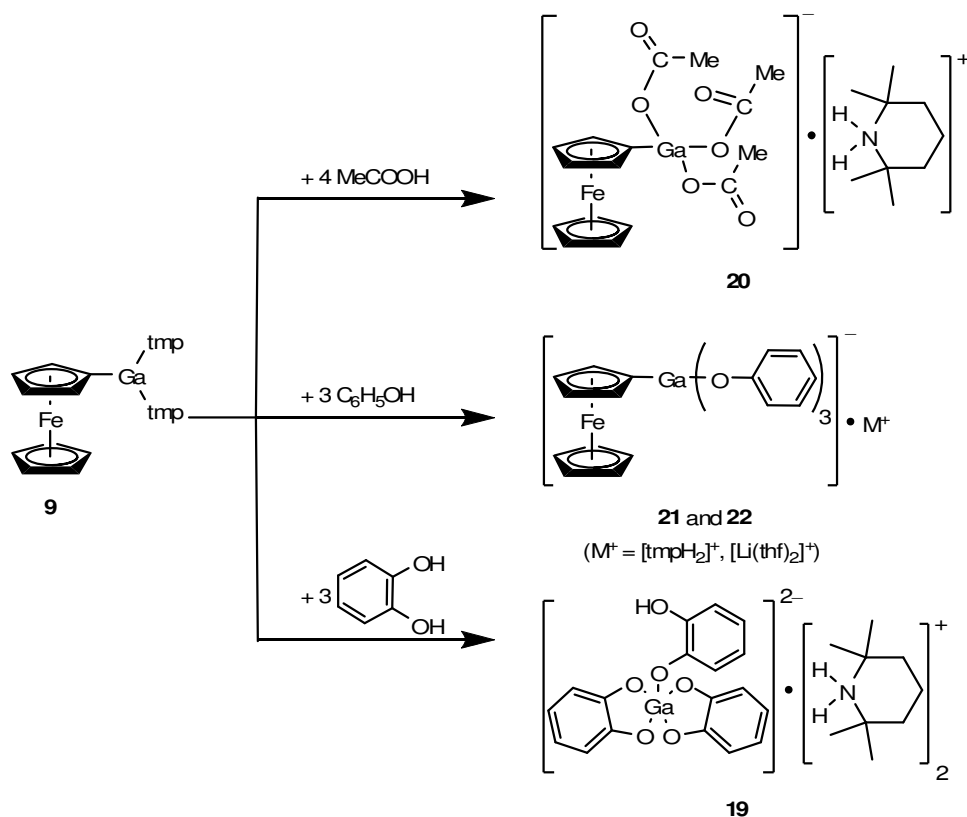
By the reaction of **9** with the Brønsted acids: MeCOOH,  $\sigma\text{-C}_6\text{H}_4(\text{OH})_2$  and  $\text{C}_6\text{H}_5\text{OH}$ , several new monogallyl ferrocene derivatives are obtained (Scheme 8).

The product **20** synthesized by the reaction of **9** with MeCOOH in a 1:4 ratio was isolated as a yellow powder. No suitable crystals could be grown. It was analyzed only by means of  $^1\text{H}$ - and  $^{13}\text{C}$ -NMR.

**21** and **22** were obtained by the reaction of **9** with phenol (exactly: 2% excess) in a 3:1 ratio in an *n*-hexane and diethyl ether mixture (see Scheme 8). The reaction took place at room temperature and was completed within few minutes. After all the volatiles were evaporated under *vacuum* and the residue was washed several times with *n*-hexane, a mixture of products **21** and **22** as an orange powder was isolated. The products were separated *via* recrystallization and further analyzed by means of  $^1\text{H}$ - and  $^{13}\text{C}$ -NMR spectroscopy. Also, suitable crystals of **22** were grown.

When a solution of catechol (1,2-dihydroxybenzene) in thf, was added dropwise to a solution of **9**, the catechol gallanate **19** as described in Chapter 4.2.1. (see Scheme 7) in good yield was obtained.

**Scheme 8:** Reactions of **9** with acids.



## 4.3.2. Spectroscopic Characterization

4.3.2.1.  $^1\text{H}$ - and  $^{13}\text{C}$ -NMR Spectroscopy

The  $^1\text{H}$  NMR spectrum of **20** (Fig. 36) exhibits one set of signals for the 2,2,6,6-tetramethylpiperidinium ion ( $\delta$   $^1\text{H}$  = 1.71, 1.63 and 1.39), one signal for the methyl groups of the acetate ligands ( $\delta$   $^1\text{H}$  = 2.03) and three signals for the hydrogen atoms of the substituted Cp ring ( $\delta$   $^1\text{H}$  = 4.29 and 4.25, br) and of the unsubstituted Cp ring ( $\delta$   $^1\text{H}$  = 4.13), respectively. One broad signal was recorded for the hydrogen atoms of  $\text{NH}_2$  moiety ( $\delta$   $^1\text{H}$  = 2.10). Until now, it was not possible to perform a single crystal structure analysis of **20**. Nevertheless, from the  $^1\text{H}$ - and  $^{13}\text{C}$ -NMR spectra recorded for **14** (see Chapter 4.2.2.1.), it was possible to confirm the structure of **20**.

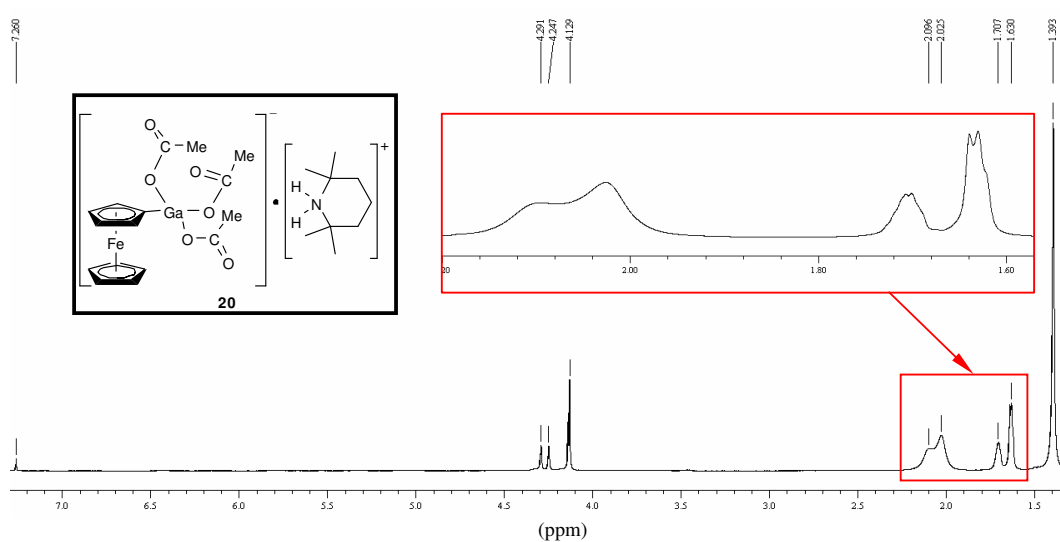


**Figure 36:**  $^1\text{H}$ -NMR spectrum of **20** in  $\text{CDCl}_3$ , at room temperature, with the inset showing an expanded view of the chemical shift range from 1.56 to 2.20 ppm.

In the  $^{13}\text{C}$  NMR broad signals for the acetate groups were recorded, which is in agreement with the predicted structure of **20**. One of the acetated group is involved in hydrogen bonding showing a different environment than the other two ( $\delta$   $^{13}\text{C}$  = 23.4 ( $\text{CH}_3$ ),  $\delta$  = 177.2, 177.8 ( $\text{H}_3\text{CCO}_2$ )). The other observed signals are in line with the expected resonance of the carbon atoms from the molecule of **20**. Last but not least, it is

important to mention that the signal for the *ipso*-carbon atom could not be observed (Fig 37).

Until now, it was not possible to perform a single crystal structure analysis of **20**. Nevertheless, from the  $^1\text{H}$ - and  $^{13}\text{C}$ -NMR spectra, and from the comparison of these spectra with the  $^1\text{H}$ - and  $^{13}\text{C}$ -NMR spectra recorded for **14** (see Chapter 4.2.2.1.), it was possible to confirm the structure of **20**.

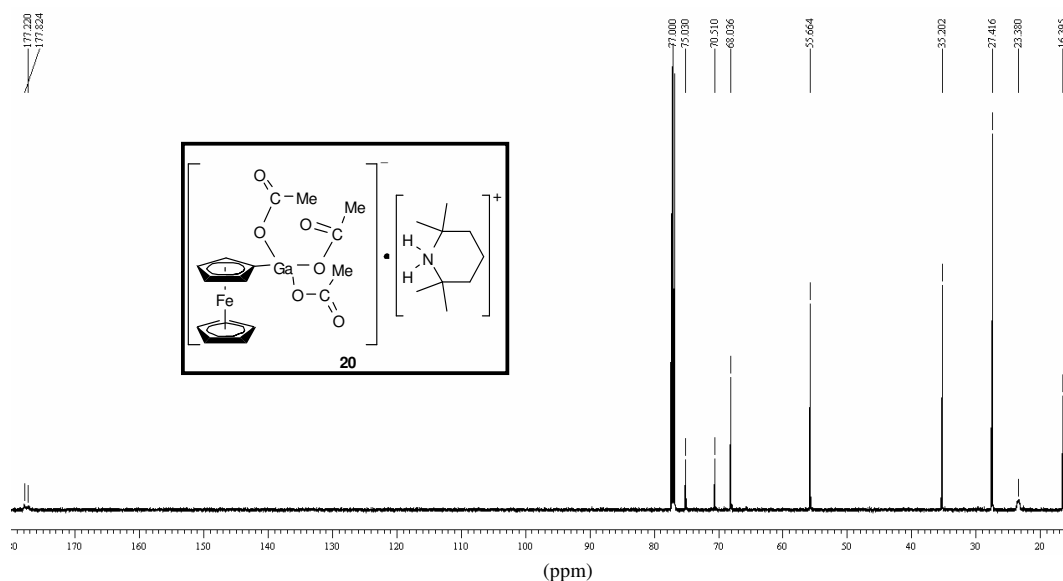


**Figure 37:**  $^{13}\text{C}$ -NMR spectrum of **20** in  $\text{CDCl}_3$ .

In the  $^1\text{H}$  NMR spectrum of **21** (Fig. 38) the expected signals for the hydrogen atoms' resonances were recorded. Thus, one doublet and two pseudo-triplets (intensity = 6:6:3) corresponding to the hydrogen atoms from *ortho*, *meta* and *para* positions of the phenolate units are exhibited ( $\delta$   $^1\text{H}$  = 7.20, 7.08 and 6.84). The protons of the cyclopentadienyl rings give rise to three signals, two for the substituted Cp-rings ( $\delta$   $^1\text{H}$  = 4.30 and 4.04) and one for the resonance of the equivalent hydrogen atoms of the unsubstituted Cp-ring ( $\delta$   $^1\text{H}$  = 3.88). On the other hand, three signals occur in the region corresponding to the tetramethylpiperidinium ions, similar with that observed for **19** or for **14** ( $\delta$   $^1\text{H}$  = 1.53, 1.37, 1.24, respectively). This is a strong sign for a salt art conformation of **21** where the cationic part built up by the tetramethylpiperidinium ion is bonded to the anionic fragment *via* hydrogen bonds.



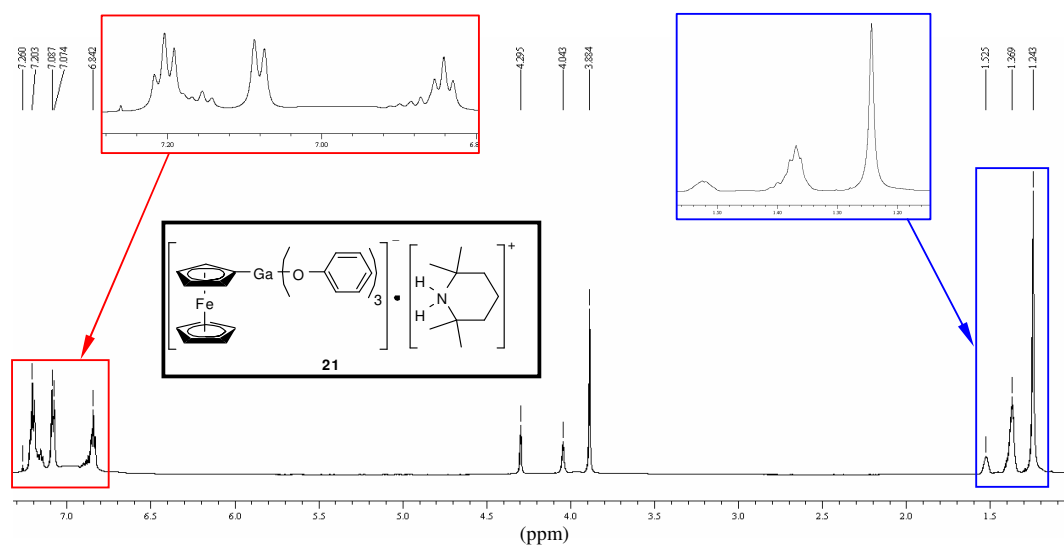


**Figure 38:**  $^1\text{H}$ -NMR spectrum of **21** in  $\text{CDCl}_3$ , at room temperature, with the inset showing an expanded view of the chemical shift range from 7.28 to 6.80 respectively from 1.56 to 1.16 ppm.

The  $^{13}\text{C}$ -NMR spectrum shows the expected signals, with the exception of the *ipso*-C atoms of the substituted cyclopentadienyl ring, which unfortunately could not be observed (see Fig. 39).

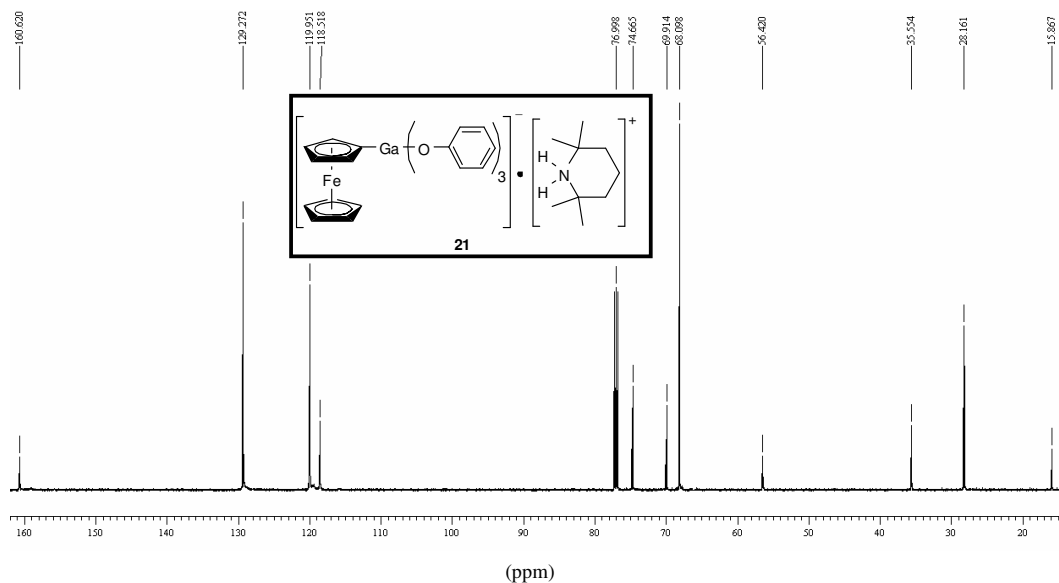


**Figure 39:**  $^{13}\text{C}$ -NMR spectrum of **21** in  $\text{CDCl}_3$ .

#### 4. Reactivity Studies on **8** and **9**

The NMR spectra of **22** are in agreement with its molecular structure. In the  $^1\text{H}$ -NMR spectrum of **22** (Fig. 40) the resonances of the phenolate rests appear in the specific aromatic area ( $\delta \text{ } ^1\text{H} = 7.13, 6.92$  and  $6.81$ ) in a 6:6:3 integral ratios. This is high field shifted compared with **21**. Three broad signals are produced by the Cp rings, two of them belong to the substituted Cp ring ( $\delta \text{ } ^1\text{H} = 4.21$  and  $3.83$ ) and the other one represents the resonance of the other five equivalent hydrogen atoms from the unsubstituted Cp ring ( $\delta \text{ } ^1\text{H} = 3.68$ ). Finally, two broad signals occur by the hydrogen atoms of the thf residues ( $\delta \text{ } ^1\text{H} = 3.77$  and  $1.76$ ).

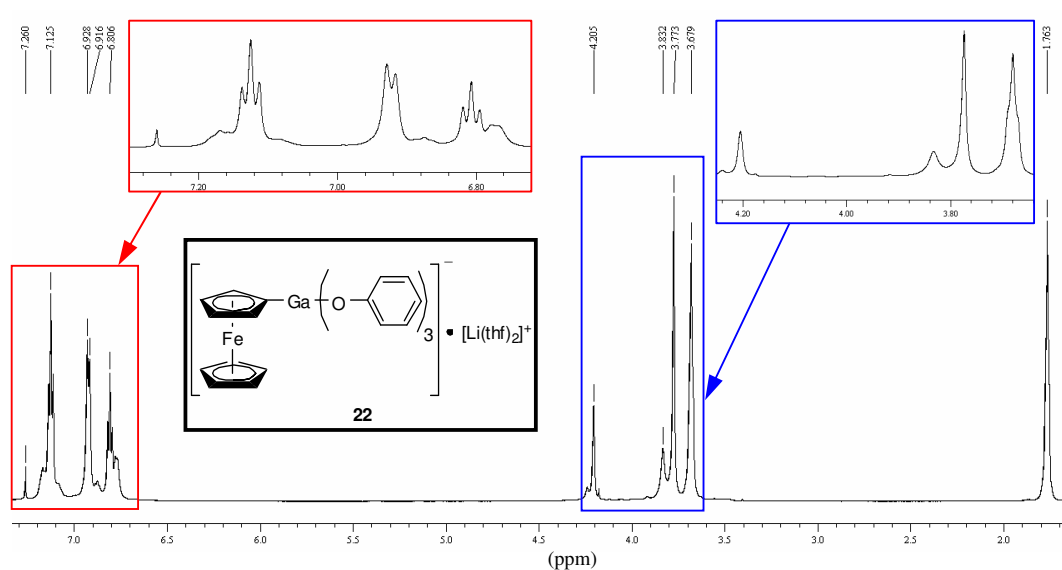


**Figure 40:**  $^1\text{H}$ -NMR spectrum of **22** in  $\text{CDCl}_3$ , at room temperature, with the inset showing an expanded view of the chemical shift range from 7.26 to 6.72 respectively from 4.24 to 3.64 ppm.

The  $^{13}\text{C}$ -NMR spectrum of **22** is similar to that of **21**, excepting the anionic part. Slight low field shifting of the substituted and unsubstituted Cp-ring carbon atoms was observed ( $\delta \text{ } ^{13}\text{C} = 74.7, 70.2$  -  $\text{CH}(\text{subst. Cp})$  and  $68.2$  -  $\text{CH}(\text{unsubst. Cp})$ ). Instead of signals for  $\text{tmpH}_2^+$ , two signals for thf groups occur ( $\delta \text{ } ^{13}\text{C} = 68.1, 25.4$ ) (Fig. 41).

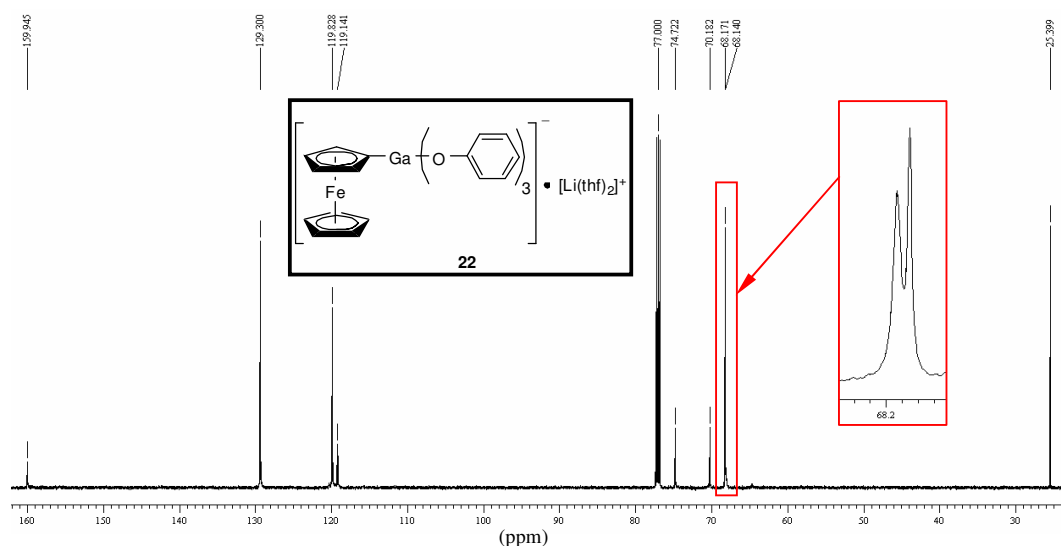


**Figure 41:**  $^{13}\text{C}$ -NMR spectrum of **22** in  $\text{CDCl}_3$ .

### 4.3.3. Crystal Structure Analysis

#### 4.3.3.1. Crystal Structure Analysis of **22**

The molecular structure of **22** is depicted in Figure 42. Suitable orange crystals for X-ray diffraction of **22** were collected from a thf: *n*-hexane solution (1:1) after several days standing at 6°C. **22** crystallizes in the triclinic system, space group  $\text{P}\bar{1}$ . The Ga atom is tetrahedral coordinated by three oxygen atoms (O1, O2 and O3) and one carbon atom (C18) from the substituted Cp-ring. The Cp-rings are in an eclipsed conformation. The Ga-O distances vary from 183.8(3) to 188.4(3) pm, are typical for Ga-O bond lengths having gallium atoms in a tetrahedral conformation. **22** exhibits the shortest reported Ga-C bond [ $d_{\text{Ga}(1)\text{-C}(18)} = 191.3$  pm] in this series of gallylferrocenes. The O-Ga-O bond angles (84.8° - 113.4°) are describing a distorted tetrahedral conformation at the gallium atoms. The O-Ga-C bond angle (112.2°) is wider than the tetrahedral angle. The lithium ion is bounded to the oxygen atoms of two of the phenolates [ $d_{\text{Li-O}} = 195.1$  pm and 195.8 pm]. A tetrahedral coordination at the lithium atom is afforded. The O-Li-O bond angles are describing a distorted tetrahedral conformation. Two angles are wider than the tetrahedral angle (110.1° and 132.6°) and the other two are narrower than the tetrahedral angle (108.8°).

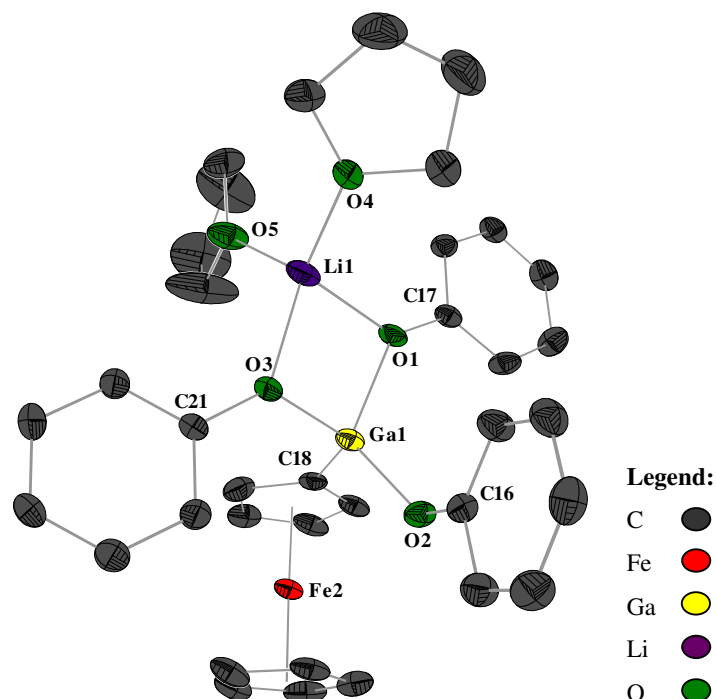


**Figure 42:** Solid state structure of **22** showing thermal ellipsoids at the 25% probability level. Selected bond lengths [pm] and angles [°]: Ga(1)-C(18) 191.3(6), Ga(1)-O(1) 188.4(3), Ga(1)-O(2) 183.8(3), Ga(1)-O(3) 185.8(4), Li(1)-O(1) 195.8(12), Li(1)-O(3) 195.1(8), Li(1)-O(4) 190.6(10), Li(1)-O(5) 192.8(10), Ga(1)···Li(1) 286.5(10), Ga(1)···Fe(2) 353.8(13), O(1)-C(17) 134.6(6), O(2)-C(16) 134.3(6), O(3)-C(21) 136.9(6), O(4)-C(32) 143.8(7), O(4)-C(45) 142.7(7), O(5)-C(24) 140.5(7), O(5)-C(43) 140.7(8); O(1)-Ga(1)-C(18) 115.51(17), O(2)-Ga(1)-C(18) 112.2(2), O(3)-Ga(1)-C(18) 116.4(2), O(1)-Ga(1)-O(2) 113.4(15), O(1)-Ga(1)-O(3) 84.8(15), O(2)-Ga(1)-O(3) 112.0(16), O(1)-Li(1)-O(3) 80.4(4), O(1)-Li(1)-O(4) 110.1(5), O(1)-Li(1)-O(5) 114.3(5), O(3)-Li(1)-O(4) 132.6(5), O(3)-Li(1)-O(5) 107.7(4), O(4)-Li(1)-O(5) 108.8(5).

#### 4.4. Comparison of Important Bond Lengths

The main features of interest of **8** and **9** are of course the Ga-C and Ga-N bond lengths and the Ga···Fe and respectively Ga···Ga interactions (only for **9**). Several gallyl ferrocenes derivatives are discussed from the above mentioned features point of view. Also, it is necessary to mention that until now almost all of the reported gallyl ferrocenes exhibits in their backbones, attached ligands to the gallium atoms, which include carbon and nitrogen atoms resulting in Ga-C and Ga-N bonds,<sup>[1]-[9]</sup> with four exceptions where instead of nitrogen atoms, oxygen atoms are presented, giving rise to Ga-O moieties.<sup>[8], [9]</sup> All Ga-C and Ga-N bond lengths determined for compounds **8** and

**9** and all reported Ga-C and Ga-N bond lengths in different gallyl ferrocenes derivatives are summarized in Table 4.

**Table 4:** Summary of Ga-C and Ga-N bond lengths.

Compound	$d_{\text{Ga-C}}$ [pm]	$d_{\text{Ga-N}}$ [pm]
<b>8</b> <sup>[10]</sup>	197.4(3) and 197.9(3) 197.7 (ave.)	187.9(2), 188.0(2), <b>187.2(2)<sup>b</sup></b> and 187.3(2) <b>187.6<sup>b</sup></b> (ave.)
<b>9</b>	200.9(4)	188.0(4) and 190.7(3) 189.4 (ave.)
$[\{\text{Fe}(\eta^5\text{-C}_5\text{H}_4)_2\}\{\text{GaC}(\text{SiMe}_3)_2(\text{SiMe}_2\text{NMe}_2)\}]^{[5]}$	200.8(3), 201.7(3) and 204.8(3) 202.4 (ave.)	210.5(2)
$[\{(\eta^5\text{-C}_5\text{H}_5)\text{Fe}(\eta^5\text{-C}_5\text{H}_3)\}\{\text{GaMe}_2(\text{CH}_2\text{NMe}_2)\}]_2^{[2]}$	199.5(4), 200.4(3) and 201.6(4) 200.5 (ave.)	217.8(2)
$[\{\text{Fe}(\eta^5\text{-C}_5\text{H}_4)_2\}\{\text{GaMe}_2\}]_n^{[7]}$	197.8(2), <b>277.5(2)<sup>a</sup></b> , 196.5(3), 195.7(2), 198.9(2), 241.0(2), 196.9(2) and 197.4(2) <b>212.7<sup>a</sup></b> (ave.)	-
$[\{\text{Fe}(\eta^5\text{-C}_5\text{H}_4)_2\}\{\text{GaMe}_2(\text{Phenazine})\}]_n^{[7]}$	197.1(4), 198.0(4) and 197.5(4) 197.5 (ave.)	<b>240.8(3)<sup>a</sup></b>
$[\{\text{Fe}(\eta^5\text{-C}_5\text{H}_4)_2\}\{\text{GaCH}(\text{SiMe}_3)_2\}]^{[3]}$	196.9(4), 193.4(4) and <b>193.3(4)<sup>b</sup></b> <b>194.5<sup>b</sup></b> (ave.)	-
$[\{\text{Fe}(\eta^5\text{-C}_5\text{H}_4)_2\}\{\text{Ga}(\text{Pytsi})_2\}]^{[4]}$	198.8(3), 195.1(4) and 196.3(3) 196.7 (ave.)	217.8(3)
$[\{\text{Fe}(\eta^5\text{-C}_5\text{H}_4)_2\}_3\{\text{Ga}(\text{Pyridine})\}]_2^{[6]}$	196.8(19), 196.5(17) and 197.3(17) 196.8 (ave.)	214.3(14)
$[\{\text{Fe}(\eta^5\text{-C}_5\text{H}_4)_2\}\{\text{GaMe}\}]_2^{[8]}$	194.42(15), 194.56(15) and 195.02(18) 194.7 (ave.)	-

#### 4. Reactivity Studies on **8** and **9**

**Table 4:** (Continuation).

Compound	$d_{\text{Ga-C}}$ [pm]	$d_{\text{Ga-N}}$ [pm]
$[\{\text{Fe}(\eta^5\text{-C}_5\text{H}_4)_2\}_2\{\text{GaMe}(\text{Et}_2\text{O})\}_2]^{[8]}$	196.2(4), 195.7(3) and 197.7(4) 196.5 (ave.)	-
$[\{\text{Fe}(\eta^5\text{-C}_5\text{H}_4)_2\}_2\{\text{GaMe}(\text{Pyridine})\}_2]^{[8]}$	198.1(6), 195.7(6) and 197.6(7) 197.1 (ave.)	214.4(5)
$[\{\text{Fe}(\eta^5\text{-C}_5\text{H}_4)_2\}_2\{\text{GaMe}(\text{Pyrimidine})\}_2]^{[8]}$	197.0(2), 196.1(2) and 197.6(2) 196.9 (ave.)	215.08(16)
$[\{\text{Fe}(\eta^5\text{-C}_5\text{H}_4)_2\}_2\{\text{GaMe}(\text{Quinoxaline})\}_2]^{[8]}$	196.30(19), 196.5(2) and 197.8(2) 196.9 (ave.)	221.92(16)
$[\{\text{Fe}(\eta^5\text{-C}_5\text{H}_4)_2\}_2\{\text{GaMe}(\text{Pyrazine})\}_2]^{[8]}$	196.05(17), 196.56(17) and 197.75(19) 196.8 (ave.)	218.54(14)
$[\{\text{Fe}(\eta^5\text{-C}_5\text{H}_4)_2\}_2\{\text{GaMe}(\text{Diox})\}_2]^{[8]}$	195.5(2), 196.1(3) and 198.6(3) 196.7 (ave.)	-
$[\{(\eta^5\text{-C}_5\text{H}_5)\text{Fe}(\eta^5\text{-C}_5\text{H}_4)\}\{\text{GaMe}_2\}_2]^{[1]}$	199.1 (5) and 196.4 (5) 197.8 (ave.)	-
$[\{\text{Fe}(\eta^5\text{-C}_5\text{H}_4)_2\}_3\{\text{Ga}(\text{Et}_2\text{O})\}_2]^{[9]}$	195.16(16), 194.61(16) and 194.99(16) 194.9 (ave.)	-
$[\{\text{Fe}(\eta^5\text{-C}_5\text{H}_4)_2\}_3\{\text{Ga}(\text{Pyridine})\}_2]^{[9]}$	196.8(19), 196.5(17) and 197.3(17) 196.9 (ave.)	214.3(14)
$[\{\text{Fe}(\eta^5\text{-C}_5\text{H}_4)_2\}_3\{\text{Ga}(\text{DMSO})\}_2]^{[9]}$	195.2(2), 195.8(2) and 195.7(2) 195.6 (ave.)	-
$[\{\text{Fe}(\eta^5\text{-C}_5\text{H}_4)_2\}_3\{\text{Ga}(\text{Pyrazine})\}_2]^{[9]}$	196.3(4), 194.3(4) and 196.1(4) 195.6 (ave.)	228.0(3)

<sup>a</sup> – largest bond length

<sup>b</sup> – shortest bond length

It can be easily seen that Ga-C bond lengths in **8** and **9** are in line with other reported Ga-C bond lengths in gallium substituted ferrocene. But, when we take a look to the Ga- N bond lengths, then, one can say that the shortest Ga-N bond length

is exhibited by **8** follow closely by **9** [ $d_{\text{Ga-N}} = 187.6$  pm and 189.4 pm]. Their values are much closer to the other compounds of type  $\text{tmp}_2\text{GaX}$  where X is a less electron withdrawing groups as Ph [ $d_{\text{Ga-N}} = 188.3(2)$  pm],  $\text{tmp}_2\text{Ga}$  [ $d_{\text{Ga-N}} = 190.1(4)$  pm],<sup>[14]</sup>  $\text{P}^t\text{Bu}_2$  [ $d_{\text{Ga-N}} = 190.8$  pm].<sup>[15]</sup>

The intermolecular Ga $\cdots$ Ga separation in **8** is 717.1 pm. Due to the conformation of **8** is much longer than in other gallyl ferrocenes derivatives (see Table 5) and in the same time is roughly four times the van der Waals radius of gallium (187 pm<sup>[16]</sup>). However, there is one reported gallyl ferrocene ( $\{[\text{Fe}(\eta^5\text{-C}_5\text{H}_4)_2]\{[\text{GaMe}_2(\text{Phenazine})_2]_n\}$ <sup>[7]</sup>) with the Ga $\cdots$ Ga separation of 619.2 pm, which is the most close value to that of **8**. Another Ga $\cdots$ Ga separation with a value of approximately 700 pm is presented by **14** [ $d_{\text{Ga}\cdots\text{Ga}} = 690.0$  pm] (see Table 7).

The intermolecular Ga $\cdots$ Fe average distance of 370.8 pm in **8** and respectively of 379.0 pm in **9** indicate no attractive interactions between the electron-rich Fe atoms and the electron deficient Ga atoms (empty p orbital).

**Table 5:** Summary of Ga $\cdots$ Fe and Ga $\cdots$ Ga separation.

Compound	$d_{\text{Ga}\cdots\text{Ga}}$ [pm]	$d_{\text{Ga}\cdots\text{Fe}}$ [pm]
<b>8</b> <sup>[10]</sup>	717.1	374.2 and 367.4 370.8 (ave.)
<b>9</b>	-	379.0
$\{[\text{Fe}(\eta^5\text{-C}_5\text{H}_4)_2]\{[\text{GaC}(\text{SiMe}_3)_2(\text{SiMe}_2\text{NMe}_2)]\}$ <sup>[5]</sup>	-	281.8
$\{[(\eta^5\text{-C}_5\text{H}_5)\text{Fe}(\eta^5\text{-C}_5\text{H}_3)]\{[\text{GaMe}_2(\text{CH}_2\text{NMe}_2)]_2\}$ <sup>[2]</sup>	473.7	352.2
$\{[\text{Fe}(\eta^5\text{-C}_5\text{H}_4)_2]\{[\text{GaMe}_2]_2\}_n$ <sup>[7]</sup>	304.4	311.2 and 341.9 326.6 (ave.)
$\{[\text{Fe}(\eta^5\text{-C}_5\text{H}_4)_2]\{[\text{GaMe}_2(\text{Phenazine})_2]_n\}$ <sup>[7]</sup>	619.2	345.6
$\{[\text{Fe}(\eta^5\text{-C}_5\text{H}_4)_2]_2\{[\text{GaCH}(\text{SiMe}_3)_2]_2\}$ <sup>[3]</sup>	462.5	354.0 and 351.3 352.7 (ave.)
$\{[\text{Fe}(\eta^5\text{-C}_5\text{H}_4)_2]_2\{[\text{Ga}(\text{Pytsi})_2]_2\}$ <sup>[4]</sup>	473.4	371.0 and 351.5 361.2 (ave.)
$\{[\text{Fe}(\eta^5\text{-C}_5\text{H}_4)_2]_3\{[\text{Ga}(\text{Pyridine})]_2\}$ <sup>[6]</sup>	386.4	365.3, 369.3 and 375.2 369.9 (ave.)
$\{[\text{Fe}(\eta^5\text{-C}_5\text{H}_4)_2]_2\{[\text{GaMe}]_2\}$ <sup>[8]</sup>	441.4	348.1 and 353.6 350.8 (ave.)
$\{[\text{Fe}(\eta^5\text{-C}_5\text{H}_4)_2]_2\{[\text{GaMe}(\text{Et}_2\text{O})]_2\}$ <sup>[8]</sup>	464.7	361.8 and 353.0 357.4 (ave.)

**Table 5:** (Continuation).

Compound	$d_{\text{Ga}\dots\text{Ga}}$ [pm]	$d_{\text{Ga}\dots\text{Fe}}$ [pm]
$[\{\text{Fe}(\eta^5\text{-C}_5\text{H}_4)_2\}_2\{\text{GaMe}(\text{Pyridine})\}_2]^{[8]}$	476.8	368.2 and 354.0 361.1 (ave.)
$[\{\text{Fe}(\eta^5\text{-C}_5\text{H}_4)_2\}_2\{\text{GaMe}(\text{Pyrimidine})\}_2]^{[8]}$	463.1	357.1 and 360.8 359.0 (ave.)
$[\{\text{Fe}(\eta^5\text{-C}_5\text{H}_4)_2\}_2\{\text{GaMe}(\text{Quinoxaline})\}_2]^{[8]}$	473.4	362.6 and 359.4 361.0 (ave.)
$[\{\text{Fe}(\eta^5\text{-C}_5\text{H}_4)_2\}_2\{\text{GaMe}(\text{Pyrazine})\}_2]^{[8]}$	458.1	357.1, 357.3, 359.6 and 356.1 357.5 (ave.)
$[\{\text{Fe}(\eta^5\text{-C}_5\text{H}_4)_2\}_2\{\text{GaMe}(\text{Diox})\}_2]^{[8]}$	447.6	345.7 and 359.5 352.6 (ave.)
$[\{(\eta^5\text{-C}_5\text{H}_5)\text{Fe}(\eta^5\text{-C}_5\text{H}_4)\}_2\{\text{GaMe}_2\}_2]^{[11]}$	299.9	466.1 and 317.7 391.9 (ave.)
$[\{\text{Fe}(\eta^5\text{-C}_5\text{H}_4)_2\}_3\{\text{Ga}(\text{Et}_2\text{O})\}_2]^{[9]}$	372.1	368.7, 366.1 and 365.1 366.3 (ave.)
$[\{\text{Fe}(\eta^5\text{-C}_5\text{H}_4)_2\}_3\{\text{Ga}(\text{DMSO})\}_2]^{[9]}$	379.5	364.9, 368.4, 370.0, 362.7, 363.6 and 371.2 366.8 (ave.)
$[\{\text{Fe}(\eta^5\text{-C}_5\text{H}_4)_2\}_3\{\text{Ga}(\text{Pyrazine})\}_2]^{[9]}$	381.4	364.7, 364.3, 369.6, 367.8, 366.0 and 361.8 365.7 (ave.)

The bond lengths (Ga-C and Ga-O) and the intermolecular separations (Ga $\cdots$ Fe, Ga $\cdots$ Ga and Fe $\cdots$ Fe) of the other gallyl substituted ferrocenes presented in this chapter are discussed as follow. Thus, the Ga-C and respectively the Ga-O bonds lengths in the gallyl substituted ferrocenes reported in this thesis and other gallyl substituted ferrocenes reported in the literature (instead of the gallyl substituted ferrocenes **8** and **9**), which exhibits also Ga-C and Ga-O bonds, are summarized in Table 6.



**Table 6:** Summary of Ga-C and Ga-O bond lengths.

Compound	$d_{\text{Ga-C}}$ [pm]	$d_{\text{Ga-O}}$ [pm]
<b>13</b> <sup>[10]</sup>	193.8(9) and <b>191.7(9)</b> <sup>b*</sup> <b>192.8</b> <sup>b</sup> (ave.)	188.6(5), 242.4(5), 193.6(6), 189.2(5), 189.8(5), 190.7(6), 194.6(6), and 234.1(5) 202.9 (ave.)
<b>14</b> <sup>[10]</sup>	194.4(3)	189.5(2), 189.2(2) and 189.4(2) 189.4 (ave.)
<b>15</b> <sup>[10]</sup>	192.3(19) ÷ 199.3(19) 195.8 (ave.)	<b>179.5(12)</b> <sup>b</sup> ÷ 194.3(13) <b>186.9</b> <sup>b</sup> (ave.)
$[\{\text{Fe}(\eta^5\text{-C}_5\text{H}_4)_2\}_2\{\text{GaMe}(\text{Et}_2\text{O})\}_2]$ <sup>[8]</sup>	196.2(4), 195.7(3) and 197.7(4) 196.5 (ave.)	215.3(2)
$[\{\text{Fe}(\eta^5\text{-C}_5\text{H}_4)_2\}_2\{\text{GaMe}(\text{Diox})\}_2]$ <sup>[8]</sup>	195.5(2), 196.1(3) and 198.6(3) 196.7 (ave.)	<b>220.00(17)</b> <sup>a</sup>
$[\{\text{Fe}(\eta^5\text{-C}_5\text{H}_4)_2\}_3\{\text{Ga}(\text{Et}_2\text{O})\}_2]$ <sup>[9]</sup>	195.16(16), 194.61(16) and 194.99(16) 194.9 (ave.)	215.51(12)
$[\{\text{Fe}(\eta^5\text{-C}_5\text{H}_4)_2\}_3\{\text{Ga}(\text{DMSO})\}_2]$ <sup>[9]</sup>	195.2(2), 195.8(2) and 195.7(2) 195.6 (ave.)	209.84(13)

<sup>a</sup> – largest bond length<sup>b</sup> – shortest bond length

\* – see Table 4

If we take a look at the Ga-C bond lengths presented in Table 6 and respectively at the Ga-C bond lengths exhibited by Table 4 it can be observed that the Ga-C bond lengths reported for the gallyl substituted ferrocenes synthesized in this thesis, in big line, are at similar lengths with the other gallyl substituted ferrocenes reported in the literature. The shortest Ga-C bond length reported so far is afforded by the digallyl substituted ferrocenes **13** [ $d_{\text{Ga-C}} = 191.7$  pm]. This can be an effect of the substituents directed bonded at the gallium atoms.

On the other hand, the shortest Ga-O bond lengths is afforded by the gallaferrocenophane **15** [ $d_{\text{Ga-O}} = 179.5$  pm] which is 41 pm shorter than the longest reported Ga-O moiety [ $d_{\text{Ga-O}} = 220.0$  pm].<sup>[8]</sup> The other gallyl substituted ferrocenes discussed in this chapter shows Ga-O bond lengths in agreement with the reported values for this type of moiety.

A large intermolecular Ga $\cdots$ Ga separation is observed for the digallyl substituted ferrocene **14** [ $d_{\text{Ga}\cdots\text{Ga}} = 690.0$  pm], but a little bit smaller than that reported for **8** (see Table 5). These two values of the intermolecular Ga $\cdots$ Ga separation are the largest reported so far. Having so big separation values between the gallium atoms, it can be concluded that no metal-metal interactions between gallium atoms are presented.

The Ga $\cdots$ Fe distance values reported for **13**, **14** and **15** are not so different from the other Ga $\cdots$ Fe distance values reported in the literature (see Table 7) and in the same time big enough to have no interaction between the Ga and Fe atoms.

Only **15** exhibit in its backbone more than one ferrocenyl unit giving rise to a possible intermolecular Fe $\cdots$ Fe interaction. As it was observed from its single crystal X-ray analysis (see Chapter 4.2.5.3.), in its structure, four ferrocenyl fragments are bonded through a gallium-oxygen cage. Here, the distance between the Fe atoms is the largest distance reported for a gallaferrocenophane, so far [ $d_{\text{Fe}\cdots\text{Fe}} = 748.3$  pm (ave.)] that can explain its electrochemical behavior in comparison with  $[\{\text{Fe}(\eta^5\text{-C}_5\text{H}_4)_2\}_3\{\text{Ga}(\text{Do})\}_2]$ <sup>[9]</sup> which has the Fe $\cdots$ Fe distance with about 200 pm shorter than **15**. A similar value of the Fe $\cdots$ Fe distance was reported for the ferrocenylgallane dimer  $[\{(\eta^5\text{-C}_5\text{H}_5)\text{Fe}(\eta^5\text{-C}_5\text{H}_4)\}\{\text{GaMe}_2\}]_2$ <sup>[11]</sup> [ $d_{\text{Fe}\cdots\text{Fe}} = 739.2$  pm (ave.)].

**Table 7:** Summary of intermolecular Ga<sup>III</sup>-Fe, Ga<sup>III</sup>-Ga and Fe<sup>III</sup>-Fe separations.

Compound	$d_{\text{Ga}\dots\text{Ga}}$ [pm]	$d_{\text{Ga}\dots\text{Fe}}$ [pm]	$d_{\text{Fe}\dots\text{Fe}}$ [pm]
<b>13</b> <sup>[10]</sup>	372.4	351.2 and 351.6 351.4 (ave.)	-
<b>14</b> <sup>[10]</sup>	690.0	345.0	-
<b>15</b> <sup>[10]</sup>	316.8, 319.6, 318.0 and 319.6 318.5 (ave.)	355.8, 356.6, 354.8, 355.4, 356.8, 359.6, 357.6 and 352.4 356.1 (ave.)	778.0, 728.8, 754.8 and 731.6 748.3 (ave.)
$[\{\text{Fe}(\eta^5\text{-C}_5\text{H}_4)_2\}_2\{\text{GaCH}(\text{SiMe}_3)_2\}_2]$ <sup>[3]</sup>	*	*	532.5
$[\{\text{Fe}(\eta^5\text{-C}_5\text{H}_4)_2\}_2\{\text{Ga}(\text{Pytsi})_2\}_2]$ <sup>[4]</sup>	*	*	546.2
$[\{\text{Fe}(\eta^5\text{-C}_5\text{H}_4)_2\}_3\{\text{Ga}(\text{Pyridine})\}_2]$ <sup>[6]</sup>	*	*	540.3, 540.3 and 558.2 546.3 (ave.)
$[\{\text{Fe}(\eta^5\text{-C}_5\text{H}_4)_2\}_2\{\text{GaMe}\}_2]$ <sup>[8]</sup>	*	*	545.5
$[\{\text{Fe}(\eta^5\text{-C}_5\text{H}_4)_2\}_2\{\text{GaMe}(\text{Et}_2\text{O})\}_2]$ <sup>[8]</sup>	*	*	543.2
$[\{\text{Fe}(\eta^5\text{-C}_5\text{H}_4)_2\}_2\{\text{GaMe}(\text{Pyridine})\}_2]$ <sup>[8]</sup>	*	*	542.7
$[\{\text{Fe}(\eta^5\text{-C}_5\text{H}_4)_2\}_2\{\text{GaMe}(\text{Pyrimidine})\}_2]$ <sup>[8]</sup>	*	*	548.5
$[\{\text{Fe}(\eta^5\text{-C}_5\text{H}_4)_2\}_2\{\text{GaMe}(\text{Quinoxaline})\}_2]$ <sup>[8]</sup>	*	*	545.0
$[\{\text{Fe}(\eta^5\text{-C}_5\text{H}_4)_2\}_2\{\text{GaMe}(\text{Pyrazine})\}_2]$ <sup>[8]</sup>	*	*	549.0
$[\{\text{Fe}(\eta^5\text{-C}_5\text{H}_4)_2\}_2\{\text{GaMe}(\text{Diox})\}_2]$ <sup>[8]</sup>	*	*	545.1
$[\{(\eta^5\text{-C}_5\text{H}_5)\text{Fe}(\eta^5\text{-C}_5\text{H}_4)\}\{\text{GaMe}_2\}_2]$ <sup>[11]</sup>	*	*	739.2
$[\{\text{Fe}(\eta^5\text{-C}_5\text{H}_4)_2\}_3\{\text{Ga}(\text{Et}_2\text{O})\}_2]$ <sup>[9]</sup>	*	*	545.2, 545.2 and 551.0 547.1 (ave.)
$[\{\text{Fe}(\eta^5\text{-C}_5\text{H}_4)_2\}_3\{\text{Ga}(\text{DMSO})\}_2]$ <sup>[9]</sup>	*	*	547.1, 535.8 and 548.0 543.6 (ave.)
$[\{\text{Fe}(\eta^5\text{-C}_5\text{H}_4)_2\}_3\{\text{Ga}(\text{Pyrazine})\}_2]$ <sup>[9]</sup>	*	*	545.5, 539.7 and 536.1 540.4 (ave.)

\* - see Table 5

### References

- [1] B. Lee, W. T. Pennington, J. A. Laske, and G. H. Robinson, *Organometallics*, **1990**, *9*, 2864-2865.
- [2] E. Hecht, *Z.Anorg.Allg.Chem.*, **2000**, *626*, 759-765.
- [3] W. Uhl, I. Hahn, A. Jantschak, and T. Spies, *J. Org. Chem.*, **2001**, *637-639*, 300-303.
- [4] J. A. Schachner, G. A. Orłowski, J. W. Quail, H.-B. Kraatz, and J. Müller, *Inorg. Chem.*, **2006**, *45*, 454-459.
- [5] C. L. Lund, J. A. Schachner, J. W. Quail, and J. Müller, *Organometallics*, **2006**, *25*, 5817-5823.
- [6] P. Jutzi, N. Lenze, B. Neumann, and H.-G. Stammer, *Angew. Chem. Int. Ed.*, **2001**, *40(8)*, 1423-1427.
- [7] A. Althoff, P. Jutzi, N. Lenze, B. Neumann, A. Stammer, and H.-G. Stammer, *Organometallics*, **2002**, *21*, 3018-3022.
- [8] A. Althoff, P. Jutzi, N. Lenze, B. Neumann, A. Stammer, and H.-G. Stammer, *Organometallics*, **2003**, *22*, 2766-2774.
- [9] A. Althoff, D. Eisner, P. Jutzi, N. Lenze, B. Neumann, W. W. Schoeller, and H.-G. Stammer, *Chem. Eur. J.*, **2006**, *12(21)*, 5471-5480.
- [10] O. Feier-Iova, and G. Linti, *Z. Anorg. Allg. Chem.* **2008**, *634*, 559-564.
- [11] O. Feier-Iova, and G. Linti, *WCECS*, **2007**, Proceedings, ISBN: 978-988-98671-6-4, 182-187.
- [12] F. Fabrizi de Biani, T. Gmeinwieser, E. Herdtweck, F. Jäkle, F. Laschi, M. Wagner, and P. Zanello, *Organometallics*, **1997**, *16*, 4776-4787.
- [13] M. C. Schnitzler, A. S. Mangrich, W. A. A. Macedo, J. D. Ardisson, and A. J. G. Zarbin, *Inorg. Chem.*, **2006**, *45*, 10642-10650.
- [14] G. Linti, R. Frey, and M. Schmidt, *Z. Naturforsch. Teil B*, **1994**, *49b*, 958-962.
- [15] G. Linti, R. Frey, W. Köstler, and H. Schwenk, *Chem. Ber.*, **1997**, *130*, 663-668.
- [16] A. Bondi, *J. Phys. Chem.*, **1964**, *68*, 441-451.

## 5. Conclusion and Outlook

With the bis(amino)gallium substituted ferrocene derivative **8**, a useful synthetic tool is available to synthesize various digallyl substituted ferrocenes (**13**, **14**, **16** and **17**) or digallylferrocenophane derivatives (**15**). **9** also proves to be a valuable synthon for the synthesis of other monogallyl substituted ferrocene (**20**, **21** and **22**).

Due to the insertion of carbon dioxide in the gallium-nitrogen bonds, new expectations are opened on using these compounds for the synthesis of new ferrocenyl gallane with different “inert molecules”.

A new type of ferrocenyl oligomers is obtained together with the first member of this class (**15**) prepared by mixed alcoholysis/hydrolysis, whose structure is determined by a gallium/oxo cage.

The reported new gallyl substituted ferrocene derivatives complete the small family of ferrocene substituted gallanes, and together with compounds **18** and **19** exhibit great possibilities to be further used as precursors in the synthesis of semiconductors. Also, these compounds might be used as single-source molecular precursors in the synthesis of Ga-O-N thin films, with addition of other elements as Fe.

An interesting further research work could be the synthesis of new oligomers or polymers *via* thermolysis reaction, having in their backbones these gallyl substituted ferrocenes. As well, using these gallyl substituted ferrocenes in the metalorganic chemical vapor deposition of GaN : Fe and (Ga,Fe)N layers, as single-source molecular precursors might be possible.

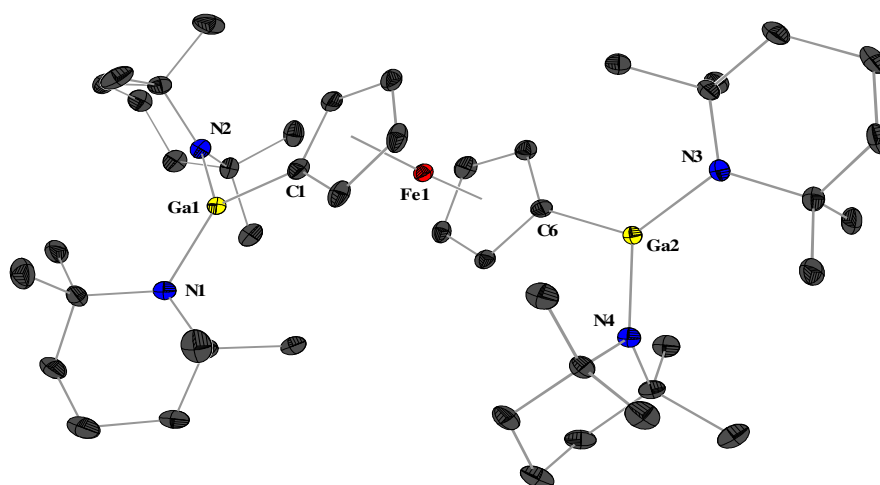


## 6. Summary

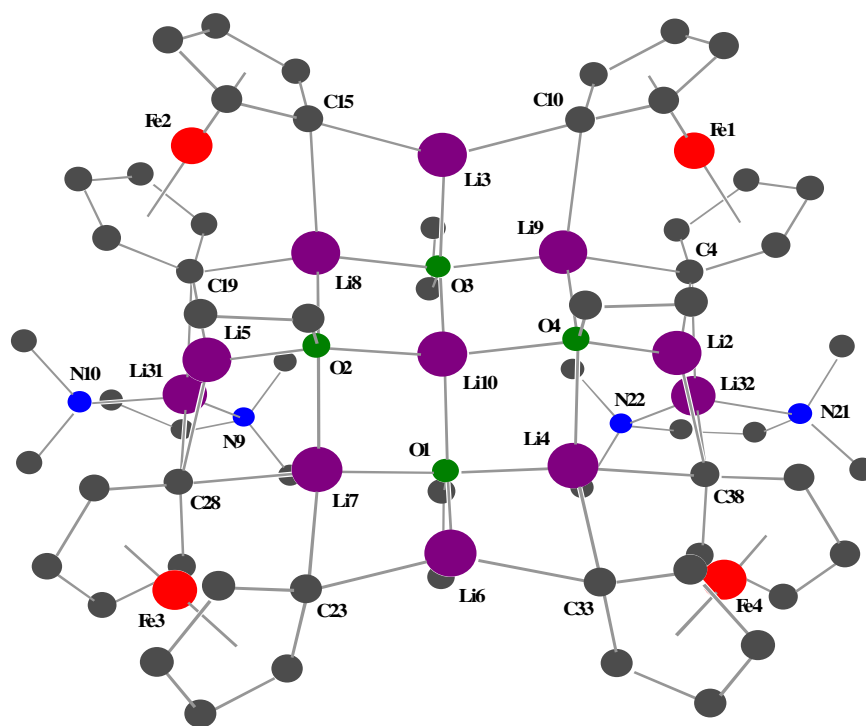
Because of the lowest development in the gallyl substituted ferrocenes chemistry, although the ferrocenyl derivatives found many applications, a new insight in the chemical and physical properties of the previous mentioned compounds was required. With this thesis, new informations regarding the stability, different properties and atoms arrangement in solid state structures of a serie of mono- and bisubstituted ferrocenyl gallanes are presented.

As starting materials two gallyl substituted ferrocenes **8** and **9** from actually four synthesized gallyl substituted (also **10** and **11**) ferrocenes were used. The disubstituted and the monosubstituted gallyl ferrocenes **10** and **11** could not be further used as starting materials because of their low yields.

The disubstituted gallyl ferrocene **8** was synthesized by treating of the monomeric bis(2,2,6,6,-tetramethylpiperidino)gallium chloride **1** with a suspension of  $[\text{Li}_2\{\text{Fe}(\eta^5\text{-C}_5\text{H}_4)_2\} \cdot 2/3 \text{ TMEDA}]$  in hexane. It leads not only to the isolation of the first starting material, but also to the isolation of a side product which shows a lithium ferrocene cage of nine lithium atoms and four disubstituted ferrocenyl rests (**12**).



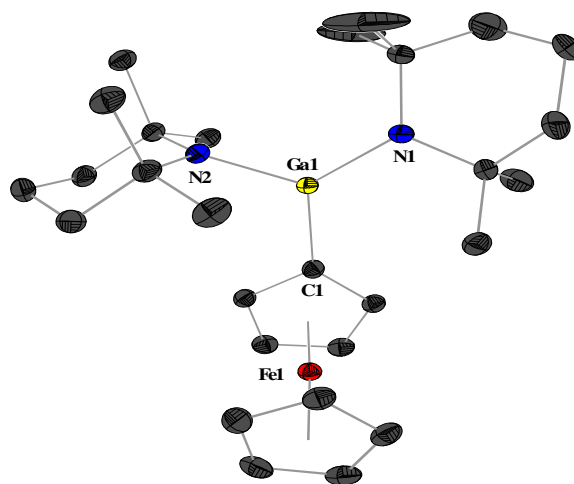
8



12

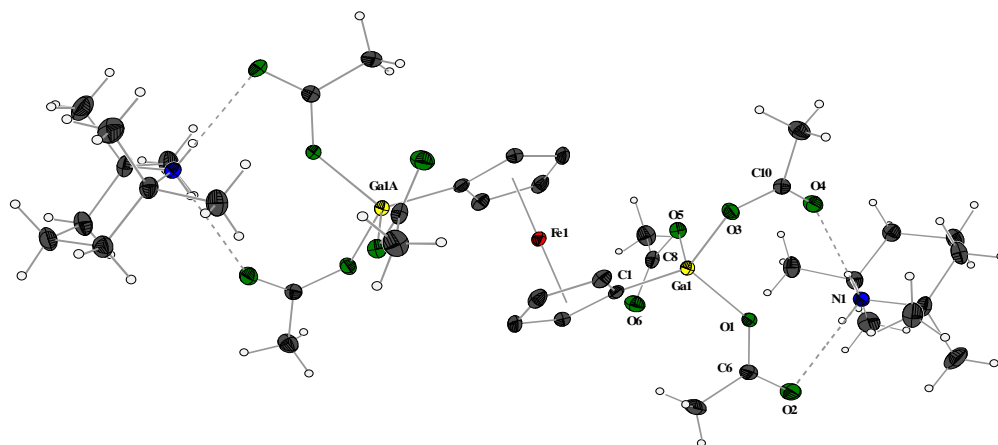
The monosubstituted gallyl ferrocene **9**, which is in fact the second starting material, was achieved in moderate yield from the reaction of **1** with monolithiated ferrocene obtained *in situ*.



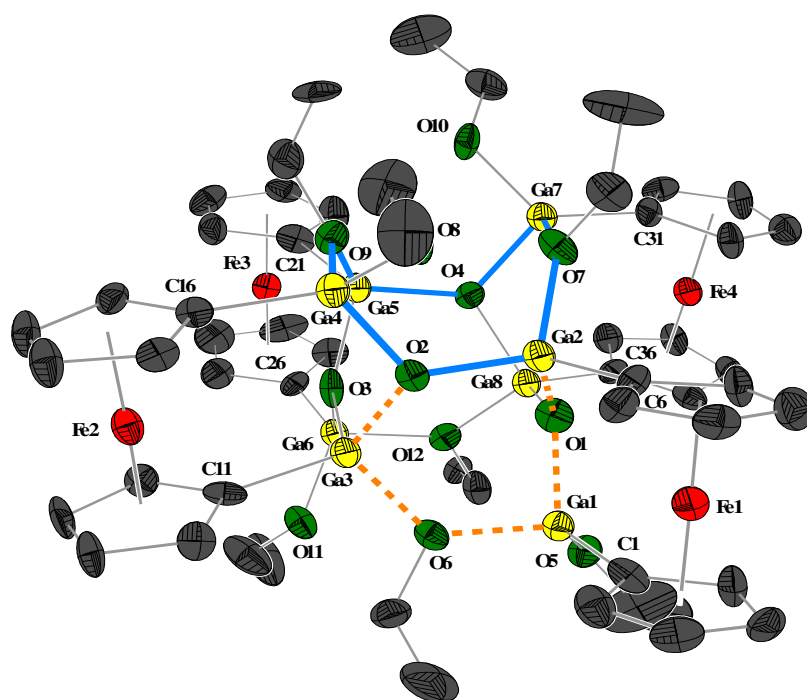


9

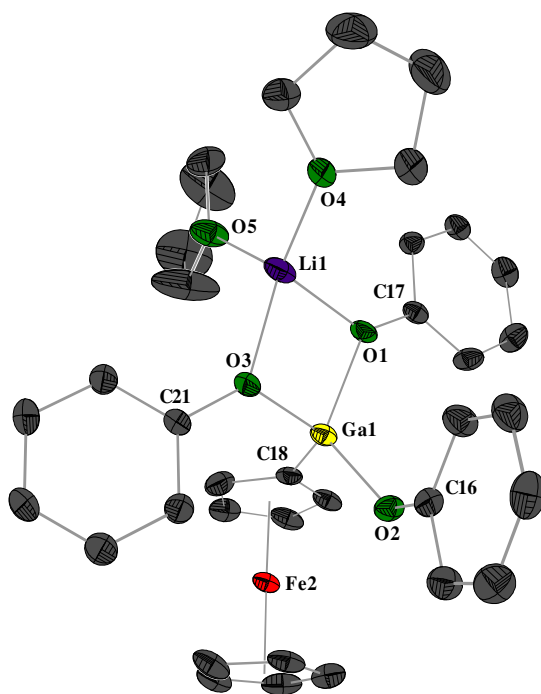
In the course of our investigations on the chemical properties of the mono- or disubstituted gallyl ferrocenes **8** and **9**, we observed a different behavior of the previous mentioned gallyl substituted ferrocenes in the reaction with mono- and diacids. When **8** or **9** react with monoacids as acetic acid, ethanol or phenol different gallyl substituted ferrocenes and a gallaferrocenophane are obtained. The new gallyl substituted ferrocenes obtained in these reactions, are formed from a substitution reaction at the gallium atoms where the tmp units are replaced with carboxylato groups (**14** and **20**), phenolato groups (**16**, **17**, **21** and **22**) or with ethoxylato rests, where the first member (**15**) of a new gallaferrocenophane class was synthesized. Several from these new products could be characterized by single crystal X-ray analyses.



14

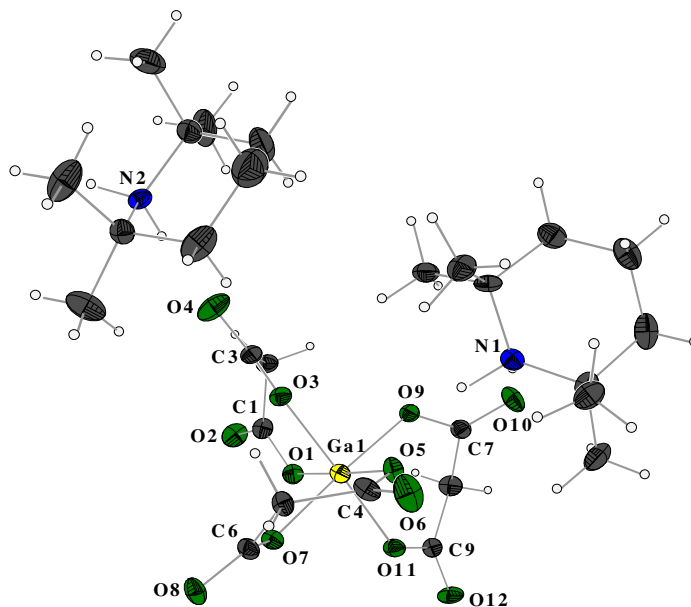
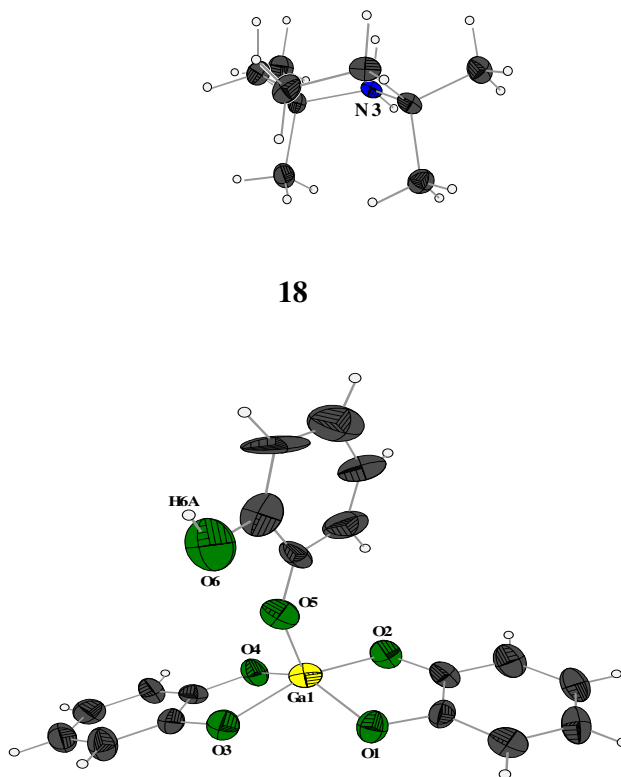


15

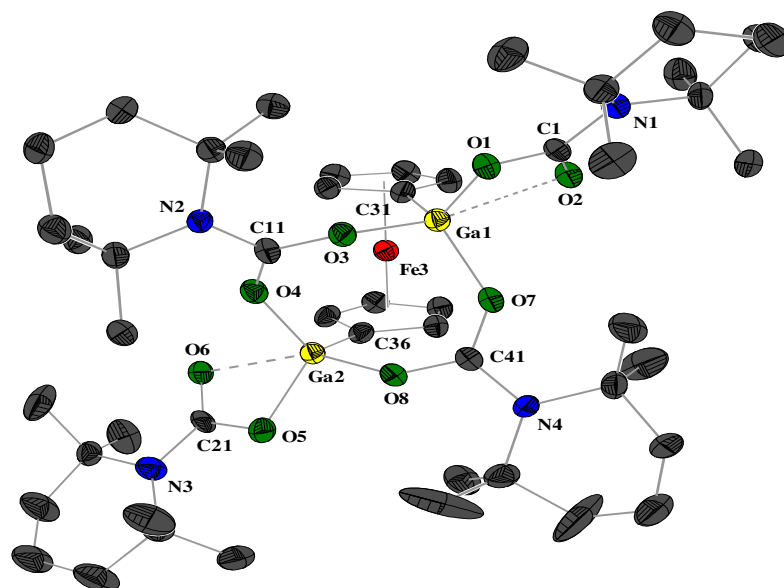


22

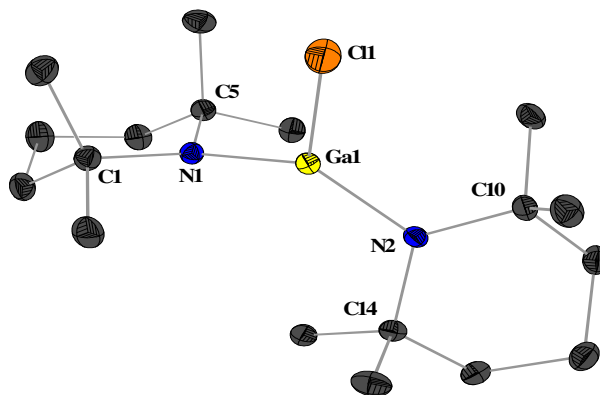
By the reaction of **8** or **9** with diacids malonic acid and catechol, not only the cleavage of the Ga-tmp bonds is observed but also the Ga-C moiety is broken, resulting in new gallium alkoxide complexes as **18** and **19**.

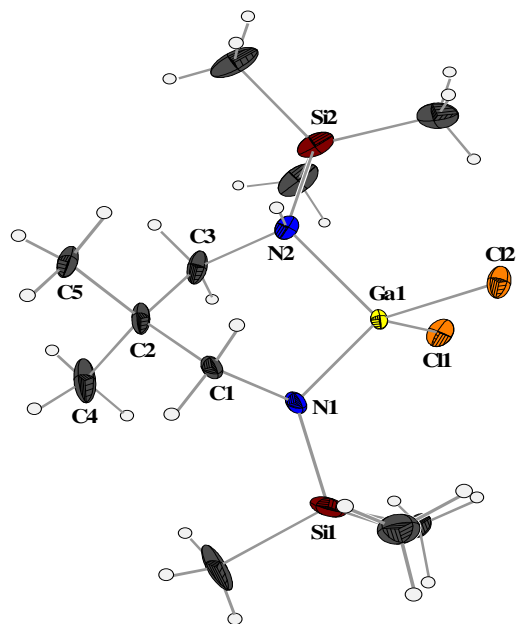
**18****19**

Even almost inert molecules, as carbon dioxide, could be activated through an insertion of CO<sub>2</sub> into all four gallium-nitrogen bonds of **8** giving the new gallium carbamate **13**.

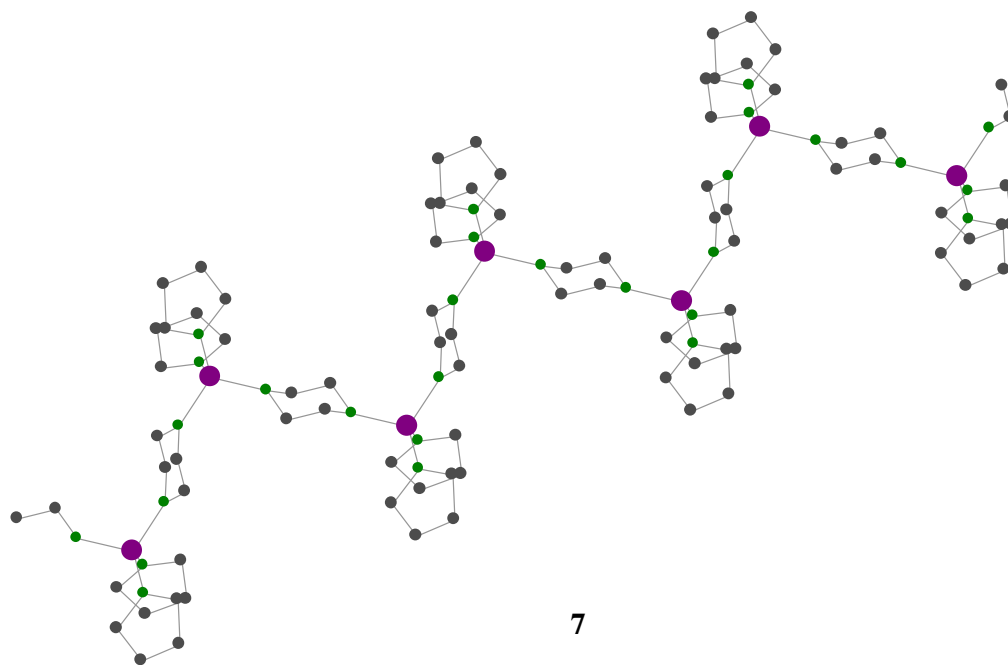
**13**

Three other suitable crystals for analysis were collected. The first one came from the monomeric **1**, which till now was not possible because of the low melting point of its crystals. From the synthesis of the monomeric **6**, the second convenient single crystals for further X-ray analyses were collected accompanied by the colorless crystals of the side product **7**. **7** shows a polymeric cationic chain in solid state.

**1**



6



7

The electrochemical behaviour of **8**, **9**, **13**, **14** and **15** was determined *via* cyclic voltammetry. Here, the higher oxidation potential was recorded for the monosubstituted gallyl ferrocene **8** ( $E_{1/2} = 121$  mV). This indicates that the monosubstituted gallyl ferrocene **8** is more difficult oxidized than ferrocene and than the other gallyl substituted ferrocenes. In the same time for the

## 6. Summary

---

tetranuclear species **15** only one oxidation-reduction peak is observed. This could be an effect of the well separated ferrocenyl units and because of that, probably, no delocalization is possible.

Usually, the mass spectra recorded for these substituted ferrocenyl gallanes did not show the molecular ion peaks, indicating a low stability in gas phase. The only one molecular ion was observed for **13** that indicates a highest stability of **13** in comparison with the other gallyl ferrocenyl derivatives.

Several quantum chemical calculations on the model compound  $[\text{Fc}\{\text{Ga}(\text{NR}_2)\}_n]$  ( $\text{Fc} = \{(\eta^5\text{-C}_5\text{H}_5)\text{Fe}(\eta^5\text{-C}_5\text{H}_4)\}$  or  $\{\text{Fe}(\eta^5\text{-C}_5\text{H}_4)_2\}$ ,  $\text{R} = \text{tmp}$ ,  $n = 0, 1$  or  $2$ ) have been performed. These bring a new insight in the energetical characteristics of the previous mentioned substituted gallyl ferrocenes **8** and **9**.

## 7. Experimental

### 7.1. General Remarks

All operations were performed in vacuum or under purified and dried argon using Schlenk techniques. Solvents were dried prior to use, using standard techniques, and stored under argon atmosphere. All other chemicals were of commercial reagent grade and used without any further purification directly as purchased.

#### 7.1.1. NMR Spectroscopy

The NMR spectra were recorded using three different spectrometers: Bruker ARX 200, Bruker Advance II 400 and Bruker Advance III 600. All the chemical shifts were referenced to internal solvent resonance and reported to external standard tetramethylsilane ( $^1\text{H}$ ,  $^{13}\text{C}$ ,  $^{29}\text{Si}$ ).

#### 7.1.2. Elementary Analysis

Elementary analyses (EA) were recorded by the Micro Analytical Laboratory of the Institute of Inorganic Chemistry, Heidelberg. The measured samples were embedded in two micro aluminum containers and put in the machine. A Vario EL Elementar analysis apparatus was used. The deviations which appeared in the results from calculated values are due to the extremely air-sensitive and hygroscopic nature of some of the compounds.

### 7.1.3. Mass Spectrometry

The mass spectra were recorded on a JEOL JMS-700 (EI) and a Finnigan TSQ 700 (ESI) machine. For all EI mass spectra, 70 eV electron beam energy was operated. All the samples were directly brought in the ionization field using a glass tube.

### 7.1.4. Cyclovoltammetry

All electrochemical experiments were carried out with a Princeton Applied Research Potentiostat/Galvanostat Model 263A respectively the corresponding software Power Suite 2.11. A three-electrode system was used. The working electrode employed was a glass carbon electrode (2 mm diameter). A silver wire, immersed in a solution of 0.1 M tetrabutylammonium hexafluorophosphate (NBu<sub>4</sub>PF<sub>6</sub>) in thf, was the pseudo reference electrode. Platinum wire was used as the auxiliary electrode. For all the CVs measurements, IR compensation was applied in order to reduce the thf resistance. The scan rate used was 25 mV/s. Bis(pentamethylcyclopentadienyl)cobaltocene tetrafluoroborate was added for each measurement as an internal standard. All the measured redox potentials were later converted into ferrocene/ferrocenium ([FeCp<sub>2</sub>]/[FeCp<sub>2</sub>]<sup>+</sup>) potentials ( $E([\text{CoCp}^*_2]) = -585 \text{ mV (in thf vs. [FeCp}_2\text{]/[FeCp}_2\text{]}^+;$  our own measurement). Experiments were performed under strict inert conditions. Measurements were taken at room temperature (296 K) in thf as solvent with NBu<sub>4</sub>PF<sub>6</sub> as supporting electrolyte.

### 7.1.5. X-ray Analysis

Suitable single crystals were mounted with perfluorated polyether oil on the tip of a glass fiber and cooled immediately on the goniometric head. Data collections were performed with Mo(K<sub>α</sub>) radiation (graphite monochromated) on a Stoe IPDSI diffractometer. The structures were solved and refined using the Bruker AXS SHELXTL (PC) package<sup>[1]</sup>. The non-hydrogen atoms were given anisotropic displacement parameters. All hydrogen atoms bonded to carbon atoms were included in calculated positions and refined using a *riding model* with fixed isotropic U's in the final refinement. All the crystal structures were solved by Direct Methods and refined by full-matrix least-squares against  $F^2$ . The positions of other hydrogen atoms were



taken from a difference Fourier map and refined isotropically. For supplementary details, see appendices on crystallographic data, without structure factors, or see the Cambridge Crystallographic Data Center where have been deposited some structures reported in this thesis. The supplementary publication numbers are: CCDC - 652002 - 652004 (**1**, **8**, **13**). These data can be obtained free of charge from via [www.ccdc.cam.ac.uk/data\\_request/cif](http://www.ccdc.cam.ac.uk/data_request/cif), or on application to CCDC, 12 Union Road, Cambridge CB 2 1 EZ, UK [Fax: int. code +44(1223)336-033; E-mail: [deposit@ccdc.cam.ac.uk](mailto:deposit@ccdc.cam.ac.uk)]. The data for the other structures (**6**, **7**, **9**, **12**, **14**, **15**, **18**, **19**, **22**) reported in this thesis are deposited at Prof. Dr. Gerald Linti, University of Heidelberg, Institute of Inorganic Chemistry, Im Neuenheimer Feld 270, D-69120 Heidelberg, Germany Fax: +49-6221-546617, E-mail: [gerald.linti@aci.uni-heidelberg.de](mailto:gerald.linti@aci.uni-heidelberg.de)

All the structures were solved by Prof. Dr. Gerald Linti.

#### 7.1.6. Quantum Chemical Calculations

Theory level used: B3LYP/6-311G(d) for all the atoms. Single-points energies were calculated with GAUSSIAN 03<sup>[2]</sup> software and the crystals coordinate from the structures of **8** and **9** were used, respectively.

For ab initio Electronic Structure Calculations of ferrocene, the same (GAUSSIAN 03<sup>[2]</sup>) software was used.

#### 7.1.7. EPR Spectroscopy

A Bruker Biospin Elexsys spectrometer equipped with a variable temperature accessory from Eurotherm and a *Super High Q* Cavity was used. The X-band was about 9 GHz. EPR spectrum had been measured in a glassy solution obtained by freezing (at 105 K) the disubstituted gallyl ferricenium in a thf/toluene (1:1) solution mixture. The sample was measured in seals quartz tubes (under argon) place in the Eurotherm (B-VT-2000) dewar filled with liquid nitrogen, respectively. The spectrum was visualized by using the Bruker Xepr software (Version 2.4b.12).

### 7.1.8. Melting Point

Melting points were measured with a Gallenkamp Melting Point Apparatus. The measurements were made using sealed capillaries. The reported values of the melting points are the one directly recorded from the apparatus, without further corrections.

### 7.1.9. Chemical used

$[\text{N}(\text{SiMe}_3)_2]_2\text{GaCl}$ ,<sup>[3]</sup>  $\text{Me}_2\text{C}\{[\text{CH}_2\text{N}(\text{Li})\text{SiMe}_3]\{\text{CH}_2\text{N}(\text{H})\text{SiMe}_3\}\}$ ,<sup>[4]</sup>  $\text{tmpLi}$ ,<sup>[5]</sup>  $\text{tmp}_2\text{GaCl}$ ,<sup>[6],[7]</sup>  $[\text{Li}_2\{\text{Fe}(\eta^5\text{-C}_5\text{H}_4)_2\} \cdot 2/3 \text{ TMEDA}]$ ,<sup>[8]</sup>  $[\text{Li}(\eta^5\text{-C}_5\text{H}_4)\text{Fe}(\eta^5\text{-C}_5\text{H}_5)]$ <sup>[9]</sup> were prepared as described in the literature.

## 7.2. Preparation of Amino Gallium Halides

### 7.2.1. Synthesis of **6** and **7**

A solution of the *N,N'*-disilylated amine **3** (1.6 g, 6.34 mmol) was lithiated with a solution of <sup>t</sup>BuLi in hexane (0.41 g, 6.4 mmol) cooling the solution at -78 °C. The resulting solution was stirred further for 2 hours (10 minutes at -78 °C and 110 minutes by room temperature) until the evolution of butane was finished. The amide solution was transferred to a dropping funnel and added slowly (over a period of 20 minutes) to a solution of GaCl<sub>3</sub> (1.12 g, 6.34 mmol) in 10 ml thf/diox (10:1) (at -78 °C). Then the cooling bath was removed continuing the stirring over night.

After stirring the mixture for 18 hours, all volatiles were evaporated under *vacuum* and a white jelly was obtained. This residue was treated with diethyl ether (50 ml), upon a while LiCl precipitated. Then the mixture was filtrated and the filtrate concentrated to 1/3 of the original volume. On cooling the solution at -32 °C for several days, 1.79 g of **6** (yield: 73 %) precipitated as colorless crystals.

M.p.: 71-73 °C, (216-220 °C dec.);

<sup>1</sup>H NMR (600 MHz, CDCl<sub>3</sub>, 25°C): δ = 3.04 (d, <sup>2</sup>J<sub>H,H</sub> = 13.2 Hz, 1H, NCH<sub>2</sub>), 2.86 (t, <sup>3</sup>J<sub>H,H</sub> = 12.4 Hz, 1H, N(H)CH<sub>2</sub>), 2.75 (dd, <sup>4</sup>J<sub>H,H</sub> = 13.2 Hz, 1H, NCH<sub>2</sub>),

2.59 (dt,  $^4J_{\text{H,H}} = 12.4$  Hz, 1H,  $\text{NCH}_2$ ), 1.96 (d,  $^3J_{\text{H,H}} = 12.4$  Hz, 1H,  $\text{NH}$ ), 1.05 (s, 3H,  $\text{CH}_3$ ), 0.89 (s, 3H,  $\text{CH}_3$ ), 0.47 (s, 9H,  $\text{Si}(\text{CH}_3)_3\text{NH}$ ), 0.09 (s, 9H,  $\text{Si}(\text{CH}_3)_3$ );

$^{13}\text{C}$  NMR ( $\text{CDCl}_3$ , 25°C):  $\delta = 56.5, 55.2$  ( $\text{CH}_2$ ), 35.0 ( $\text{C}(\text{CH}_3)_2$ ), 26.7, 21.6 ( $\text{CH}_3$ ), 0.8, -1.0 ( $\text{Si}(\text{CH}_3)_3$ );

EA  $\text{C}_{11}\text{H}_{29}\text{GaN}_2\text{Si}_2$  (386.17): calcd. C 34.21, H 7.57, N 7.25; found C 33.81, H 7.52, N 7.20;

MS (70eV, EI-MS,  $^{69}\text{Ga}$ ):  $m/z$  (%) = 281 (12)  $[\text{M} - 7\text{CH}_3]^+$ , 268 (5)  $[\text{M} - \text{Si}(\text{CH}_3)_3 - 3\text{CH}_3]^+$ , 253 (8)  $[\text{M} - \text{Si}(\text{CH}_3)_3 - 4\text{CH}_3]^+$ , 170 (30)  $[\text{M} - 2\text{Si}(\text{CH}_3)_3 - 2\text{CH}_3 - \text{C}(\text{CH}_2)_2]^+$ , 30 (100)  $[2\text{CH}_3]^+$ .

### 7.3. Preparation of Ferrocenyl Substituted Bis(amino)gallanes

#### 7.3.1. Synthesis of **8** and **12**

A solution of 2.71 g (7.02 mmol) **1** in 60 ml *n*-hexane was cooled at -78 °C and a suspension of 0.97 g (3.52 mmol)  $[\text{Li}_2\{\text{Fe}(\eta^5\text{-C}_5\text{H}_4)_2\} \cdot 2/3\text{TMEDA}]$  in 30 ml *n*-hexane was added dropwise. The solution was stirred for 18 h. During this time, the color changed to red-orange and a precipitate of LiCl was formed. The reaction mixture was filtrated and the filtrate was reduced to one-third of its original volume and stored at -32 °C for several days, resulting in a deposition of 2.58 g (yield: 83 %) of red-orange crystals of **8**. In the same time, some red crystals were collected and investigated by X-ray single crystal analysis giving rise to a new dilithioferrocene-TMEDA adduct with eleven lithium atoms and four ferrocenyl units in its backbone **12**.

M.p.: 198-200 °C;

$^1\text{H}$  NMR (400 MHz,  $\text{C}_6\text{D}_6$ , 25 °C):  $\delta = 4.62$  (pseudo-t,  $^3J_{\text{H,H}} = ^4J_{\text{H,H}} = 1.6$  Hz, 4 H,  $\text{Cp-H}^2 / \text{H}^5$  or  $\text{Cp-H}^3 / \text{H}^4$ ), 4.53 (pseudo-t,  $^3J_{\text{H,H}} = ^4J_{\text{H,H}} = 1.6$  Hz, 4 H,  $\text{Cp-H}^2 / \text{H}^5$  or  $\text{Cp-H}^3 / \text{H}^4$ ), 1.77 ( $m_c$ , 8 H, tmp- $\gamma\text{-CH}_2$ ), 1.57 (s, 48 H, tmp- $\text{CH}_3$ ), 1.51 (pseudo-t,  $^2J_{\text{H,H}} = ^3J_{\text{H,H}} = 6.3$  Hz, 16 H, tmp- $\beta\text{-CH}_2$ );

## 7. Experimental

---

$^{13}\text{C}$  NMR ( $\text{C}_6\text{D}_6$ , 25 °C):  $\delta$  = 80.4 (*ipso*-C, subst. Cp-ring), 77.9 (Cp- $\text{C}^3/\text{C}^4$  or Cp- $\text{C}^2/\text{C}^5$ ), 71.9 (Cp- $\text{C}^3/\text{C}^4$  or Cp- $\text{C}^2/\text{C}^5$ ), 54.2 (tmp- $\text{C}^2/\text{C}^6$ ), 40.7 (tmp- $\text{C}^3/\text{C}^5$ ), 34.9 (tmp- $\text{C}^7/\text{C}^8/\text{C}^9/\text{C}^{10}$ ), 18.6 (tmp- $\text{C}^4$ );

EA  $\text{C}_{46}\text{H}_{80}\text{FeGa}_2\text{N}_4$  (884.47): calcd.: C 62.47, H 9.12, N 6.33, found: C 59.80, H 8.62, N 5.92;

MS (70eV, EI-MS,  $^{69}\text{Ga}$ ):  $m/z$  (%) = 489 (0.6) [ $\text{tmp}_3\text{Ga}$ ] $^+$ , 253 (0.8) [ $\{\text{Fe}(\eta^5\text{-C}_5\text{H}_4)_2\}\text{Ga}$ ] $^+$ , 186 (94) [ $\text{C}_{10}\text{H}_{10}\text{Fe}$ ] $^+$ , 141 (31) [ $\text{C}_9\text{H}_{19}\text{N}$ ] $^+$ , 126 (100) [ $\text{tmpH-Me}$ ] $^+$ , 121 (44) [ $\text{C}_5\text{H}_5\text{Fe}$ ] $^+$ , 69 (100) [ $\text{Ga}$ ] $^+$ , 58 (100) [ $\text{Fe}$ ] $^+$ .

### 7.3.2. Synthesis of **8a**

A solution of 0.033 g (0.205 mmol) bromine in 5 ml *n*-hexane was added dropwise *via* a syringe to a solution of 0.360 g (0.41 mmol) **8** in 15 ml *n*-hexane. The reaction took place at room temperature. The color changed rapidly from orange to green and then to blue, with the formation of a precipitate. All volatiles were evacuated under *vacuum* and the resulting solid was washed several times with *n*-hexane yielding (0.084 g, 21% yield) the disubstituted gallyl ferricenium species, as a blue solid.

### 7.3.3. Synthesis of **9**

To a solution of 2.35 g (12.63 mmol) ferrocene in 30 ml thf, chilled at -20 °C, 11.15 ml (18.95 mmol) of 1.7 M  $t\text{-BuLi}$  in pentane were added dropwise (over a period of 20 min.). After the addition was complete, the mixture was stirred further for 120 min. and allowed to warm up slowly at -10 °C. Then it was stirred another 2 h and allowed to warm at r.t. and stirred further for another 30 min. During this time, the color changed to deep red. The monolithioferrocene solution was transferred into a dropping funnel and added dropwise into a solution of 4.87 g (12.63 mmol) **1** in 60 ml *n*-hexane. The reaction mixture was stirred over night and the color changed to red-orange. All volatiles were evacuated under *vacuum* and the resulting solid was dissolved in 70 ml *n*-hexane with the precipitation of LiCl. The reaction mixture was filtrated and the filtrate was reduced to one-third of its original volume and stored at -32 °C for several days, resulting in a deposition of 3.11 g (yield: 46 %) of red-orange crystals of **9**.

$^1\text{H}$  NMR (600 MHz,  $\text{C}_6\text{D}_6$ , 25 °C):  $\delta$  = 4.55 (pseudo-t,  $^3\text{J}_{\text{H,H}} = ^4\text{J}_{\text{H,H}} = 1.6$  Hz, 2 H, Cp- $H^2 / H^5$  or Cp- $H^3 / H^4$ ), 4.31 (pseudo-t,  $^3\text{J}_{\text{H,H}} = ^4\text{J}_{\text{H,H}} = 1.6$  Hz, 2 H, Cp- $H^2 / H^5$  or Cp- $H^3 / H^4$ ), 4.07 (s, 5 H unsubst. Cp-ring), 1.74 (m<sub>c</sub>, 4 H, tmp- $\gamma$ -CH<sub>2</sub>), 1.51 (s, 24 H, tmp-CH<sub>3</sub>), 1.46 (pseudo-t,  $^2\text{J}_{\text{H,H}} = ^3\text{J}_{\text{H,H}} = 6.2$  Hz, 8 H, tmp- $\beta$ -CH<sub>2</sub>);

$^{13}\text{C}$  NMR ( $\text{C}_6\text{D}_6$ , 25 °C):  $\delta$  = 81.0 (*ipso*-C, subst. Cp-ring), 77.6 (Cp- $C^3/C^4$  or Cp- $C^2/C^5$ ), 71.2 (Cp- $C^3/C^4$  or Cp- $C^2/C^5$ ), 68.7 (unsubst. Cp-ring), 54.1 (tmp- $C^2/C^6$ ), 40.8 (tmp- $C^3/C^5$ ), 34.8 (tmp- $C^7/C^8/C^9/C^{10}$ ), 18.7 (tmp- $C^4$ );

EA  $\text{C}_{28}\text{H}_{45}\text{FeGa}\text{N}_2$  (535.26): calcd.: C 62.83, H 8.47, N 5.23, found: C 61.25, H 7.66, N 3.99;

#### 7.3.4. Synthesis of **10**

A suspension of (1.28 g, 4.65 mmol)  $[\text{Li}_2\{\text{Fe}(\eta^5\text{-C}_5\text{H}_4)_2\} \cdot 2/3\text{TMEDA}]$  in 40 ml *n*-hexane was added dropwise into a solution of (3.51 g, 9.11 mmol) **2** in 50 ml *n*-hexane with continuous stirring at room temperature. In a few minutes, the solution gets an orange color. Then, the reaction mixture was stirred over night. At the end of reaction, a white precipitate was formed and the solution color turned red-orange. After the removal of the precipitate, by filtration and the removal of all volatiles under *vacuum*, the product **10** as an orange solid was afforded. Yield: 42 %.

$^1\text{H}$  NMR (600 MHz,  $\text{C}_6\text{D}_6$ , 25 °C):  $\delta$  = 4.61 (pseudo-t,  $^3\text{J}_{\text{H,H}} = ^4\text{J}_{\text{H,H}} = 1.6$  Hz, 4 H, Cp- $H^2 / H^5$  or Cp- $H^3 / H^4$ ), 4.41 (pseudo-t,  $^3\text{J}_{\text{H,H}} = ^4\text{J}_{\text{H,H}} = 1.6$  Hz, 4 H, Cp- $H^2 / H^5$  or Cp- $H^3 / H^4$ ), 0.40 (s, 72 H, N(Si(CH<sub>3</sub>)<sub>3</sub>)<sub>2</sub>).

$^{13}\text{C}$  NMR ( $\text{C}_6\text{D}_6$ , 25 °C):  $\delta$  = 77.4 (Cp- $C^3/C^4$  or Cp- $C^2/C^5$ ), 72.0 (Cp- $C^3/C^4$  or Cp- $C^2/C^5$ ), 6.1 (N(Si(CH<sub>3</sub>)<sub>3</sub>)<sub>2</sub>).

#### 7.3.5. Synthesis of **11**

To a solution of 0.98 g (5.27 mmol) ferrocene in 15 ml thf, chilled at - 20 °C, 4.65 ml (7.91 mmol) of 1.7 M  $t\text{BuLi}$  in pentane was added dropwise (over a period of 20 min.). After the addition was complete, the mixture was stirred further for 120 min and allowed to warm up slowly at - 10 °C. Then it was stirred another 2 h and allowed to

warm at r.t. and stirred further for another 30 min. During this time, the color changed to deep red. The monolithioferrocene solution was put into a dropping funnel and added dropwise into a solution of 3.02 g (5.27 mmol) **2** in 30 ml *n*-hexane. The reaction mixture was stirred over night and the color change to red-orange. All volatiles were evacuated under *vacuum* and the resulting solid was treated with 40 ml *n*-hexane. The reaction mixture was filtrated and the filtrate was reduced to one-third of its original volume and stored at -32 °C for several days, resulting in a deposition of 1.10 g (yield: 29 %) of red-orange crystals of **11**.

<sup>1</sup>H NMR (600 MHz, C<sub>6</sub>D<sub>6</sub>, 25 °C): δ = 4.31 (pseudo-t, <sup>3</sup>J<sub>H,H</sub> = <sup>4</sup>J<sub>H,H</sub> = 1.6 Hz, 2 H, Cp-*H*<sup>2</sup> / *H*<sup>5</sup> or Cp-*H*<sup>3</sup> / *H*<sup>4</sup>), 4.27 (pseudo-t, <sup>3</sup>J<sub>H,H</sub> = <sup>4</sup>J<sub>H,H</sub> = 1.6 Hz, 2 H, Cp-*H*<sup>2</sup> / *H*<sup>5</sup> or Cp-*H*<sup>3</sup> / *H*<sup>4</sup>), 4.11 (s, 5 H, unsubst. Cp-ring), 0.51 (s, 36 H, N(Si(CH<sub>3</sub>)<sub>3</sub>)<sub>2</sub>).

<sup>13</sup>C NMR (C<sub>6</sub>D<sub>6</sub>, 25 °C): δ = 76.7 (Cp-*C*<sup>3</sup>/*C*<sup>4</sup> or Cp- *C*<sup>2</sup>/*C*<sup>5</sup>), 71.8 (Cp-*C*<sup>3</sup>/*C*<sup>4</sup> or Cp- *C*<sup>2</sup>/*C*<sup>5</sup>), 68.9 (unsubst. Cp), 6.3 (N(Si(CH<sub>3</sub>)<sub>3</sub>)<sub>2</sub>).

### 7.4. Preparation of Different Derivatives of Mono- and Bisgallyl Substituted Ferrocenes

#### 7.4.1. Synthesis of **13**

Into a stirred solution of 0.21 g (0.23 mmol) **8** in 10 ml of thf, cooled at -78 °C, was added dry ice in excess. Within a few seconds the color changed from red-orange to yellow. Then the mixture was warmed up slowly at ambient temperatures and stirred for another 20 minutes. The clear yellow solution was reduced to one-third of its original volume and stored at -32 °C for several days. 0.23 g (yield: 94 %) **13** as yellow crystals formed.

M.p.: 216-219 °C;

<sup>1</sup>H NMR (400 MHz, CDCl<sub>3</sub>, 25 °C): δ = 4.39 (pseudo-t, <sup>3</sup>J<sub>H,H</sub> = <sup>4</sup>J<sub>H,H</sub> = 1.5 Hz, 4 H, Cp-*H*<sup>2</sup> / *H*<sup>5</sup> or Cp-*H*<sup>3</sup> / *H*<sup>4</sup>), 4.36 (pseudo-t, <sup>3</sup>J<sub>H,H</sub> = <sup>4</sup>J<sub>H,H</sub> = 1.5 Hz, 4 H, Cp-*H*<sup>2</sup> / *H*<sup>5</sup> or Cp-*H*<sup>3</sup> / *H*<sup>4</sup>), 1.70 (pseudo-t, 8 H, tmp-γ-CH<sub>2</sub>), 1.58 (m<sub>c</sub>, 16 H, tmp-β-CH<sub>2</sub>), 1.53 (s, 24 H, tmp-CH<sub>3</sub>), 1.44 (s, 24 H, μ<sup>2</sup>-tmp-CH<sub>3</sub>);

$^{13}\text{C}$  NMR ( $\text{CDCl}_3$ , 25 °C):  $\delta$  = 165.8 ( $\text{CO}_2\text{N}$ ), 161.3 ( $\text{CO}_2\text{N}$ ), 75.8 ( $\text{Cp-C}^3/\text{C}^4$  or  $\text{Cp-C}^2/\text{C}^5$ ), 71.6 ( $\text{Cp-C}^3/\text{C}^4$  or  $\text{Cp-C}^2/\text{C}^5$ ), 64.7 (*ipso*-C, subst. Cp-ring), 57.4 ( $\text{tmp-C}^2/\text{C}^6$ ), 56.7 ( $\text{tmp-C}^2/\text{C}^6$ ), 42.9 ( $\text{tmp-C}^3/\text{C}^5$ ), 40.7 ( $\text{tmp-C}^3/\text{C}^5$ ), 29.7 ( $\text{tmp-C}^7/\text{C}^8/\text{C}^9/\text{C}^{10}$ ), 29.6 ( $\text{tmp-C}^7/\text{C}^8/\text{C}^9/\text{C}^{10}$ ), 16.4 ( $\text{tmp-C}^4$ ), 15.7 ( $\text{tmp-C}^4$ );

EA  $\text{C}_{50}\text{H}_{80}\text{FeGa}_2\text{N}_4\text{O}_8$  (1060.52): calcd.: C 56.63, H 7.60, N 5.28, found: C 56.46, H 7.79, N 5.04;

MS (70eV, EI-MS,  $^{69}\text{Ga}$ ):  $m/z$  (%) = 1060 (0.4)  $[\text{M}]^+$ , 972 (7)  $[\text{M}-2\text{CO}_2]^+$ , 875 (0.4)  $[\text{M}-\text{tmpCO}_2]^+$ , 832 (14)  $[\text{M}-\text{tmp}_2\text{CO}_2]^+$ , 194 (3)  $[\text{tmpGa-Me}]^+$ , 186 (99)  $[\text{C}_{10}\text{H}_{10}\text{Fe}]^+$ , 141 (31)  $[\text{tmpH}]^+$ , 126 (100)  $[\text{tmpH-Me}]^+$ , 121 (27)  $[\text{C}_5\text{H}_5\text{Fe}]^+$ , 69 (100)  $[\text{Ga}]^+$ , 58 (100)  $[\text{Fe}]^+$ , 44 (97)  $[\text{CO}_2]^+$ .

#### 7.4.2. Synthesis of **14**

Into a solution of 0.43 g **8** (0.49 mmol) in 20 ml of diethyl ether, cooled at  $-78$  °C, a solution of 0.17 ml water free  $\text{H}_3\text{CCOOH}$  (2.99 mmol) in 5 ml of diethyl ether was added dropwise. Within a few seconds the color changed from red-orange to yellow. Then the mixture was allowed to warm up slowly at ambient temperature and stirred for an additional hour. A deposition of a yellow precipitate was observed. All volatiles were removed in *vacuum* (0.01 mbar) and the remaining solid was washed with hexane several times. Then the solid was dissolved in a 10:1 mixture of tetrahydrofuran/hexane and stored at  $-32$  °C for several days. 0.46 g **14** (Yield: 97 %) as yellow crystals were collected.

M.p.: 132 – 135 °C;

$^1\text{H}$  NMR (600 MHz,  $\text{CDCl}_3$ , 25 °C):  $\delta$  = 4.28 (br, H,  $\text{Cp-H}^2 / \text{H}^5$  or  $\text{Cp-H}^3 / \text{H}^4$ ), 4.24 (br, 4 H,  $\text{Cp-H}^2 / \text{H}^5$  or  $\text{Cp-H}^3 / \text{H}^4$ ), 2.10 (br, 4H,  $\text{tmpH}_2^+-\text{NH}_2$ ), 2.02 (br, 18 H,  $\text{O}_2\text{CCH}_3$ ), 1.69 (br, 4H,  $\text{tmpH}_2^+-\gamma\text{-CH}_2$ ), 1.62 (br, 8H,  $\text{tmpH}_2^+-\beta\text{-CH}_2$ ), 1.39 (br, 24H,  $\text{tmpH}_2^+-\text{CH}_3$ );

$^{13}\text{C}$  NMR ( $\text{CDCl}_3$ , 25 °C):  $\delta$  = 177.8 ( $\text{CO}_2\text{CH}_3$ ), 177.3 ( $\text{CO}_2\text{CH}_3$ ), 75.0 ( $\text{Cp-C}^3/\text{C}^4$  or  $\text{Cp-C}^2/\text{C}^5$ ), 70.5 ( $\text{Cp-C}^3/\text{C}^4$  or  $\text{Cp-C}^2/\text{C}^5$ ), 55.7 ( $\text{tmp-C}^2/\text{C}^6$ ), 35.2 ( $\text{tmp-C}^3/\text{C}^5$ ), 27.5 ( $\text{tmp-C}^7/\text{C}^8/\text{C}^9/\text{C}^{10}$ ), 23.6 ( $\text{CO}_2\text{CH}_3$ ), 16.4 ( $\text{tmp-C}^4$ );

## 7. Experimental

---

EA C<sub>40</sub>H<sub>66</sub>FeGa<sub>2</sub>N<sub>2</sub>O<sub>12</sub> (962.25): calcd. C 49.93, H 6.91, N 2.91, found C 50.25, H 7.06, N 3.05;

MS (5.5 kV, ESI-MS, thf, 8  $\mu$ l/min, <sup>69</sup>Ga): m/z (%) = (-): 431 (100) [Fe( $\eta^5$ -C<sub>5</sub>H<sub>4</sub>)GaAc<sub>3</sub>]<sup>-</sup>, 389 (53) [Fe( $\eta^5$ -C<sub>5</sub>H<sub>4</sub>)GaAc<sub>2</sub>OH]<sup>-</sup>. (Ac = CH<sub>3</sub>COO<sup>-</sup>).

### 7.4.3. Synthesis of **15**

0.64 g **8** (0.73 mmol) were dissolved in 20 ml of benzene at room temperature and 0.35 ml of 90%-ethanol (5.94 mmol) were added dropwise. Within a few seconds the color changed from red-orange to light yellow. Then the reaction mixture was stirred for another 15 minutes. The clear yellow solution was reduced to one-third of its original volume in *vacuum* and stored at -32 °C for several days. 0.22 g **15** (yield: 18 %) as yellow crystals precipitated.

M.p.: 119 – 123 °C, (240 °C dec.);

EA C<sub>56</sub>H<sub>72</sub>Fe<sub>4</sub>Ga<sub>8</sub>O<sub>12</sub> (1718.42): calcd. C 39.14, H 4.22, found C 36.22, H 4.43;

MS (70eV, EI-MS, <sup>69</sup>Ga): m/z (%) = 858 (0.2) [M/2]<sup>+</sup>, 186 (96) [C<sub>10</sub>H<sub>10</sub>Fe]<sup>+</sup>, 121 (60) [C<sub>5</sub>H<sub>5</sub>Fe]<sup>+</sup>, 69 (100) [Ga]<sup>+</sup>, 56 (30) [Fe]<sup>+</sup>.

### 7.4.4. Synthesis of **16** and **17**

A solution of C<sub>6</sub>H<sub>5</sub>OH (0.298 g, 3.17 mmol) in 5 ml thf was added dropwise *via* a syringe to a solution of **8** (0.458 g, 0.52 mmol) in 15 ml thf with continuous stirring at room temperature. The solution color turned immediately yellow. After the removal of all volatiles in *vacuum*, the residue was washed several times with *n*-hexane yielding a yellow powder of the mixture of **16** and **17**; 67 % yield based upon consumed **8**.

<sup>1</sup>H NMR (600 MHz, CDCl<sub>3</sub>, 25 °C):  $\delta$  = 7.11 (m, H, phenol-*p*-CH), 6.91 (m, H, phenol-*o*-CH), 6.75 (m, H, phenol-*m*-CH), 3.81 (br, 4H, subst. Cp-*H*<sup>2</sup> / *H*<sup>5</sup> or Cp-*H*<sup>3</sup> / *H*<sup>4</sup>), 3.74 (m<sub>c</sub>, 8H, [Li(*thf*)<sub>2</sub>]), 3.55 (br, 4H, subst. Cp-*H*<sup>2</sup> / *H*<sup>5</sup> or Cp-*H*<sup>3</sup> / *H*<sup>4</sup>), 1.84 (m<sub>c</sub>, 8H, [Li(*thf*)<sub>2</sub>]), 1.66 (m<sub>c</sub>, 4H, tmp- $\gamma$ -CH<sub>2</sub>), 1.47 (m<sub>c</sub>, 8 H, tmp- $\beta$ -CH<sub>2</sub>), 1.31 (s, 24 H, tmp-CH<sub>3</sub>);



$^{13}\text{C}$  NMR ( $\text{CDCl}_3$ , 25 °C):  $\delta$  = 161.0 and 160.0 (Ph-COGa), 129.2 and 129.1 (Ph-*m*-CH), 120.0 and 119.6 (Ph-*o*-CH), 118.8 and 118.0 (Ph-*p*-CH), 74.6 (subst. Cp- $\text{C}^3/\text{C}^4$  or Cp- $\text{C}^2/\text{C}^5$ ), 70.7 (subst. Cp- $\text{C}^3/\text{C}^4$  or Cp- $\text{C}^2/\text{C}^5$ ), 67.9 ( $\text{Li}(\text{thf})_2$ ), 53.9 (tmp- $\text{C}^2/\text{C}^6$ ), 36.8 (tmp- $\text{C}^3/\text{C}^5$ ), 29.3 (tmp- $\text{C}^7/\text{C}^8/\text{C}^9/\text{C}^{10}$ ), 25.5 ( $\text{Li}(\text{thf})_2$ ), 16.8 (tmp- $\text{C}^4$ );

#### 7.4.5. Synthesis of **18**

0.65 g (0.74 mmol) of **8** were dissolved in 15 ml thf. Into this solution was added 0.31 g (3.00 mmol) of a solution of malonic acid in thf. The reaction took place at room temperature with continuous stirring. In a few seconds, a yellow precipitate was formed. After the addition was finished, the mixture was stirred for another 20 minutes. Then all the volatiles were evaporated under *vacuum* at room temperature, and the residue was washed several times with *n*-hexane and then with diethyl ether. The yellow jelly proved to be insoluble in thf at room temperature and also after refluxing for 30 minutes. By refluxing the residue for 20 minutes in acetonitrile, a clear pale yellow solution was obtained. The last solution was cool down slowly to room temperature and let for several days at 6°C yielding 0.423 g of colorless crystals of **18** (yield: 71%).

$^1\text{H}$  NMR (600 MHz,  $\text{CDCl}_3$ , 25 °C):  $\delta$  = 3.34 (br, 6H, Mal-(COO) $_2\text{CH}_2$ ), 1.67 (br, 18 H, tmp- $\gamma\text{-CH}_2$  and tmp- $\beta\text{-CH}_2$ ), 1.41 (s, 36 H, tmp- $\text{CH}_3$ );

$^{13}\text{C}$  NMR ( $\text{CDCl}_3$ , 25 °C):  $\delta$  = 174.1 (Mal-(COO) $_2\text{CH}_2$ ), 56.5 (tmp- $\text{C}^2/\text{C}^6$ ), 45.0 (Mal-(COO) $_2\text{CH}_2$ ), 34.8 (tmp- $\text{C}^3/\text{C}^5$ ), 27.4 (tmp- $\text{C}^7/\text{C}^8/\text{C}^9/\text{C}^{10}$ ), 16.3 (tmp- $\text{C}^4$ ).

#### 7.4.6. Synthesis of **19**

a) Into a solution of 0.36 g **8** (0.40 mmol) in 20 ml of thf, cooled at -78°C, 0.18 g 1,2-dihydroxybenzene (1.66 mmol) dissolved in 5 ml of thf were added dropwise. The color changed immediately from red-orange to yellow and a white precipitate was formed. Then the reaction mixture was heated to reflux for 10 minutes and a clear yellow solution was obtained. The mixture was stirred for another 30 minutes at room temperature. The clear yellow solution was reduced to one-third of its original volume and stored at -32 °C for several days. 0.28 g **19** (yield: 93 %) as colorless crystals were formed.

## 7. Experimental

---

b) By a similar reaction, to a solution of 0.37 g (0.69 mmol) **9** in 10 ml thf, at room temperature, was added dropwise a solution of 0.228 g (2.07 mmol) 1,2-dihydroxybenzene, in 5 ml thf. In a few minutes the color turned yellow. Then three quarter volumes were evaporated under *vacuum*. After several days standing at 7°C, colorless prismatic crystals of **19** were formed (yield: 87%).

M.p.: 247 – 250 °C (with dec.);

<sup>1</sup>H NMR (600 MHz, CDCl<sub>3</sub>, 25 °C): δ = 8.40 (br, 1 H, OH), 6.85 (br, 2 H, CH), 6.66 (br, 6 H, CH), 6.55 (br, 4 H, CH), 1.69 (m, 4H, tmp-γCH<sub>2</sub>), 1.58 (m, 8 H, tmp-βCH<sub>2</sub>), 1.28 (s, 24 H, tmp-CH<sub>3</sub>);

<sup>13</sup>C NMR (CDCl<sub>3</sub>, 25 °C): δ = 150.0 (COGa), 145.2 (COH), 120.3 (o-CH), 117.7 (o-CH), 114.2 (m-CH), 56.0 (tmp-C<sup>2</sup>/C<sup>6</sup>), 35.8 (tmp-C<sup>3</sup>/C<sup>5</sup>), 27.9 (tmp-C<sup>7</sup>/C<sup>8</sup>/C<sup>9</sup>/C<sup>10</sup>), 16.1 (tmp-C<sup>4</sup>);

EA C<sub>40</sub>H<sub>57</sub>GaN<sub>2</sub>O<sub>7</sub> (747.61): calcd. C 64.26, H 7.68, N 3.75, found C 60.55, H 7.42, N 3.68.

MS (5.0 kV, ESI-MS, thf, 8 μl/min, <sup>69</sup>Ga): m/z (%) = (-) 321 (100) [Ga(C<sub>6</sub>H<sub>4</sub>O<sub>2</sub>){C<sub>6</sub>H<sub>4</sub>O(OH)}(OH)<sub>2</sub>]<sup>-</sup>, 109 (3) [C<sub>6</sub>H<sub>4</sub>O(OH)]<sup>-</sup>.

### 7.4.7. Synthesis of **20**

A solution of 0.49 g **9** (0.92 mmol) in 10 ml diethyl ether was treated with a solution of acetic acid (0.22 g, 3.67 mmol) in 5 ml diethyl ether. The reaction took place at room temperature. The color changed immediately from orange to yellow with the formation of a yellow precipitate. All volatiles were removed under *vacuum* (0.01 mbar) and the remaining solid was washed with hexane several times. 0.41 g **20** (yield: 78 %) as yellow powder was collected.

<sup>1</sup>H NMR (600 MHz, CDCl<sub>3</sub>, 25 °C): δ = 4.29 (br, 2H, Cp-H<sup>2</sup> / H<sup>5</sup> or Cp-H<sup>3</sup> / H<sup>4</sup>), 4.25 (br, 2H, Cp-H<sup>2</sup> / H<sup>5</sup> or Cp-H<sup>3</sup> / H<sup>4</sup>), 4.13 (br, 5H, unsubst. Cp), 2.10 (br, 2H, tmpH<sub>2</sub><sup>+</sup>-NH<sub>2</sub>), 2.03 (br, 9 H, O<sub>2</sub>CCH<sub>3</sub>), 1.71 (br, 2H, tmpH<sub>2</sub><sup>+</sup>-γ-CH<sub>2</sub>), 1.63 (br, 4H, tmpH<sub>2</sub><sup>+</sup>-β-CH<sub>2</sub>), 1.39 (br, 12H, tmpH<sub>2</sub><sup>+</sup>-CH<sub>3</sub>);

$^{13}\text{C}$  NMR ( $\text{CDCl}_3$ , 25 °C):  $\delta = 177.8$  ( $\text{CO}_2\text{CH}_3$ ), 177.2 ( $\text{CO}_2\text{CH}_3$ ), 75.0 ( $\text{Cp-C}^3/\text{C}^4$  or  $\text{Cp-C}^2/\text{C}^5$ ), 70.5 ( $\text{Cp-C}^3/\text{C}^4$  or  $\text{Cp-C}^2/\text{C}^5$ ), 68.0 (unsubst. Cp), 55.7 ( $\text{tmp-C}^2/\text{C}^6$ ), 35.2 ( $\text{tmp-C}^3/\text{C}^5$ ), 27.4 ( $\text{tmp-C}^7/\text{C}^8/\text{C}^9/\text{C}^{10}$ ), 23.4 ( $\text{CO}_2\text{CH}_3$ ), 16.4 ( $\text{tmp-C}^4$ );

#### 7.4.8. Synthesis of **21** and **22**

To a stirred solution of **9** (0.659 g, 1.23 mmol) in 15 ml *n*-hexane was added dropwise a solution of  $\text{C}_6\text{H}_5\text{OH}$  (0.355 g, 3.77 mmol) in 10 ml mixture of *n*-hexane and diethyl ether (8:2). The reaction took place at room temperature. The solution color turned yellow and the products mixture as an orange precipitate was formed. Product mixture yield 72%, based upon consumed **9**. The products **21** and **22** were separated by recrystallization from a thf:*n*-hexane solution (1:1) yielding suitable crystals of **22** (32% yield, based on product mixture yield) and the other product **21** remained in the solution.

##### a) **21**: $^1\text{H}$ - and $^{13}\text{C}$ -NMR

$^1\text{H}$  NMR (600 MHz,  $\text{CDCl}_3$ , 25 °C):  $\delta = 7.20$  (pseudo-t,  $^3\text{J}_{\text{H,H}} = ^5\text{J}_{\text{H,H}} = 7.8$  Hz, 6H, Ph-*m*-CH), 7.08 (d,  $^3\text{J}_{\text{H,H}} = 7.8$  Hz, 6H, Ph-*o*-CH), 6.84 (pseudo-t,  $^3\text{J}_{\text{H,H}} = ^5\text{J}_{\text{H,H}} = 7.2$  Hz, 3H, Ph-*p*-CH), 4.30 (br, 2H, subst.  $\text{Cp-H}^2 / \text{H}^5$  or  $\text{Cp-H}^3 / \text{H}^4$ ), 4.04 (br, 2H, subst.  $\text{Cp-H}^2 / \text{H}^5$  or  $\text{Cp-H}^3 / \text{H}^4$ ), 3.88 (s, 5H, unsubst. Cp-ring), 1.53 (m, 2H, tmp- $\gamma\text{CH}_2$ ), 1.37 (m, 4 H, tmp- $\beta\text{CH}_2$ ), 1.24 (s, 12 H, tmp- $\text{CH}_3$ );

$^{13}\text{C}$  NMR ( $\text{CDCl}_3$ , 25 °C):  $\delta = 160.6$  (Ph, COGa), 129.3 (Ph, *m*-CH), 120.0 (Ph, *o*-CH), 118.5 (Ph, *p*-CH), 74.7 (subst.  $\text{Cp-C}^3/\text{C}^4$  or  $\text{Cp-C}^2/\text{C}^5$ ), 69.9 (subst.  $\text{Cp-C}^3/\text{C}^4$  or  $\text{Cp-C}^2/\text{C}^5$ ), 68.1 (unsubst. Cp), 56.4 ( $\text{tmp-C}^2/\text{C}^6$ ), 35.6 ( $\text{tmp-C}^3/\text{C}^5$ ), 28.2 ( $\text{tmp-C}^7/\text{C}^8/\text{C}^9/\text{C}^{10}$ ), 15.9 ( $\text{tmp-C}^4$ );

##### b) **22**: $^1\text{H}$ - and $^{13}\text{C}$ -NMR

$^1\text{H}$  NMR (600 MHz,  $\text{CDCl}_3$ , 25 °C):  $\delta = 7.13$  (pseudo-t,  $^3\text{J}_{\text{H,H}} = ^5\text{J}_{\text{H,H}} = 7.5$  Hz, 6H, Ph-*m*-CH), 6.92 (d,  $^3\text{J}_{\text{H,H}} = 7.5$  Hz, 6H, Ph-*o*-CH), 6.81 (pseudo-t,  $^3\text{J}_{\text{H,H}} = ^5\text{J}_{\text{H,H}} = 7.2$  Hz, 3H, Ph-*p*-CH), 4.21 (br, 2H, subst.  $\text{Cp-H}^2 / \text{H}^5$  or  $\text{Cp-H}^3 / \text{H}^4$ ), 3.83 (br, 2H, subst.  $\text{Cp-H}^2 / \text{H}^5$  or  $\text{Cp-H}^3 / \text{H}^4$ ), 3.77 (br, 4H, thf- $\text{CH}_2$ ), 3.68 (s, 5H, unsubst. Cp-ring), 1.76 (br, 4H, thf- $\text{CH}_2$ );

## 7. Experimental

---

$^{13}\text{C}$  NMR ( $\text{CDCl}_3$ , 25 °C):  $\delta$  = 159.9 (Ph, COGa), 129.3 (Ph, *m*-CH), 119.8 (Ph, *o*-CH), 119.1 (Ph, *p*-CH), 74.7 (subst. Cp- $\text{C}^3/\text{C}^4$  or Cp- $\text{C}^2/\text{C}^5$ ), 70.2 (subst. Cp- $\text{C}^3/\text{C}^4$  or Cp- $\text{C}^2/\text{C}^5$ ), 68.2 (unsubst. Cp-ring), 68.1 (thf- $\text{CH}_2$ ), 25.4 (thf- $\text{CH}_2$ ).

## References

- [1] SHELXTL, *Bruker*, 1998.
- [2] M. J. Frisch, G. W. Trucks, H. B. Schlegel, G.E. Scuseria, M. A. Robb, J. R. Cheeseman, J. A. Montgomery, J. T. Vreven, K. N. Kudin, J. C. Burant, J. M. Millam, S. S. Iyengar, J. Tomasi, V. Barone, B. Mennucci, M. Cossi, G. Scalmani, N. Rega, G. A. Petersson, H. Nakatsuji, M. Hada, M. Ehara, K. Toyota, R. Fukuda, J. Hasegawa, M. Ishida, T. Nakajima, Y. Honda, O. Kitao, H. Nakai, M. Klene, X. Li, J. E. Knox, H. P. Hratchian, J. B. Cross, C. Adamo, J. Jaramillo, R. Gomperts, R. E. Stratmann, O. Yazyev, A. J. Austin, R. Cammi, C. Pomelli, J. W. Ochterski, P. Y. Ayala, K. Morokuma, G. A. Voth, P. Salvador, J. J. Dannenberg, V. G. Zakrzewski, S. Dapprich, A. D. Daniels, M. C. Strain, O. Farkas, D. K. Malick, A. D. Rabuck, K. Raghavachari, J. B. Foresman, J. V. Ortiz, Q. Cui, A. G. Baboul, S. Clifford, J. Cioslowski, B. B. Stefanov, G. Liu, A. Liashenko, P. Piskorz, I. Komaromi, R. L. Martin, D. J. Fox, T. Keith, M. A. Al-Laham, C. Y. Peng, A. Nanayakkara, M. Challacombe, P. M. W. Gill, B. Johnson, W. Chen, M. W. Wong, C. Gonzalez, J. A. Pople, Gaussian 03, Revision B.03 ed., Gaussian, Inc., Pittsburgh PA, **2003**.
- [3] P. J. Brothers, R. J. Wehmschulte, M. M. Olmstead, K. Ruhlandt-Senge, S. R. Parkin, and P. P. Power, *Organometallics*, **1994**, *13*, 2792-2799.
- [4] G. Linti, H. Nöth, K. Polborn, C. Robl, and M. Schmidt, *Chem. Ber.*, **1995**, *128*, 487-492.
- [5] M. F. Lappert, M. J. Slade, and A. Singh, *J. Am. Chem. Soc.*, **1983**, *105*, 302-304.
- [6] G. Linti, R. Frey, K. Polborn, and M. Schmidt, *Chem. Ber.*, **1994**, *127*, 1387-1393.
- [7] R. Frey, G. Linti, and K. Polborn, *Chem. Ber.*, **1994**, *127*, 101-103.
- [8] I. R. Butler, W. R. Cullen, J. Ni, and S. J. Rettig, *Organometallics*, **1985**, *4*, 2196-2201.
- [9] F. Rebiere, O. Samuel, and H. B. Kagan, *Tetrahedron Lett.*, **1990**, *31(22)*, 3121-3124.



## 8. Crystals Data

	1	6
Identification code	of4	li_of2
Empirical formula	C <sub>18</sub> H <sub>36</sub> ClGaN <sub>2</sub>	C <sub>11</sub> H <sub>29</sub> Cl <sub>2</sub> GaN <sub>2</sub> Si <sub>2</sub>
Molar mass [g mol <sup>-1</sup> ]	385.66	386.16
Data collection temp. [K]	200(2)	200(2)
Wavelength [pm]	71.073	71.073
Crystal system	monoclinic	monoclinic
Space group	<i>P2<sub>1</sub>/c</i>	<i>P2<sub>1</sub>/n</i>
Unit cell dimensions:		
<i>a</i> [Å]	10.876(2)	13.534(3)
<i>b</i> [Å]	23.807(5)	11.113(2)
<i>c</i> [Å]	7.951(2)	13.613(3)
$\alpha$ [°]	90.00	90.00
$\beta$ [°]	104.09(3)	106.52(3)
$\gamma$ [°]	90.00	90.00
Volume [Å <sup>3</sup> ]	1996.7(7)	1962.9(7)
Z	4	4
Density (calculated) [g/cm <sup>3</sup> ]	1.283	1.307
Absorption coefficient [mm <sup>-1</sup> ]	1.512	1.785
F(000) [e]	824	808
Crystal size [mm <sup>3</sup> ]	0.48 x 0.24 x 0.22	0.25 x 0.25 x 0.20
$\theta$ range for data collection [°]	1.93 to 24.12	1.87 to 30.51
Index ranges	-12 ≤ <i>h</i> ≤ 12 -26 ≤ <i>k</i> ≤ 25 -9 ≤ <i>l</i> ≤ 9	-19 ≤ <i>h</i> ≤ 18 0 ≤ <i>k</i> ≤ 15 0 ≤ <i>l</i> ≤ 19
Reflections collected	12794	5980
Independent reflections	3076 [R <sub>int</sub> = 0.0299]	5980 [R <sub>int</sub> = 0]
Completeness to...	$\theta = 24.12^\circ$ ; 96.4%	$\theta = 30.51^\circ$ ; 100%
Refinement method	Full-matrix least-squares on F <sup>2</sup>	Full-matrix least-squares on F <sup>2</sup>
Data/restraints/parameters	3076/0/207	5980/0/205
Goodness-of-fit on F <sup>2</sup>	1.058	1.068
Final <i>R</i> indices [ <i>I</i> > 2σ( <i>I</i> )]	<i>R</i> <sub>1</sub> = 0.0248 <i>wR</i> <sub>2</sub> = 0.0647	<i>R</i> <sub>1</sub> = 0.0625 <i>wR</i> <sub>2</sub> = 0.1580
<i>R</i> indices (all data)	<i>R</i> <sub>1</sub> = 0.0292 <i>wR</i> <sub>2</sub> = 0.0686	<i>R</i> <sub>1</sub> = 0.0706 <i>wR</i> <sub>2</sub> = 0.1647
Largest difference peak and hole [eÅ <sup>-3</sup> ]	0.274 and -0.342	3.342 and -2.492
X-ray diffractometer	STOE IPDS I	STOE IPDS I

## 8. Crystals Data

	7	8
Identification code	of14	of9
Empirical formula	(C <sub>12</sub> H <sub>24</sub> Cl <sub>4</sub> GaLiO <sub>4</sub> ) <sub>n</sub>	C <sub>46</sub> H <sub>80</sub> FeGa <sub>2</sub> N <sub>4</sub>
Molar mass [g mol <sup>-1</sup> ]	(450.77)n	884.43
Data collection temp. [K]	200(2)	200(2)
Wavelength [pm]	71.073	71.073
Crystal system	monoclinic	triclinic
Space group	<i>P</i> 2 <sub>1</sub> / <i>c</i>	<i>P</i> $\bar{1}$
Unit cell dimensions:		
<i>a</i> [Å]	9.906(2)	10.999(2)
<i>b</i> [Å]	15.733(3)	13.803(3)
<i>c</i> [Å]	13.292(3)	15.830(3)
$\alpha$ [°]	90.00	91.82(3)
$\beta$ [°]	91.22(3)	106.32(3)
$\gamma$ [°]	90.00	104.62(3)
Volume [Å <sup>3</sup> ]	2071.0(7)	2218.0(8)
<i>Z</i>	4	2
Density (calculated) [g/cm <sup>3</sup> ]	1.446	1.324
Absorption coefficient [mm <sup>-1</sup> ]	1.854	1.564
F(000) [e]	920	944
Crystal size [mm <sup>3</sup> ]	0.65 x 0.30 x 0.24	0.32 x 0.24 x 0.10
$\theta$ range for data collection [°]	2.01 to 20.88	1.93 to 24.11
Index ranges	-9 ≤ <i>h</i> ≤ 9 -15 ≤ <i>k</i> ≤ 15 -13 ≤ <i>l</i> ≤ 13	-12 ≤ <i>h</i> ≤ 12 -15 ≤ <i>k</i> ≤ 15 -18 ≤ <i>l</i> ≤ 18
Reflections collected	8740	14381
Independent reflections	2151 [R <sub>int</sub> = 0.1325]	6594 [R <sub>int</sub> = 0.0422]
Completeness to...	$\theta = 20.88^\circ$ ; 98.3%	$\theta = 24.11^\circ$ ; 93.5%
Refinement method	Full-matrix least-squares on F <sup>2</sup>	Full-matrix least-squares on F <sup>2</sup>
Data/restraints/parameters	2151/0/199	6594 /0/494
Goodness-of-fit on F <sup>2</sup>	1.468	0.940
Final <i>R</i> indices [I > 2σ( <i>I</i> )]	<i>R</i> <sub>1</sub> = 0.1238 <i>wR</i> <sub>2</sub> = 0.2812	<i>R</i> <sub>1</sub> = 0.0332 <i>wR</i> <sub>2</sub> = 0.0813
<i>R</i> indices (all data)	<i>R</i> <sub>1</sub> = 0.1967 <i>wR</i> <sub>2</sub> = 0.3043	<i>R</i> <sub>1</sub> = 0.0403 <i>wR</i> <sub>2</sub> = 0.0832
Largest difference peak and hole [eÅ <sup>-3</sup> ]	1.494 and -0.686	0.647 and -0.801
X-ray diffractometer	STOE IPDS I	STOE IPDS I



	9	12
Identification code	of36	of13
Empirical formula	C <sub>28</sub> H <sub>45</sub> FeGaN <sub>2</sub>	C <sub>72</sub> H <sub>124</sub> Fe <sub>4</sub> Li <sub>12</sub> N <sub>8</sub> O <sub>4</sub> •2(H <sub>5</sub> C <sub>2</sub> ) <sub>2</sub> O
Molar mass [g mol <sup>-1</sup> ]	535.23	1612.65
Data collection temp. [K]	200(2)	200(2)
Wavelength [pm]	71.073	71.073
Crystal system	monoclinic	triclinic
Space group	<i>P2<sub>1</sub>/n</i>	<i>P</i> $\bar{1}$
Unit cell dimensions:		
<i>a</i> [Å]	10.293(2)	15.607(3)
<i>b</i> [Å]	12.504(3)	16.654(3)
<i>c</i> [Å]	21.388(4)	20.577(4)
$\alpha$ [°]	90.00	80.19(3)
$\beta$ [°]	101.07(3)	71.69(3)
$\gamma$ [°]	90.00	64.57(3)
Volume [Å <sup>3</sup> ]	2701.6(9)	4581.5(16)
<i>Z</i>	4	2
Density (calculated) [g/cm <sup>3</sup> ]	1.316	1.169
Absorption coefficient [mm <sup>-1</sup> ]	1.552	0.670
F(000) [e]	1136	1720
Crystal size [mm <sup>3</sup> ]	0.48 x 0.44 x 0.37	0.40 x 0.39 x 0.29
$\theta$ range for data collection [°]	1.94 to 23.99	1.58 to 24.11
Index ranges	-11 ≤ <i>h</i> ≤ 11 -14 ≤ <i>k</i> ≤ 14 -24 ≤ <i>l</i> ≤ 24	-17 ≤ <i>h</i> ≤ 17 -18 ≤ <i>k</i> ≤ 19 -23 ≤ <i>l</i> ≤ 23
Reflections collected	16689	29649
Independent reflections	4179 [R <sub>int</sub> = 0.0685]	13614 [R <sub>int</sub> = 0.1007]
Completeness to...	$\theta = 23.99^\circ$ ; 98.4%	$\theta = 24.11^\circ$ ; 93.5%
Refinement method	Full-matrix least-squares on F <sup>2</sup>	Full-matrix least-squares on F <sup>2</sup>
Data/restraints/parameters	4179/0/297	13614/0/991
Goodness-of-fit on F <sup>2</sup>	1.057	1.041
Final <i>R</i> indices [I>2σ( <i>I</i> )]	<i>R</i> <sub>1</sub> = 0.0476 <i>wR</i> <sub>2</sub> = 0.1284	<i>R</i> <sub>1</sub> = 0.1890 <i>wR</i> <sub>2</sub> = 0.5312
<i>R</i> indices (all data)	<i>R</i> <sub>1</sub> = 0.0540 <i>wR</i> <sub>2</sub> = 0.1319	<i>R</i> <sub>1</sub> = 0.2358 <i>wR</i> <sub>2</sub> = 0.5469
Largest difference peak and hole [eÅ <sup>-3</sup> ]	1.970 and -0.758	3.338 and -1.166
X-ray diffractometer	STOE IPDS I	STOE IPDS I

## 8. Crystals Data

	13	14
Identification code	of16	of24
Empirical formula	C <sub>50</sub> H <sub>80</sub> FeGa <sub>2</sub> N <sub>4</sub> O <sub>8</sub> •2 thf	C <sub>40</sub> H <sub>66</sub> FeGa <sub>2</sub> N <sub>2</sub> O <sub>12</sub>
Molar mass [g mol <sup>-1</sup> ]	1204.68	962.26
Data collection temp. [K]	200(2)	200(2)
Wavelength [pm]	71.073	71.073
Crystal system	triclinic	triclinic
Space group	<i>P</i> $\bar{1}$	<i>P</i> $\bar{1}$
Unit cell dimensions:		
<i>a</i> [Å]	12.322(3)	10.580(2)
<i>b</i> [Å]	15.243(3)	11.072(2)
<i>c</i> [Å]	17.673(4)	11.438(2)
$\alpha$ [°]	103.40(3)	64.81(3)
$\beta$ [°]	102.20(3)	84.86(3)
$\gamma$ [°]	103.38(3)	75.75(3)
Volume [Å <sup>3</sup> ]	3015.9(10)	1174.9(4)
<i>Z</i>	2	1
Density (calculated) [g/cm <sup>3</sup> ]	1.327	1.360
Absorption coefficient [mm <sup>-1</sup> ]	1.182	1.500
F(000) [e]	1280	504
Crystal size [mm <sup>3</sup> ]	0.20 x 0.18 x 0.14	0.20 x 0.14 x 0.13
$\theta$ range for data collection [°]	2.15 to 24.14	1.97 to 24.03
Index ranges	-14 ≤ <i>h</i> ≤ 14 -17 ≤ <i>k</i> ≤ 17 -20 ≤ <i>l</i> ≤ 20	-12 ≤ <i>h</i> ≤ 12 -12 ≤ <i>k</i> ≤ 12 -13 ≤ <i>l</i> ≤ 13
Reflections collected	19531	7517
Independent reflections	8975 [R <sub>int</sub> = 0.0485]	3458 [R <sub>int</sub> = 0.0480]
Completeness to...	$\theta = 24.14^\circ$ ; 93.2%	$\theta = 24.03^\circ$ ; 93.6%
Refinement method	Full-matrix least-squares on F <sup>2</sup>	Full-matrix least-squares on F <sup>2</sup>
Data/restraints/parameters	8975/0/677	3458/0/267
Goodness-of-fit on F <sup>2</sup>	1.008	0.828
Final <i>R</i> indices [I > 2σ( <i>I</i> )]	<i>R</i> <sub>1</sub> = 0.0731 <i>wR</i> <sub>2</sub> = 0.1920	<i>R</i> <sub>1</sub> = 0.0284 <i>wR</i> <sub>2</sub> = 0.0596
<i>R</i> indices (all data)	<i>R</i> <sub>1</sub> = 0.1051 <i>wR</i> <sub>2</sub> = 0.2174	<i>R</i> <sub>1</sub> = 0.0442 <i>wR</i> <sub>2</sub> = 0.0622
Largest difference peak and hole [eÅ <sup>-3</sup> ]	0.684 and -0.842	0.371 and -0.380
X-ray diffractometer	STOE IPDS I	STOE IPDS I

	15	18
Identification code	of26	of46o
Empirical formula	C <sub>56</sub> H <sub>72</sub> Fe <sub>4</sub> Ga <sub>8</sub> O <sub>12</sub> •2C <sub>6</sub> H <sub>6</sub>	C <sub>36</sub> H <sub>66</sub> GaN <sub>3</sub> O <sub>12</sub>
Molar mass [g mol <sup>-1</sup> ]	1874.51	802.64
Data collection temp. [K]	200(2)	200(2)
Wavelength [pm]	71.073	71.073
Crystal system	monoclinic	orthorhombic
Space group	<i>P</i> 2 <sub>1</sub>	<i>P</i> 2 <sub>1</sub> 2 <sub>1</sub> 2 <sub>1</sub>
Unit cell dimensions:		
<i>a</i> [Å]	12.646(3)	11.909(2)
<i>b</i> [Å]	13.037(3)	14.958(3)
<i>c</i> [Å]	22.861(5)	22.798(5)
$\alpha$ [°]	90.00	90.00
$\beta$ [°]	104.41(3)	90.00
$\gamma$ [°]	90.00	90.00
Volume [Å <sup>3</sup> ]	3650.3(13)	4061.1(14)
<i>Z</i>	2	4
Density (calculated) [g/cm <sup>3</sup> ]	1.705	1.313
Absorption coefficient [mm <sup>-1</sup> ]	3.725	0.740
F(000) [e]	1880	1720
Crystal size [mm <sup>3</sup> ]	0.57 x 0.15 x 0.09	0.24 x 0.30 x 0.46
$\theta$ range for data collection [°]	1.69 to 23.98	2.01 to 26.1
Index ranges	-14 ≤ <i>h</i> ≤ 13 -14 ≤ <i>k</i> ≤ 14 -26 ≤ <i>l</i> ≤ 26	-14 ≤ <i>h</i> ≤ 14 -18 ≤ <i>k</i> ≤ 18 -27 ≤ <i>l</i> ≤ 28
Reflections collected	22714	32848
Independent reflections	11199 [R <sub>int</sub> = 0.1208]	8045 [R <sub>int</sub> = 0.2118]
Completeness to...	$\theta = 23.98^\circ$ ; 99.2%	$\theta = 26.10^\circ$
Refinement method	Full-matrix least-squares on $F^2$	Full-matrix least-squares on $F^2$
Data/restraints/parameters	11199/1/837	8045/2/499
Goodness-of-fit on $F^2$	0.861	0.573
Final <i>R</i> indices [ $I > 2\sigma(I)$ ]	<i>R</i> <sub>1</sub> = 0.0710 <i>wR</i> <sub>2</sub> = 0.1671	<i>R</i> <sub>1</sub> = 0.0468 <i>wR</i> <sub>2</sub> = 0.0906
<i>R</i> indices (all data)	<i>R</i> <sub>1</sub> = 0.1226 <i>wR</i> <sub>2</sub> = 0.1957	<i>R</i> <sub>1</sub> = 0.1291 <i>wR</i> <sub>2</sub> = 0.0904
Largest difference peak and hole [eÅ <sup>-3</sup> ]	1.012 and -1.846	0.44 and -0.33
X-ray diffractometer	STOE IPDS I	STOE IPDS I

## 8. Crystals Data

	19	22
Identification code	of25	of47
Empirical formula	C <sub>36</sub> H <sub>53</sub> GaN <sub>2</sub> O <sub>6</sub> •thf	C <sub>36</sub> H <sub>40</sub> FeGaLiO <sub>5</sub>
Molar mass [g mol <sup>-1</sup> ]	747.60	685.22
Data collection temp. [K]	200(2)	200(2)
Wavelength [pm]	71.073	71.073
Crystal system	orthorhombic	triclinic
Space group	<i>P</i> 2 <sub>1</sub> 2 <sub>1</sub> 2 <sub>1</sub>	<i>P</i> $\bar{1}$
Unit cell dimensions:		
<i>a</i> [Å]	13.917(3)	8.9821(18)
<i>b</i> [Å]	14.254(3)	11.100(2)
<i>c</i> [Å]	20.509(4)	16.770(3)
$\alpha$ [°]	90.00	101.56(3)
$\beta$ [°]	90.00	92.31(3)
$\gamma$ [°]	90.00	97.10(3)
Volume [Å <sup>3</sup> ]	4068.5(14)	1621.9(6)
<i>Z</i>	4	2
Density (calculated) [g/cm <sup>3</sup> ]	1.221	1.403
Absorption coefficient [mm <sup>-1</sup> ]	0.724	1.319
F(000) [e]	1592	712
Crystal size [mm <sup>3</sup> ]	0.53 x 0.32 x 0.19	0.28 x 0.23 x 0.15
$\theta$ range for data collection [°]	1.99 to 19.48	1.89 to 22.39
Index ranges	-12 ≤ <i>h</i> ≤ 12 -13 ≤ <i>k</i> ≤ 13 -19 ≤ <i>l</i> ≤ 19	-9 ≤ <i>h</i> ≤ 9 -11 ≤ <i>k</i> ≤ 11 -17 ≤ <i>l</i> ≤ 17
Reflections collected	14436	8610
Independent reflections	3479 [R <sub>int</sub> = 0.0724]	3954 [R <sub>int</sub> = 0.0598]
Completeness to...	$\theta$ = 19.48°; 99.0%	$\theta$ = 22.39°; 94.5%
Refinement method	Full-matrix least-squares on F <sup>2</sup>	Full-matrix least-squares on F <sup>2</sup>
Data/restraints/parameters	3479/24/526	3954/0/397
Goodness-of-fit on F <sup>2</sup>	1.030	0.822
Final <i>R</i> indices [I > 2σ( <i>I</i> )]	<i>R</i> <sub>1</sub> = 0.0558 <i>wR</i> <sub>2</sub> = 0.1421	<i>R</i> <sub>1</sub> = 0.0429 <i>wR</i> <sub>2</sub> = 0.0945
<i>R</i> indices (all data)	<i>R</i> <sub>1</sub> = 0.0679 <i>wR</i> <sub>2</sub> = 0.1490	<i>R</i> <sub>1</sub> = 0.0718 <i>wR</i> <sub>2</sub> = 0.1000
Largest difference peak and hole [eÅ <sup>-3</sup> ]	0.412 and -0.225	0.468 and -0.540
X-ray diffractometer	STOE IPDS I	STOE IPDS I

## 9. Publications

1. “*Synthesis and Structure of a Carbamato-bridged Digallyl-ferrocenophane – Fixation of Carbon Dioxide with Aminogallanes*”  
Ovidiu Feier-Iova and Gerald Linti, *Z. Anorg. Allg. Chem.* **2008**, 634, 559-564.
2. “*Reactivity Studies on a Versatile Bis(diaminogallyl)ferrocene*”  
Ovidiu Feier-Iova and Gerald Linti, *WCECS*, **2007**, Proceedings, ISBN: 978-988-98671-6-4, 182-187.